Optimal Synthesis, Design and Operation of Hybrid Separation Processes

Tajalasfia M. M. Barakat

September 2006

A thesis submitted for the degree of Doctor of Philosophy of the University of London

Department of Chemical Engineering
University College London
London, WC1E 7JE, United Kingdom

Abstract

Hybrid separation systems have recently been hailed as one of the most promising alternatives to conventional capital and energy intensive separation processes. Hybrid separation systems are able to effectively separate mixtures commonly encountered in the fine chemical and pharmaceutical industries that are difficult or impossible to separate by conventional distillation processes due to azeotropic behaviour or low relative volatilities.

In a hybrid process where a distillation column unit and a pervaporation unit are integrated into one process, the shortcomings of one method are outweighed by the benefits of the other. The addition of a pervaporation unit to the conventional distillation process, either before, after or fully integrated, adds complexity to the system but also more degrees of freedom which, if properly chosen, can result in capital and operating costs savings and can consequently increase the overall profitability of the system, particularly for difficult separations.

The objective of this work was to study the optimal configuration, design and operation of hybrid distillation/membrane processes taking into account the extra degrees of freedom afforded by these processes. This is achieved by firstly developing detailed mathematical models from first principles to accurately describe the distillation, membrane and their hybrid processes. Secondly, rigorous optimisation strategies were employed to study the hybrid systems and their constituents processes.

The feasibility of the hybrid system was investigated through various studies. In the first study, the *batch* configuration, design and operation of the hybrid system was considered for the first time. The second study considers the optimal synthesis of continuous hybrid processes where more degree of freedoms have been explored than previously reported. The third study considered the *novel* multi-criteria optimisation of these systems. It was demonstrated in these studies that significant savings can be achieved when the optimal hybrid process is used instead of distillation or pervaporation alone.

Acknowledgments

I would like to express my gratitude and greatest thanks to my supervisor, Dr Eva Sørensen who supported, encouraged and contributed invaluably to this research and to my general academic progress. I would also like to thank my secondary supervisor, Professor Eric Fraga for his guidance and contribution to this research.

Special thanks to Professor Alan Jones and Professor David Bogle for their help and support. The members of the CPSE at UCL have provided useful discussions and company during this research which is greatly appreciated. Special mention should go to those who helped in proof-reading this thesis.

I would like to acknowledge the financial support of UCL Graduate School and the CPSE that made this research possible. Conference funding from UCL Graduate School, IChemE Fluid Separation Subject Group, EPSRC and INYS is also greatly acknowledged.

Finally, I would like to thank my family and friends for their support and encouragement.

Contents

PAGE

MISSING

IN

ORIGINAL

List of Tables

List of Figures

Chapter 1

Introduction

In this chapter, a general background to hybrid distillation/membrane separation processes is given and a review of work presented in the open literature on theses processes is presented. The potential of hybrid separation processes is discussed followed by an outline of the motivations and objectives of this project.

1.1 Background

Distillation remains the most commonly used technique for separating liquid mixtures in the chemical industries despite being an energy and capital intensive process. Many industrially valuable mixtures, however, are difficult to separate by simple continuous distillation due to azeotropic phase behaviour, tangent pinch, or an overall low relative volatility (Pressly and Ng, 1998). Nevertheless, the extensive use of distillation even in these cases has resulted in significant academic and industrial research effort to develop more efficient distillation-based systems.

The separation principle of distillation is based on the difference in volatilities between the constituent components of the mixture. The successive boiling and condensation of the mixture will cause the vapour to become richer in the lighter components while the liquid

will become richer in the heavier components. The separation mechanism in membranes, however, is fundamentally different, as the membrane acts as a barrier that preferentially diffuses some of the components in the mixture while retaining the others regardless of the components' vapour-liquid equilibria. Membrane processes are characterised by their high selectivity, moderate operation cost-to-performance ratio, low energy consumption, and compact and modular design (Lipnizki et al., 1999). Membrane-based processes are today finding widespread use in the petrochemical, pharmaceutical, food industries and environmental applications in addition to a variety of other applications (Baker (2000) and Nunes and Peinemann (2001)) due to the many advantages of membranes over conventional distillation separation processes.

Membrane processes are still generally more costly than distillation. However, for some separations, particularly azeotropic and close boiling separations, the costs are comparable or in favour of membrane processes. Recently, hybrid processes have emerged where a distillation column unit and a membrane unit are integrated into one process. In such a process, where the shortcomings of one method are outweighed by the benefits of the other, significant savings in terms of capital investment and energy consumption can be achieved as will be demonstrated in this work.

1.2 Distillation Processes

Many mixtures commonly encountered in the chemical industries exhibit tangent-pinch, low relative volatility or close-boiling behaviour and are therefore energy intensive and often uneconomical to separate by conventional distillation processes. Nevertheless, distillation can be used to separate low relative volatility mixtures by altering their volatilities, or in the case of azeotropes, by shifting or breaking the azeotropic point. This is commonly done by adding other chemicals (known as solvents, entrainers or extractants) or by appropriately adjusting the column operating pressure. Distillation based methods for separating these difficult mixtures can be classified as follows:

- Extractive distillation processes

  Extractive distillation is characterised by the presence of a chemical agent (known as the extractive agent, entrainer or solvent). The solvent is normally a miscible, high-boiling, relatively non-volatile liquid that does not form any azeotropes with other components in the mixture. The solvent breaks the azeotrope by altering the relative volatilities of the components to permit the withdrawal of pure components from the column. The solvent is retrieved from the bottom of the column stream for subsequent re-usage.

- Azeotropic distillation processes

  In *homogeneous* azeotropic distillation, similarly to extractive distillation, a miscible liquid solvent is added to break the azeotrope, however, in contrast to extractive distillation, a solvent is used and recovered in the distillate. Another alternative is *heterogeneous* azeotropic distillation. This method is characterised by a solvent that forms one or more azeotropes with the components in the mixture resulting in two liquid phases forming. The liquid-liquid mixture is then separated in a subsequent distillation sequence.

- Pressure-swing distillation processes

  The dependence of the azeotropic point on pressure can be exploited to perform the required separation. A series of distillation columns operating at different pressures may be used to process the mixture above and below the azeotropic points.

- Reactive distillation processes

  Reactive distillation is a combination of both reaction and separation in a single unit. In this method, the separating agent reacts preferentially and reversibly with one or more of the components in the azeotropic mixture. This permits the withdrawal of the reaction products followed by a second unit to reverse the reaction in order to recover the reacted components.

- Hybrid distillation/decantation processes

  A Hybrid distillation/decantation process can also be used to separate difficult mixtures. In principles, mixtures is separated into its liquid phases by condensation and decantation. Part of separation is performed by distillation while the liquidliquid split in the decanter is used for crossing the distillation boundaries.

- Hybrid distillation/crystallisation processes

  Hybrid distillation/crystallisation processes exploit the crystallisation properties of the mixture considered. Similarly to hybrid distillation/decantation processes, part of the separation is performed by the distillation column while the solid-liquid split in the crystliser is used to overcome the distillation boundaries.

- Hybrid distillation/membrane processes

  Hybrid distillation/membrane processes, which is the main focus of this thesis, can also be used to separate close-boiling or azeotropic mixtures. The primary purpose of the membrane is to break the azeotrope and to allow the distillation column to perform the separation process either above or below the azeotropic point.

1.3 Membrane Processes

Membrane separation technology is characterised by the splitting of a feed stream into two product streams: a permeate and a retentate. The permeate product stream consists of material that has been absorbed, then diffused, through a membrane. The rejected material will then form the retentate product stream. This process is described schematically by the figure below.

Pervaporation has established itself as one of the most promising membrane technologies in recent years. Pervaporation offers potential solutions in a wide range of applications from dehydration of organic compounds to waste water treatments (Lipnizki et al., 1999). In pervaporation, a saturated liquid feed is separated by a combination of permeation and

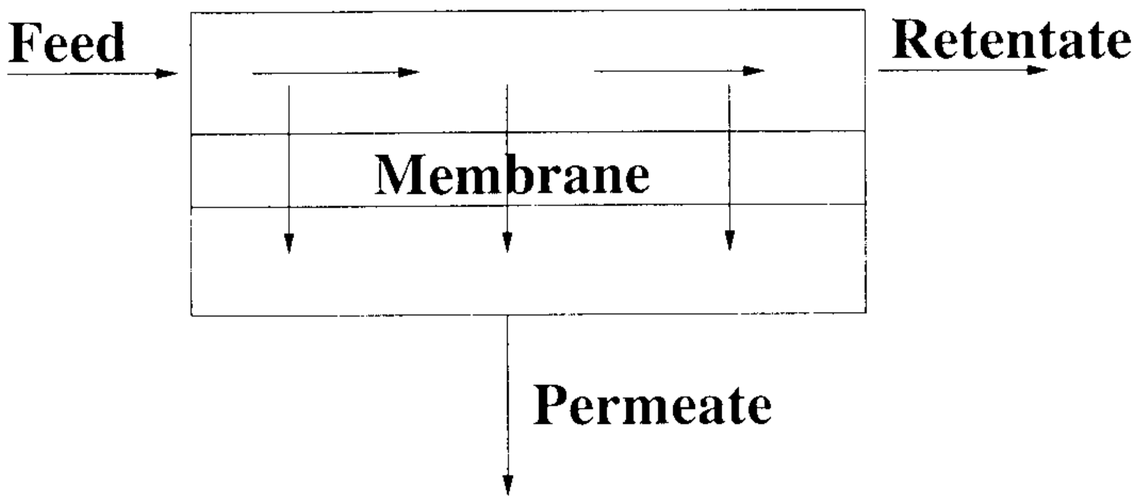

Figure 1.1: Schematic of a simple membrane separation

evaporation across a dense polymer membrane. The fugacity difference between liquid feed and vapour permeate acts as the driving force for the permeation process. In order to maintain an acceptable transport rate across the membrane, it is essential to keep the feed stream close to its saturation temperature because the permeation process across the membrane is highly temperature-dependent.

Vapour permeation is an alternative to pervaporation, where the feed stream enters as a saturated vapour which avoids the phase change across the membrane surface that happens in pervaporation. Furthermore, vapour permeation is less sensitive to concentration polarisation on the feed side of the membrane and membrane lifetime is expected to be longer than that of pervaporation due to the lower degree of membrane-swelling (Pettersen and Lien, 1995).

The decision of which membrane process to integrate into the hybrid distillation/membrane will depend on the mixture considered as well as the availability of a membrane process capable of performing the required separation duty. In this work, only pervaporation will be considered in the case studies. However, the proposed models and solution techniques can just as easily be used for other membrane processes.

1.4 Hybrid Distillation/Membrane Processes

As mentioned, several alternatives to current separation processes based on distillation have emerged in the past few years to overcome operational and environmental constraints. In particular hybrid distillation/membrane processes, consisting of combined distillation and membrane separation units, have received considerable attention due to the many potential advantages it can offer:

- Membrane units can easily be integrated into existing distillation processes with minimal process restructuring.
- Hybrid processes can separate azeotropic mixtures that are otherwise difficult to separate by conventional distillation processes.
- The addition of other components as entrainer (that is subsequently removed) is not required resulting in reduced costs and eliminated undesirable side effects.
- Higher product yield can be achieved using a hybrid process due to the high selectivity of membranes.
- Hybrid processes can cope better with distillation pressure variations (Lipnizki et al., 1999).

Consequently, hybrid processes offer opportunities for large energy savings of up to 60% reduction when compared to conventional azeotropic distillation systems as demonstrated by Guerreri (1992) and Van Hoof et al. (2004). Furthermore, hybrid processes can offer a 15-30% reduction in capital costs over a conventional distillation sequence (Kumar et al., 1992).

1.4.1 Industrial Applications of Hybrid Separation Processes

The potential applications of hybrid distillation/membrane processes generally cover all kinds of liquid mixtures in all concentration ranges (Lipnizki et al., 1999), although, hybrid

processes are more suited for azeotropic and close-boiling separations. Some examples are presented next.

Ethanol Production Process

The separation of ethanol from ethanol-water mixtures is a challenging process due to the azeotrope between water and ethanol. Tusel and Ballweg (1983) patented a process to dehydrate ethanol, where the proposed system featured a distillation column followed by two hydrophilic pervaporation membrane units. The first high flux-low selectivity membrane is fed from the column condenser drum with a primary task of splitting the azeotrope. This was followed by a second low flux-high selectivity membrane to act as a polishing step to produce the final top product ethanol with a concentration of 99.8%. Although the dehydration of high purity bioethanol can be performed in a similar fashion as that reported by Tusel and Ballweg (1983), no hybrid distillation/membrane processes has so far been reported in the open literature to investigate this.

Isopropanol Production Process

A combined pervaporation and distillation hybrid process was suggested by Binning and James (1958) for the production of isopropanol (IPA). The separation of a ternary isopropanol -ethanol-water mixture was reported to produce high purity IPA and a salable alcohol by-product of less than 0.5 wt% water. Their economical analysis revealed that the investment costs of the hybrid distillation/pervaporation were 31% lower than that of a two column azeotropic distillation process using hexane as an entrainer. The operating costs were reported to be reduced by 15%.

Benzene-Cyclohexane Production Process

A process for the separation of an equimolar benzene-cyclohexane mixture into 99.2 mol% cyclohexane and 99.5% benzene, was described by Rautenbach and Albrecht (1989). The process consisted of two extractive distillation columns using furfurol as carrier and a

benzene-philic pervaporation membrane unit. The first distillation column separated cyclohexane from a furfurol-benzene mixture while the second column recovered furfurol from the furfurol-benzene mixture. The pervaporation unit was then used to remove benzene from the cyclohexane-rich top product of the first distillation column to achieve a retentate of cyclohexane of the desired purity.

Methyl Tert-Butyl Ether Production Process

In the production of methyl tert-butyl ether (MTBE), non-reacted methanol from the reactor effluent forms azeotropes with both MTBE and C_4's. Conventionally, the reactor effluent is fed to a distillation column sequence that produces MTBE bottom product and a methanol-C_4's azeotropic mixture as a top product. The methanol is then separated by a water wash combined with molecular sieve separation or distillation. A hybrid distillation/pervaporation process consisting of a methanol-philic pervaporation unit and distillation was first proposed by Chen et al. (1988) with the aim to achieve a high purity MTBE product. It was found that the $TRIM^{TM}$ (Total Recovery Improvement for MTBE) process of Chen et al. (1988) was economically desirable as it could increase production by 5% and reduce investment costs by up to 20%.

Similarly, Kanji and Matsuo (1994) patented a process for the production of ether compounds with particular reference to MTBE. Their process consisted of an organophilic pervaporation membrane unit connected to the condenser outlet of a distillation column, however, no economical data were presented.

Hömmerich and Rautenbach (1998) conducted an economical analysis in order to compare the conventional Hülls MTBE production process (Obenaus and Droste, 1980) to their suggested alternatives of hybrid distillation/membrane process schemes. They concluded that 5.4-6% and 14-15.5% savings in capital and utility costs, respectively, could be achieved when hybrid processes are used instead.

Ethyl Tert-Butyl Ether Production Process

Ethyl tert-butyl ether (ETBE) is conventionally produced by a catalytic reaction of ethanol and isobutene in a process similar to that of MTBE. Streicher et al. (1995) proposed a hybrid process alternative to the conventional production process that included an ethanol-philic pervaporation membrane unit and distillation. They concluded that up to 60% savings in operating costs can be achieved when using hybrid distillation/pervaporation. Luo et al. (1997) has also suggested two other alternative processes for producing ETBE. Based on their first suggested layout, consisting of an organophilic pervaporation membrane to treat the top stream of the distillation column, it was concluded that ethanol recovery of 99.3% was achievable with the hybrid distillation/pervaporation instead of the significantly lower 55.2% recovery achieved when using the conventional production process. A different approach, however, was adopted by Yang and Goto (1997) when considering a reactive distillation column combined with a pervaporation unit to produce ETBE. Although they indicated that the proposed process was a more effective alternative to the conventional process, no economical evaluations of the potential was included.

1.4.2 Operation Modes

Hybrid distillation/membrane processes can be operated in both continuous and batch modes. Continuous mode is mostly employed for large production volumes whereas batch mode is better suited for high-value low-volume speciality chemicals. Batch mode offers many advantages over its continuous counterpart including its ability to cope better with different separation duties, tracing of products through batch production identity and lower cost for small scale and seasonal production.

1.4.3 Configurations

The configuration of hybrid distillation/membrane processes can be classified primarily by the position of the membrane unit relative to the distillation column and the destination of the membrane output streams. Furthermore, the distillation column operation mode, as well as the location of the feed, product and recycle streams, adds further dimensions to the possible configurations of hybrid distillation. Below, various column configurations considered in this research are defined.

Pre-Distillation Hybrid System

In this configuration, the membrane is placed before the distillation column to pretreat the feed stream for the distillation. The membrane unit permeate can then be fed to the rectifying section of the column while the retentate is fed to the stripping section as shown in Figure 1.2a. Another possibility is to collect pure retentate or permeate streams and direct the other stream into the appropriate column section (see Figures 1.2b). In all alternatives of this configuration, the bottom and top products from the distillation column are collected in product accumulators.

Post-Distillation Hybrid System

In a post-distillation hybrid system, the membrane unit is fed from the top or bottom stream of the distillation column where the main function of the membrane is to perform the final purification of the column product streams (see Figure 1.3). Depending on where the membrane unit is placed, the retentate or the permeate can then be recycled to the appropriate column section while the other stream flows directly into product accumulators.

Integrated Hybrid System

An integrated hybrid system is also known as a *parallel* hybrid system. In this configuration, the membrane is placed parallel to the distillation column where it is fed from a side stream from the distillation column. The membrane permeate or retentate can then be collected or recycled to a location in the column as shown in Figures 1.4a. Recycling membrane permeate and/or retentate streams to the column results in a fully integrated hybrid configuration. This is potentially advantageous to assist the distillation column in separating the desired mixture where the column is least effective, *i.e.* near the feed stream in the case of continuous distillation of azeotropic mixtures (see Figure 1.4b).

The addition of the membrane unit to the distillation column in a hybrid process present enormous possibilities in how the two units can be integrated and operated together. This will also add extra degrees of freedom which, if properly chosen, can further increase the potential of these processes.

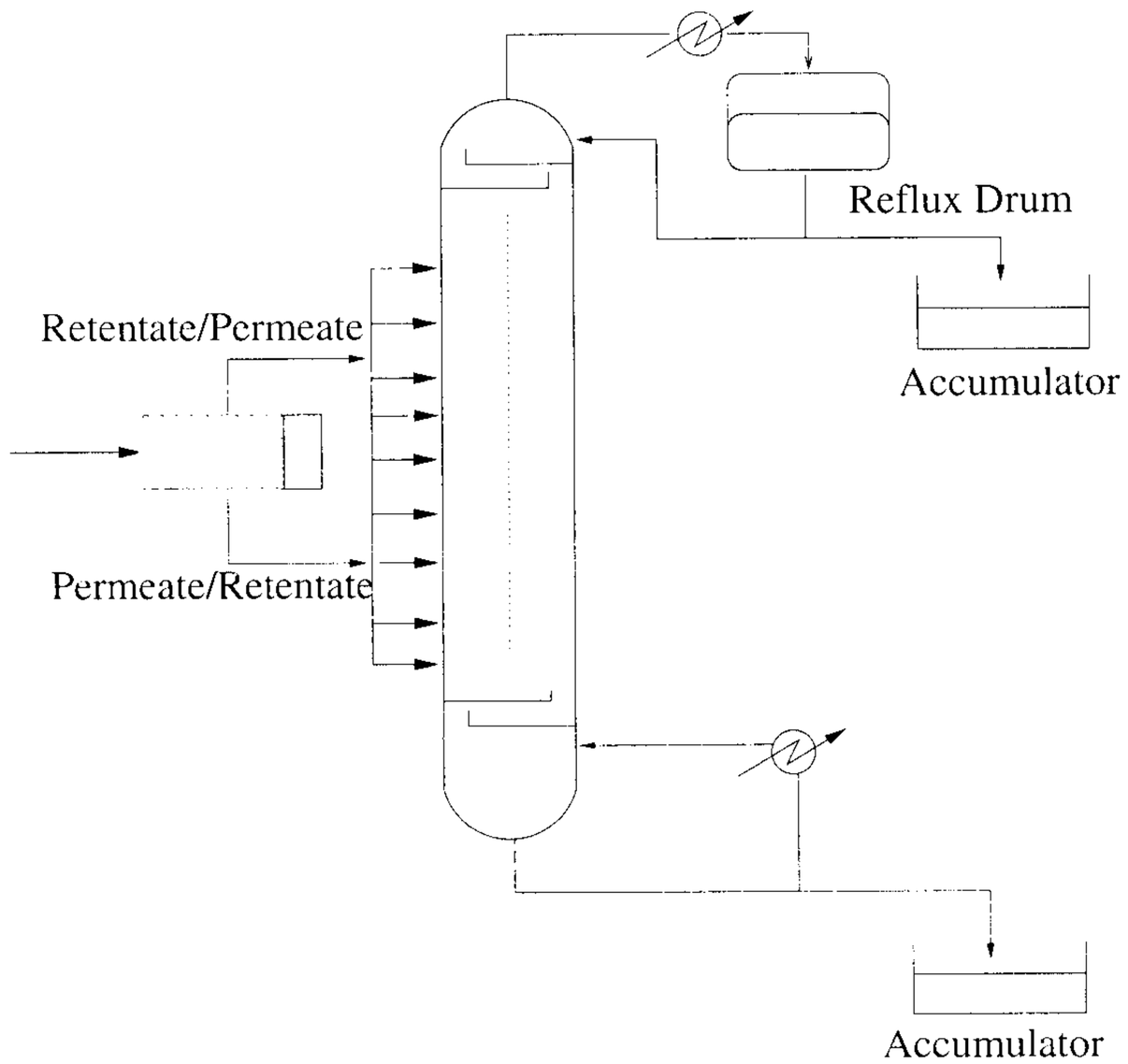

(a)

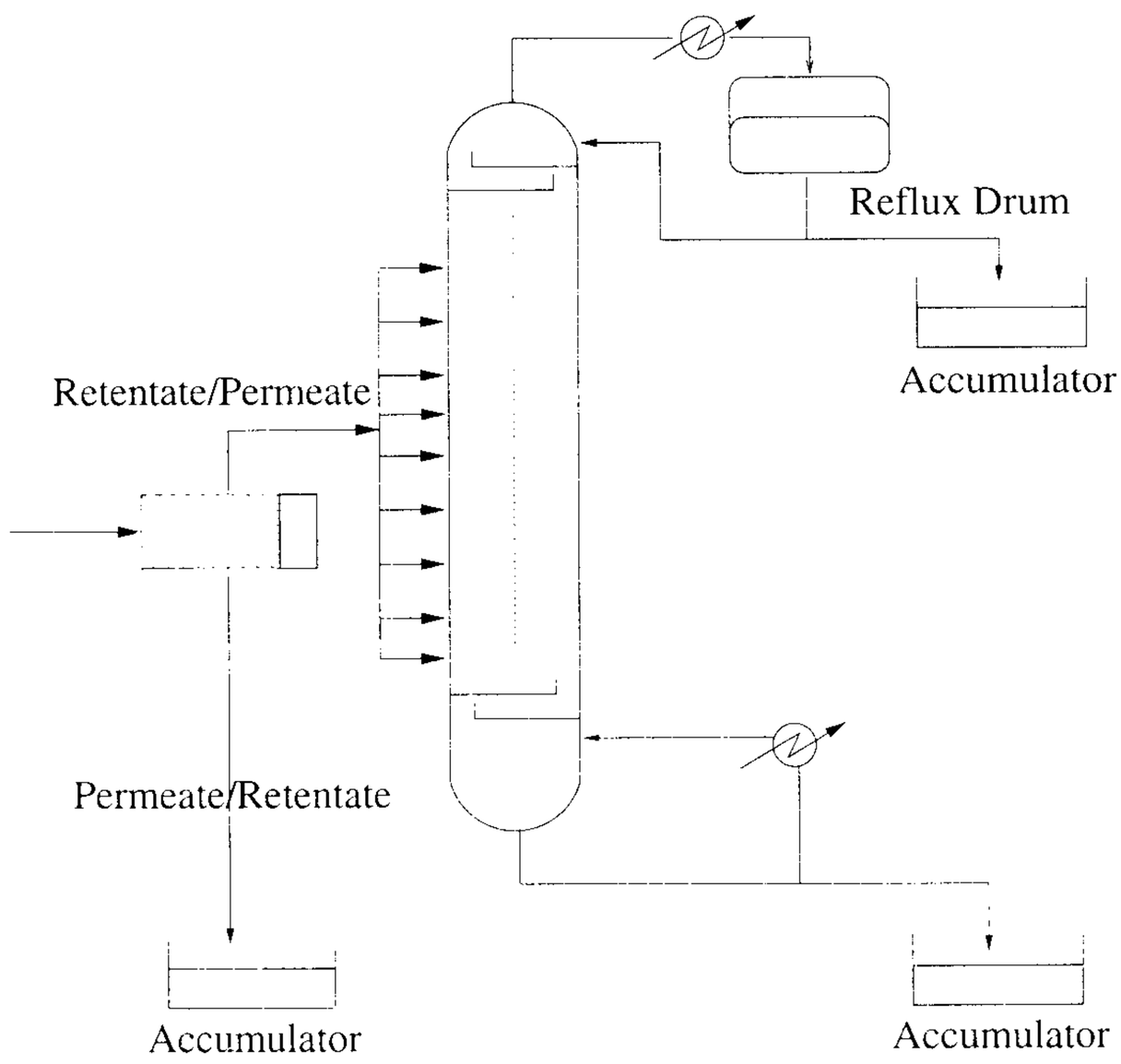

(b)

Figure 1.2: Pre-Distillation Hybrid Systems

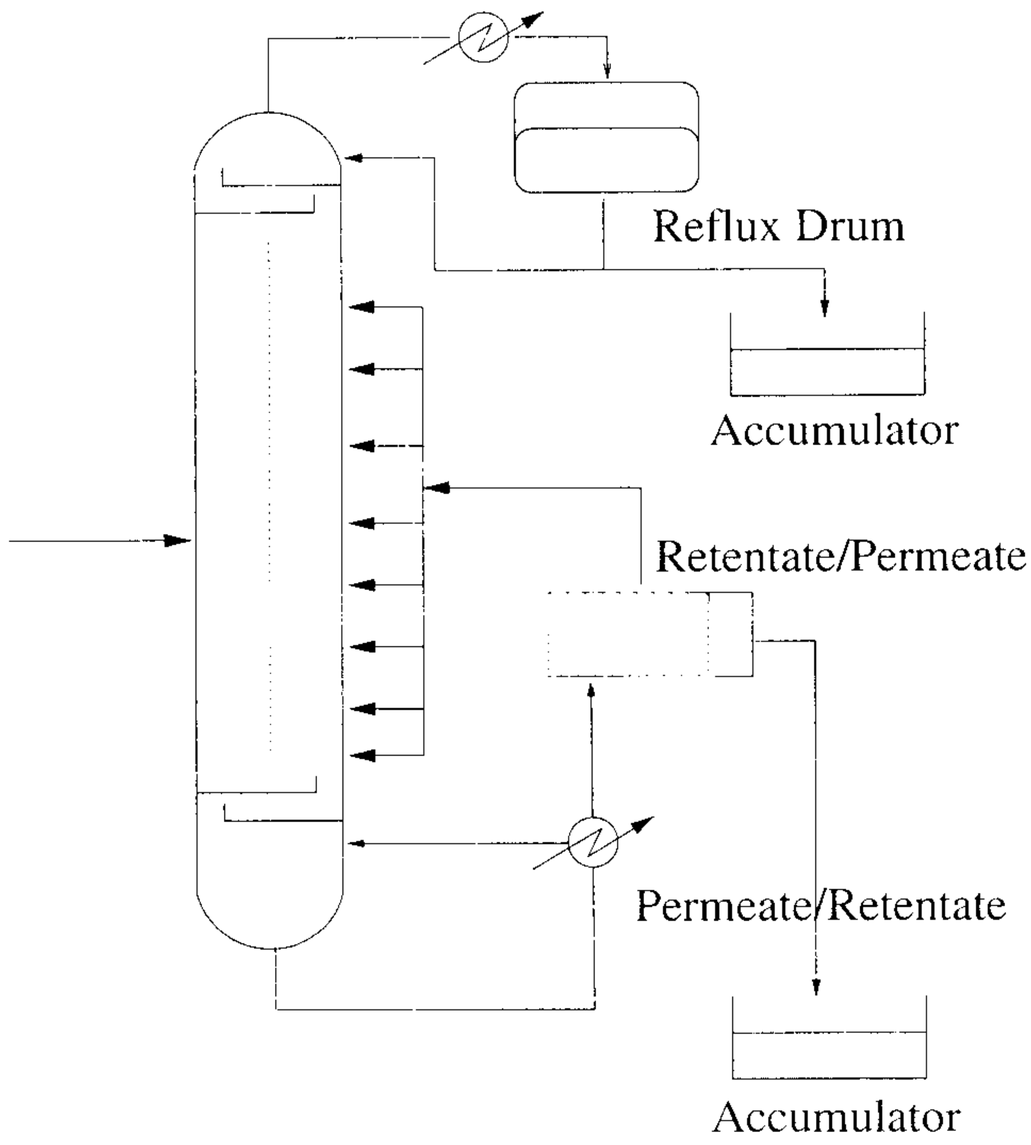

(a)

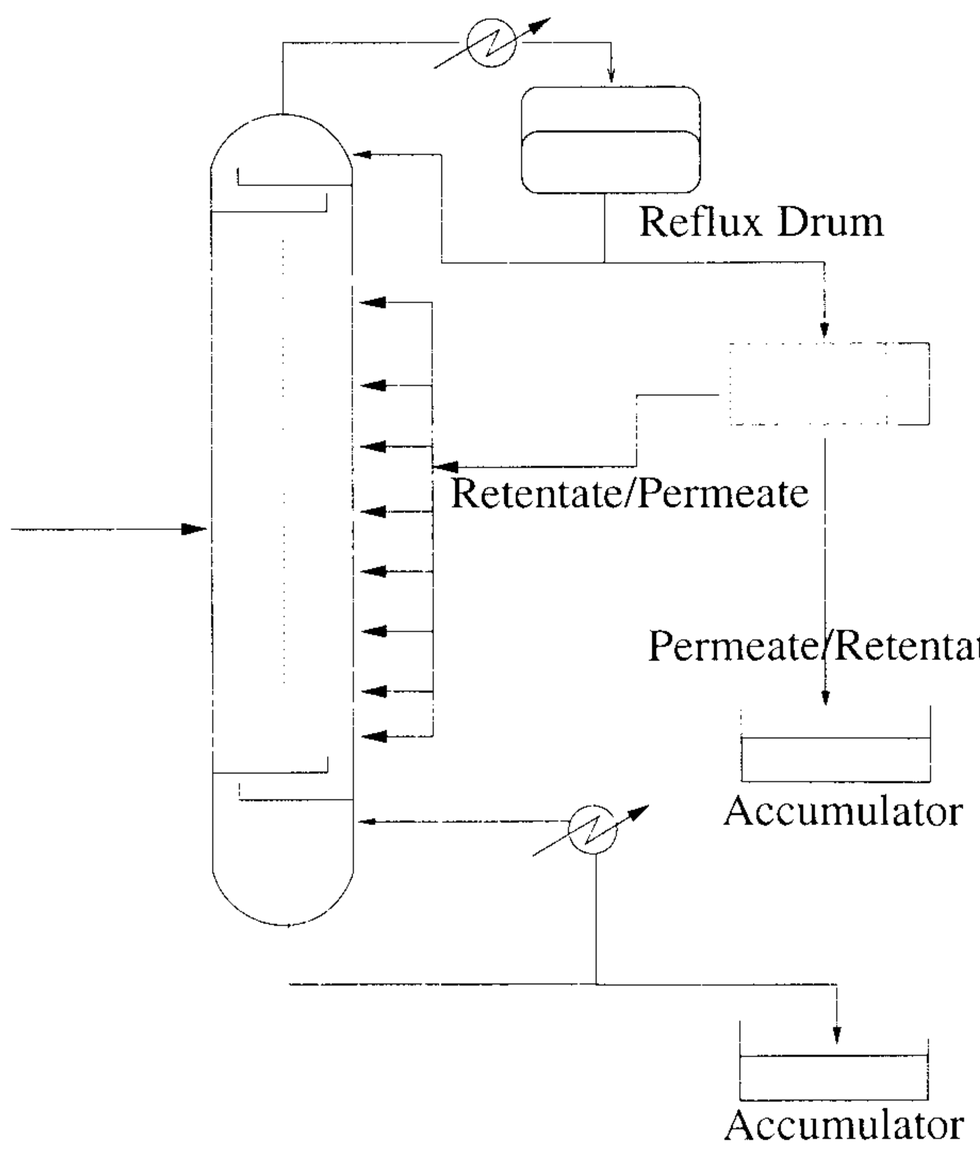

(b)

Figure 1.3: Post-Distillation Hybrid Systems

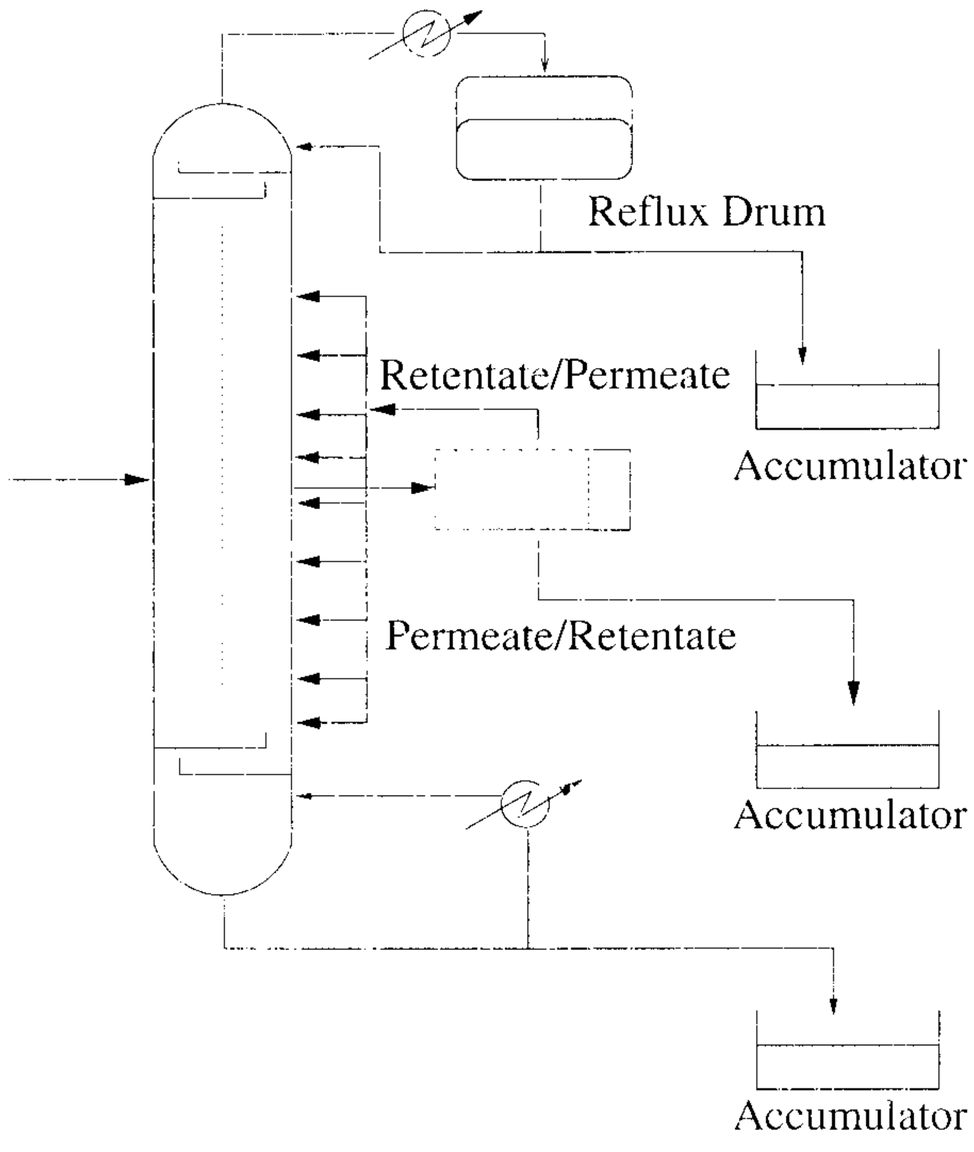

(a)

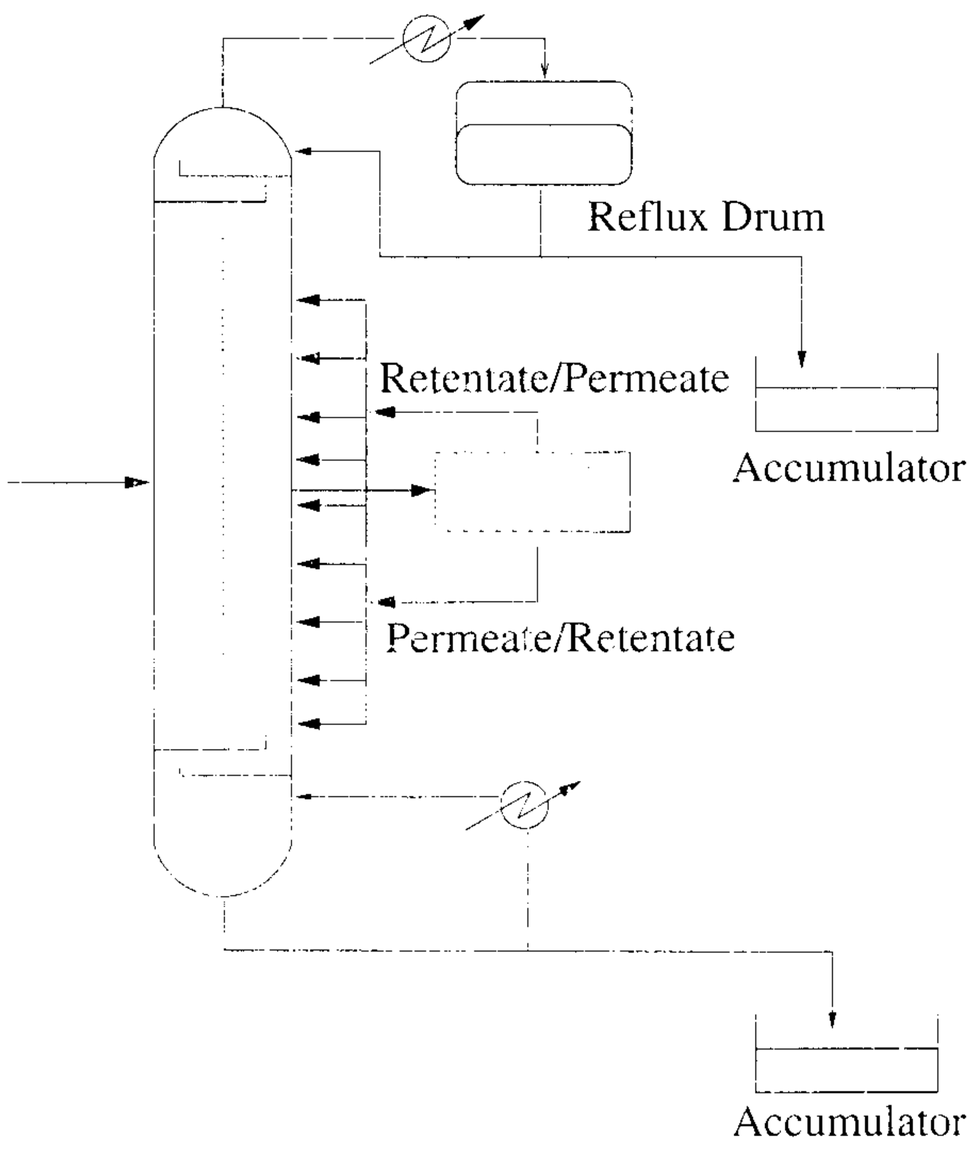

(b)

Figure 1.4: Integrated/Parallel Hybrid Systems

1.5 The Configuration, Design and Operation Problem

Hybrid distillation/pervaporation processes are inherently dynamic systems, especially when considered in a batch operation mode. Whether the unit is operated in batch or continuous mode, there exists other fundamental decision variables which need to be considered:

- Design Variables
  - Distillation column type (tray, packed, ...etc)
  - Distillation column dimensions
  - Membrane module type (hollow-fibre, spiral-wound, ..etc)
  - Membrane area per module
- Configurational Variables
  - Distillation column feed location(s)
  - Distillation product, offcut and side-stream withdrawal locations
  - Membrane location with respect to distillation column
  - Recycle stream locations
- Operation Variables
  - Operation mode (batch or continuous)
  - Distillation column pressure
  - Membrane permeate pressure
  - Heating/Cooling duties
  - Side stream and product flowrates
  - Reflux and recycle ratios

The problem is to determine not only the best design and operation of a suitable separation process, but also which separation technique to use and, if considering a hybrid system, how the two units should be integrated. The problem statement of this work is therefore: to determine the configuration, design and operation of the most suitable process with respect to given objective(s) for the separation of specified mixtures into their components to specified degrees of purity.

1.6 Motivation and Objectives

Hybrid distillation/pervaporation processes are becoming more important due to the increased industrial production of high value-added and low-volume fine-and speciality chemicals which are commonly difficult to separate. The efficiency, reduced environmental impact and cost-effectiveness of hybrid processes in separating these difficult mixtures has increased their popularity as a means to meet current and future industrial production targets, environmental regulations and overall market leadership.

The general aims of this work are to investigate the optimal design and operation policies of hybrid distillation/membrane processes by:

- Developing suitable mathematical models and applying appropriate optimisation methodologies for the determination of the most profitable configuration, design and operation for a number of case studies, and
- To investigate the optimality in order to draw conclusions that may possibly lead to specific or general guidelines for the design and operation of hybrid distillation/membrane systems.

1.7 Outline of the Thesis

The next chapter in this thesis discusses work presented in the open literature on these processes and their modelling, synthesis and optimisation. The studies surveyed are then

summarised at the end of the chapter where the research statement of this thesis is also given.

The third chapter considers the simultaneous optimisation of configuration, design and operation of hybrid batch distillation/pervaporation processes by considering all possible process structures. This study is the first where the batch operation of these processes has been studied. The overall problem is formulated as a mixed integer dynamic optimisation (MIDO) problem. The optimisation strategy comprises of an overall economics index that encompasses capital investment, operating costs and production revenues. Furthermore, rigorous dynamic models developed from first principles for distillation and pervaporation are used. Based on the optimisation results, it is shown that a significant increase in overall profitability can be achieved when hybrid configuration is used instead of conventional distillation or pervaporation processes.

The fourth chapter deals with the application of the simultaneous optimisation methodology proposed in the third chapter to continuous hybrid distillation/pervaporation processes. In this study, a number of unexplored degrees of freedom has been addressed. It is again demonstrated that hybrid process can increase overall profitability when compared to distillation alone. Furthermore, the annualised capital and operating costs are found to be significantly reduced for the continuous hybrid process.

The final chapter of the thesis considers the simultaneous multi-criteria optimisation of design and operation of batch distillation and hybrid distillation/pervaporation processes for the first time. The performance of these processes depends on a number of different criteria that are often conflicting (*e.g.* revenue versus cost or profit versus environmental impact), therefore an effective optimisation of such systems requires the consideration of multi-criteria approaches to effectively evaluate and optimise the performance, whilst still meeting the desired separation requirements. The overall problem is formulated as a multi-objective mixed integer dynamic optimisation (MO-MIDO) problem. The optimisation strategy comprises of indices that reflect capital investment and operational energy consumption. A novel genetic algorithm based multi-objective framework that can be applied to multi-dimensional engineering problems is proposed. The proposed algorithm

is found to successfully handle the multi-objective nature of the simultaneous design and operation of batch hybrid distillation/pervaporation processes.

1.8 Main Contributions of This Thesis

The following summarises the main contributions of this thesis:

- A process superstructure encompassing distillation, pervaporation and hybrid thereof was developed and implemented for the optimisation and synthesis of such processes.
- Accurate costing correlations were developed for use in the optimisation and synthesis procedures.
- Rigorous studies were conducted for the simultaneous optimisation of batch hybrid processes configuration, design and operation using different case studies.
- Continuous hybrid processes were studied using the optimal synthesis procedure to explore the majority of degrees of freedom afforded by these processes.
- A multi-criteria optimisation procedure was proposed to explore various trade-offs in the objective functions considered.
- Detailed studies to investigate the bi-criteria optimisation of configuration, design and operation of batch distillation and batch hybrid processes using different case studies were conducted.

Chapter 2

Literature Review

This chapter outlines work that has previously been undertaken within the area of modelling and design of hybrid distillation/membrane separation processes. It is found that work on the modelling and optimisation of hybrid systems has so far been restricted to simple models and no work has been done on the control of such columns. It is also noted that batch operation of hybrid distillation/membrane processes has not yet been explored.

2.1 Introduction

Hybrid separation technologies have recently emerged as some of the most promising alternatives to existing separation techniques, offering the advantages of higher product yield, lower energy consumption, lower operating costs and hence an overall increase in profitability. One of these alternatives is to combine distillation with different separation technologies, such as membrane processes. The work conducted so far in the area of hybrid distillation/membrane separation processes is summarised in Table 2.1 at the end of this chapter and will now be discussed in more detail.

2.2 Modelling and Design of Hybrid Distillation/Membrane Processes

The suggestion of Binning and James (1958) to use a distillation/pervaporation hybrid process for isopropanol-ethanol dehydration, marks the first mention in the literature of such processes. It was not, however, until the late 1980s that this was regarded as an attractive alternative for separation of difficult mixtures.

Chen et al. (1988) patented a hybrid distillation/membrane process for an improved separation of alcohols from ethers (MTBE and TAME) in etherification processes. Different separation layouts were suggested; the first layout featured a pre-treatment of the distillation feed stream to reduce the methanol concentration from about 5 to 2 wt% by using an organophilic pervaporation unit. The ethanol-rich permeate was then recycled back to the reaction section of the etherification process. The recycle stream was reported to result in a 5% increase in MTBE conversion per reaction cycle. A methanol recovery unit was placed after the distillation to recycle processed methanol to the reacting section of the process. In the second layout, they suggested the use of the pervaporation unit in conjunction with the distillation unit, with a liquid side draw feed from the distillation column, and once again a methanol recovery unit was included after the distillation. An economical comparison indicated that by integrating such technologies, investment costs could be reduced by 10-15%. In addition, a 5% increase in production capacity could be achieved when compared to conventional two stage reactor-de-butaniser MTBE production processes.

Kanji and Matsuo (1994) patented a chemical process for producing MTBE. The process reactor effluent was fed into a distillation column and the top azeotropic mixture from the distillation column was liquefied and then fed into a pervaporation unit equipped with an organophilic membrane. the methanol rich stream permeated through the pervaporation unit and was then recycled and injected in the reactor inlet stream. The patented process was described to be capable of producing MTBE of 98.6 wt% purity as the bottom stream of the hybrid distillation column.

Pettersen and Lien (1995) were the first to conduct parametric studies addressing the trade-off issues related to integrating vapour permeation membranes in a continuous post-distillation hybrid system for an ethanol dehydration process. Their studies were based on an algebraic design model for the vapour permeation system which was valid for binary mixtures and was based on a black-box representation of the transport properties across the membrane (selectivity). The design model presented, estimated the required membrane area and product recovery through a step-wise calculation procedures to meet a specified product purity. The parametric studies of Pettersen and Lien (1995) illustrated how the membrane selectivity influenced the performance of the hybrid and how the required membrane area was affected by the composition and pressure in the membrane feed.

Pettersen and Lien (1995) concluded that with increased membrane selectivity, an increased ethanol product purity and recovery was observed. With respect to the effects of the membrane feed composition and pressure on the required membrane area, they found that by reducing the feed water contents from 10 to 5 wt% water, the required membrane area could be reduced three folds. A 50% reduction in membrane area could also be achieved if the feed pressure was increased to 2 bar (from 1.15 bar). It should be noted that their model assumed no temperature changes in the membrane model and is therefore not suitable for use in pervaporation systems where significant temperature phase changes occur. Furthermore, the model is only accurate within 20% of the predicted membrane area. No details of the distillation system model or indeed how the model could be adopted for the separation of other mixtures were presented.

A McCabe-Thiele based approach was introduced by Stephan et al. (1995) to analyse different distillation/vapour permeation hybrid configurations (post-, pre- or integrated) in order to find short-cut methods to determine appropriate operating conditions for each configuration. Their studies were based on a steady state model which predicts the required number of column trays for a particular set of operating conditions. The operating

conditions resulting in minimum membrane area and number of trays was considered to be the optimal. The method presented by Stephan et al. (1995) investigated the separation of a propane/propylene mixture and consisted of the following steps:

1. For a given set of operating parameters (membrane area and feed composition), calculate the membrane stream flowrates and compositions from a total mass balance,

2. Determine the column sections, *i.e.* number of trays between membrane feed, permeate, retentate, column top and bottom streams from the membrane streams (feed, retentate, permeate) compositions and

3. Solve the mass balances for the column sections above and construct a McCabe-Thiele diagram or solve iteratively using Smoker's equation (Smoker, 1938), to find the number of column trays required.

The approach proposed by Stephan et al. (1995) led to a decoupling of the membrane system from the distillation column, and hence the two models were solved separately, *i.e.* the membrane model had to be solved first, then the distillation model. It should also be noted that their studies investigated the use of vapour permeation membranes and, as an analytical solution (McCabe-Thiele) is not attainable using saturated vapour streams, they made the assumption that all membrane streams are of saturated liquids. The assumptions made and the decoupling of the models, will of course decrease the robustness and accuracy of the solution obtained.

Pettersen et al. (1996) extended the work of Pettersen and Lien (1995) and Stephan et al. (1995) by considering a theoretical comparison of three configurations of hybrid membrane/vapour permeation processes for the separation of propylene and propane mixtures. They described the performance of the distillation column using the design model presented by Smoker (1938) to obtain the minimum number of column trays with the assumption of constant relative volatility and constant molar overflow in each section of the column. They described the transport of propane and propylene across a Nafion/Silver

based membrane by a dual-mode transport model which was first introduced by Ward (1970) and further developed by Shindo et al. (1985). Furthermore, all streams to the membrane were assumed to be saturated vapour and negligible pressure drop in the distillation column was also assumed. The binary model for the hybrid distillation/vapour permeation was then implemented in C++ to solve the two units *separately* in the same fashion as that of Stephan et al. (1995). Their results showed that if a membrane was placed parallel to the column, then the *optimal* (with respect to minimum membrane area and column trays) position for the membrane feed stream was close to the column feed plate, which represents a potential pinch point in the column. The propylene mole fraction of this configuration was found to be generally close to the optimal membrane cut rate (permeate to feed ratio). The comparison between different hybrid distillation system configurations also indicated that placing the membrane in parallel, or at the bottom stream of the hybrid distillation column, gave the best operational performance in terms of compressor duty and membrane area.

Luo et al. (1997) featured two different alternative process layouts for the processing of reactor effluent in the production of ETBE. In their first layout, the reactor outlet stream containing 10 wt% ethanol was fed to the distillation column and the overhead product stream was processed with a pervaporation unit furnished with a cellulose acetate organophilic membrane. The retentate was fed back to the distillation feed stream and the permeate containing 99.34 wt% ethanol was recycled to the reactor. In the second layout, the membrane separation was performed first. The reactor effluent containing 30% wt was introduced to the pervaporation feed stream to be mixed and processed along with the top azeotropic mixture, the retentate was recycled to the distillation column feed position and the ethanol-rich permeate was returned to the reactor. The ETBE product in both layouts was collected at the bottom of the distillation column. They reported that for the same feed and separation requirements, the ethanol recovery of 99.34 wt% using the first hybrid distillation layout was significantly higher than a 55.2 wt% ethanol recovery using the same distillation column on its own. The simulation was performed

with the assumption that the distillation feed was a binary mixture of ETBE and ethanol and hence the pervaporation model used is only valid for these components.

Lipnizki et al. (1999) reviewed most of the applications of hybrid processes involving membranes and distillation columns. They also defined a hybrid process as a "process package consisting of generally different unit operations, which are interlinked and optimised to achieve a predefined task". Lipnizki et al. (1999) suggested that the costs of the hybrid distillation/membrane processes patented by Chen et al. (1988) could further be decreased by minimising, or even eliminating, any methanol recovery units.

Pressly and Ng (1998) presented a screening classification scheme for distillation/ membrane hybrids for the separation of a binary mixture based on configuration complexity and material phase behaviour. They presented schematics for different process alternatives to suit particular separation types (*i.e.* azeotropic, tangent-pinch or close boiling binary mixtures). Pressly and Ng (1998) also presented a break-even analysis based on calculating the maximum cost of the membrane for the hybrid process for it to be a viable economical alternative. The break-even cost of the membrane is the difference between the designed hybrid process cost and that of a conventional distillation process that meet the specified separation requirements. The cost analysis was conducted using the costing procedure outlined by Douglas (1988).

The hybrid process design was determined by first solving the overall mass balance around the membrane unit for a given separation factor and membrane cut rate (ratio of permeate to feed flowrate). The distillation model was then solved based on the membrane unit mass balance to obtain the minimum number of required trays. The assumption of constant molar overflow was retained but no details of how the minimum number of trays is calculated were given. Although the method proposed by Pressly and Ng (1998) can be useful during the initial design and screening stages of hybrid process design, no directions were given on its applicability for multi-component hybrid systems.

Hömmerich and Rautenbach (1998) demonstrated the economical potential of integrating pervaporation or vapour permeation membranes into existing process designs. A process licenced by Huels AG (Obenaus and Droste, 1980) with a maximum annual capacity of 130 ktons MTBE was chosen for comparative process analysis. The purification part of the Huels system processes a stream of MTBE, methanol and $C_4's$ (from process reactors) through a sequence of two distillation columns. The first column produces mainly methanol as the top product and feeds the bottom stream to the second column. The second column produces pure MTBE as the bottom products and recycles the top product to the reaction cascade of the process.

Hömmerich and Rautenbach (1998) reported that placing the membrane unit at the bottom stream for MTBE enrichment was not economically favourable due to the very low driving force which would result in an enormous required membrane area to achieve the final product quality. They also underlined the need for membrane development to accommodate higher feed temperatures allowing higher fluxes. However, operating costs may increase as a results of preheating and pressurising of feed to ensure a liquid phase in the case of pervaporation. It should also be noted that inorganic zeolite membranes for vapour permeation have recently evolved as an interesting alternative (Kita et al., 1997).

The economical analysis of Hömmerich and Rautenbach (1998) indicated that a modified hybrid pervaporation-distillation process could save up to 5.4% of capital costs and 15.5% of utility costs when compared to the original Huels process. A further 6% of the capital costs and 14% of the utility costs could be realised if using a vapour permeation instead of the pervaporation membrane.

The analysis was conducted using the steady state simulation software Aspen Plus. Although no details of the membrane model were given, it was indicated that differential mass and energy balances of the membrane were linked to Aspen Plus through a Fortran routine.

Bausa and Marquardt (2000) presented shortcut methods for the design of hybrid processes consisting of pervaporation and distillation units. They utilised developed methods

by Bausa et al. (1998) and Watzdorf et al. (1999) to determine the minimum reflux ratio for simple and complex column arrangements for the distillation unit and a minimum membrane area characterisation of the pervaporation unit. The methodology was demonstrated by two examples of hybrid pervaporation-distillation processes; the purification of methyl tert-butyl ether (MTBE) and ethanol dehydration. The rectification body method (RBM) proposed by Bausa and Marquardt (2000) is, however, based on a geometrical analysis of plate-to-plate profiles and pinch curves, therefore graphical representation of mixtures with four, five or more components is complex and can hardly be visualised. Another limitation of the technique is the use of a linear approximation for the curved plate-to-plate trajectories, thus reducing the accuracy although also reducing the computational time.

In their MTBE purification example, Bausa and Marquardt (2000) concluded that a stripping sidedraw hybrid membrane-distillation process configuration seems to be the most favourable compared with the Huels process (Obenaus and Droste, 1980), as it resulted in a minimum membrane area requirement as well as reduced investment and energy costs involved. However, they found that the membrane feed temperature in this configuration (112 °C) needed to be higher than the allowable limit of the plasma-polymerised membrane used (T_{max} = 100 °C), and hence suggested the use of more temperature resistant inorganic zeolite membranes. It should be noted that similar shortcut techniques were also developed by Levy et al. (1985) for non-ideal distillation systems. However, their methods, similarly to that developed by Bausa and Marquardt (2000), require the calculation of many trajectories and can not easily be automated.

González and Ortiz (2001) presented a more rigorous analysis of hybrid distillation/ membrane systems than previous authors. They analysed the azeotropic separation of alcohol-ether through simulation studies. Their distillation model included mass and energy balances on each stage, coupled with vapour-liquid equilibrium relationships, that were developed with the assumptions of (i) thermal and thermodynamic equilibrium between phases at each stage, (ii) perfect mixing in both phases at each stage, (iii) conservation of enthalpy based energy balance and (iv) no chemical reaction.

The mathematical membrane model featured a plate-and-frame pervaporation module design incorporating steady state mass and energy balances by considering: (i) plug-flow for the feed liquid stream, (ii) perfect mixing in the permeated vapour, (iii) 100 % efficiency in the module, (iv) negligible pressure drop within the module, (v) negligible polarisation effects and (vi) negligible heat losses.

The model equations were solved using gPROMS (PSE, 2001) to simulate the hybrid process for different process configurations and parameters. They assessed the merit of the different configurations by calculating the minimal required membrane area to perform the desired separation duty. Their simulation studies indicated that an integrated parallel configuration similar to that shown in Figure 1.4 resulted in a minimum membrane area whether the specified main product was bottom or overhead from the column.

Szitkai et al. (2002) presented the first optimisation studies of hybrid dehydration systems using mixed integer nonlinear programming (MINLP) models. They presented a superstructure for the hybrid system consisting of a distillation column connected to a membrane train of which the retentate was collected and fed back to the column feed stream. They adopted an algebraic distillation column superstructure proposed by Viswanathan and Grossmann (1993) while the pervaporation membrane process model was numerically integrated first (for potential optimisation variables values) then imported as an algebraic model into GAMS where the optimisation problem was then solved. Furthermore, the optimisation objective was to minimise the annual operating costs of a single, post-distillation, hybrid configuration for the separation of ethanol-water systems by considering the number of trays, reflux ratio, number of membrane modules as the optimisation variables. It should be noted that only simple steady-state models of a post-distillation hybrid were used in the approach of Szitkai et al. (2002) and these may not be suitable for rigorous optimisation studies such as those presented in Chapter 4 and 5. They concluded that a 12% saving in total annual costs could be achieved when considering an optimised hybrid system compared to an existing process.

Eliceche et al. (2002) carried out optimisation studies of operating conditions for an azeotropic distillation column in a hybrid distillation/pervaporation system. They implemented models developed by González and Ortiz (2001) in solving the optimisation problem. The column reflux ratio, side draw and product flow rates and column pressure were optimised to achieve minimum operating costs. Optimisation of the membrane operating parameters (*e.g.* permeate pressure, retentate recycle ratio) were not considered. The optimisation problem was solved using the HYSYS optimiser where a Sequential Quadratic Programming (SQP) technique was employed. They concluded that the optimum operation conditions could result in a 9.7% reduction in operating costs when compared to an un-optimised base case.

Fahmy et al. (2002) investigated the integration of steam jet ejectors into hybrid dehydration processes. Jet ejectors can potentially replace the common condensation/vacuuming technique to lower pressure on the membrane permeate side in order to achieve the required driving force for the mass transfer across the membrane. A case study was carried out for the dehydration of isopropanol in a distillation-pervaporation-distillation hybrid process. It was found that the use of steam-jet ejectors was more favourable at relatively high permeate pressures where the steam requirements were relatively low. However, it should be noted that due to the exponential increase in the steam requirements (Fahmy et al., 2002), consequently the operating costs make the ejectors less attractive for lower vacuum pressures.

Lu et al. (2002) presented a design of a hybrid process for the separation of etherified C4 effluent to qualified methanol, MTBE and C4 streams. The process design featured a cellulose acetate/polyacrylonitrile pervaporation module side-connected with a distillation column in the rectifying section. The membrane was used to permeate a methanol-rich stream that could be recycled back to the reactor. They found that in order to improve the hybrid process operation, the methanol concentration of the pervaporation retentate needed to be reasonably high (0.025 mole fraction). It was also reported that 15-35%

membrane area could be saved if the pervaporation module was operated in a plug flow rather than a perfect mixing mode.

Aiouache and Goto (2003) investigated the etherification process of tert-amyl alcohol (TAA) through experimental analysis of a reactive distillation column inserted with a zeolite pervaporation membrane tube. Their experimental tests showed that temperature had a positive effect on the membrane separation factor and if separate component feeds were used, such as ethanol at the top of the column reactive section and TAA in the middle part of the column, the reaction would favour the formation of tert-amyl ethyl ether rather than that of tert-amyl alcohol.

Kookos (2003) proposed a methodology for the structural and parametric optimisation of continuous hybrid separation systems. He described the superstructure of the hybrid process using a simplified steady-state mathematical model where it was assumed that all streams taken from, or returned to, the distillation column were vapour streams. The methodology is therefore not suitable for other membrane processes, such as pervaporation, or for dynamic systems, such as batch processes. Kookos (2003) outlined that the hybrid systems can potentially reduce the operating costs by 22% if operated at optimum conditions. Kookos (2003) also proposed the use of hybrid process superstructures, but his work only allowed for the optimisation of the hybrid process and therefore exploring either distillation or pervaporation alone as the potentially best separation process, is not possible.

Van Hoof et al. (2004) compared the economics of various processes to separate a mixture of IPA and water (50/50 wt %) to a final IPA concentration of 99.5 wt%. Their comparative studies included three cases and featured (i) azeotropic distillation, (ii) hybrid distillation-pervaporation for both polymeric and ceramic membrane configurations and (iii) hybrid distillation-pervaporation-distillation for both polymeric and ceramic membrane configuration. They concluded that the distillation-pervaporation hybrid process

using ceramic zeolite membranes (Mitsui, 2005) was the most interesting among the considered alternatives from an economic point of view, and can lead to 50% savings in total costs compared to conventional azeotropic distillation.

Daviou et al. (2004) extended the work of Eliceche et al. (2002) to optimise the pervaporation portion of a hybrid distillation/pervaporation system. They considered minimising the total cost of the hybrid systems by optimising the column reflux ratio, side and bottom stream flowrates as well as the composition of the retentate stream. It is interesting to note that they treated the composition of the retentate stream as an optimisation variable rather than a specified design requirement in determining the required membrane area. This will avoid the optimisation of integer variables (*e.g.* number of modules to give the required membrane area) and hence simplifies the optimisation problem. The SQP HYSYS optimiser was used for the optimal separation of MTBE/methanol/C_4 mixtures. Daviou et al. (2004) reported that a 30% reduction in costs could be achieved compared to the base case design.

Fontalvo et al. (2005) presented simulation studies to compare the pervaporation and vapour permeation systems when integrated in a hybrid distillation/membrane process for the dehydration of acetonitrile (ACN). They used Aspen Plus to simulate the distillation column while solving the membrane model in a Matlab subroutine. The membrane model used was based on a constant membrane separation factor. They concluded that a hybrid process with vapour permeation was preferred when the membrane was used to overcome the ACN azeotrope, whereas pervaporation was more economical when the membrane was used to remove water below the azeotropic point.

Recently, Kreis and Górak (2006) analysed an integrated hybrid process similar to those shown in Figure 1.4 for the separation of an acetone-isopropanol-water mixture into pure components. They investigated the influence of operational parameters (heat duty and side

stream flowrate) on the dehydration rate for a pilot plant process and on the operational costs for an industrial scale process. A rate based model for the distillation column developed by Klöker et al. (2005) was featured while models of various complexities for the membrane unit were considered for analysis. Kreis and Górak (2006) indicated that approximately 98% of water can be removed (for the pilot-plant process scale) within a wide operating range for the heat duties and side stream flowrate. For an industrial scale process, they found that the lowest operational costs were localised in the region of the low heat duties and high side stream flowrates.

Authors	Process*	Application	Model	Optimisation	Approach	Experimental
Chen et al. (1988)	D-PV	MTBE/TAME	N/A	×	Design	×
Kanji and Matsuo (1994)	D-PV	MTBE	N/A	×	Design	×
Pettersen and Lien (1995)	D-VP	Methylamine	Unspecified	×	Procedural	√
Stephan et al. (1995)	D-VP	Propane-Propylene	Smoker's equation	×	McCabe-Thiele	√
Pettersen et al. (1996)	D-VP	Propane-Propylene	Smoker's equation	×	Simulations	√
Luo et al. (1997)	D-PV	Ethanol/ETBE	Aspen Plus	×	Simulations	√
Pressly and Ng (1998)	D-PV & D-VP	Ethanol	Unspecified	×	Classifications	√
Hömmerich and Rautenbach (1998)	D-PV & D-VP	MTBE	Aspen Plus	×	Simulations	√
Bausa and Marquardt (2000)	D-PV	Ethanol/MTBE	RBM	×	Graphical	×
González and Ortiz (2001)	D-PV	Ether	Equilibrium	×	Simulations	√
Szitkai et al. (2002)	D-PV	Ethanol	Equilibrium	√	MINLP	√
Lu et al. (2002)	D-PV	MTBE	Unspecified	×	Simulations	√
Eliceche et al. (2002)	D-PV	MTBE	Equilibrium	√	NLP	√
Fahmy et al. (2002)	D-PV & D-VP	IPA	Unspecified	×	Jet Ejectors	×
Aiouache and Goto (2003)	RE-D-PV	TAA	N/A	×	Experimental	√
Kookos (2003)	D-VP	Propane-Propylene	Equilibrium	√	MINLP	√
Van Hoof et al. (2004)	D-PV	IPA	Aspen Plus	×	Economical	√
Daviou et al. (2004)	D-PV	MTBE	Equilibrium	√	NLP	√
Fontalvo et al. (2005)	D-PV & D-VP	ACN	Aspen Plus	×	Simulations	×
Kreis and Górak (2006)	D-PV	Acetone-IPA	Rate	×	Simulations	√

* Distillation = D, Reactive = RE, Pervaporation = PV, Vapour permeation VP

Table 2.1: Summary of hybrid distillation literature surveyed.

2.3 Summary and Research Statement

The literature review conducted in this chapter summarises the work done on design, modelling and optimisation of hybrid distillation/membrane processes. The details, assumption and limitations of the studies reviewed were highlighted.

It was noted that the work conducted in the modelling of hybrid distillation/membrane systems has begun to focus more on advance modelling techniques. The optimisation work, however, has either made use of only simple models or considered a limited number of the optimisation degree of freedoms afforded by these processes. Furthermore, no work on batch operation or controllabity of these processes, has been conducted.

Most of the work undertaken on hybrid separation systems as described in this chapter has so far focussed on the design of such systems with some work on modelling and optimisation. The majority of the work presented in the literature contained some form of comparative studies to conventional distillation processes. This plays an important role in highlighting the benefits of such novel technologies for them to be widely accepted as viable and cost effective separation alternatives. While previous work has demonstrated that hybrid systems can lead to cost savings, it is noted that the extent of the savings reported differ considerably.

The simulation studies of hybrid distillation/membrane processes conducted in some work (*e.g.* Pettersen and Lien (1995) and González and Ortiz (2001)) help to aid the fundamental understanding of the theoretical flexibility, as well as limitations, of these processes compared to existing technologies. Other experimental studies (*e.g.* Kreis and Górak (2006)), were conducted to help verify the simulation studies and to test the practical viability of these systems.

Another area of research explored was the optimisation of design and operation of hybrid systems. However, most of this work was confined to simple process models or treated design and operation of the hybrid in isolation.

The main aim of this project is to conduct a more comprehensive comparative studies based on optimisation which considers not only the hybrid systems, but also its constituent dis-

tillation and pervaporation processes. The *simultaneous* single and multi-objective optimisation of the process configuration, design and operation using a processes superstructure will be investigated for the first time in this work (Chapters 4, 5 and 6).

Chapter 3

Modelling and Optimisation Strategies

In this chapter, the modelling of a tray distillation column, hollow-fibre pervaporation membrane and their hybrid is considered first, followed by the numerical integration technique used in this study. The optimisation solution strategy employed is then presented.

3.1 Introduction

The objectives of this chapter are to describe the approaches taken in modelling and optimisation of the distillation column, the membrane unit and the hybrid of the two. The next section outlines the mathematical models used for distillation and membrane processes. The numerical solution technique is then presented, followed by the optimisation strategy employed.

3.2 Distillation Modelling

The optimisation work conducted in this thesis is based on a rigorous tray distillation column model. The model considers stage-by-stage column dynamics which is described by a set of MESH (material balance, equilibrium, summation of fraction and heat balance equations). The main model features include:

- Fast energy dynamics: This eliminates column temperature initialisation making the model easier to initialise and solve. Furthermore, the energy dynamics disposes of the assumption of constant molal overflow often used in distillation modelling. The constant molal overflow assumption implies that the heat of vaporisation of the components in the mixture is the same which is often unreasonable for difficult separations (*e.g.* acetone-water $\lambda_{water} = 9.7\,kcal/mol$ and $\lambda_{acetone} = 7.2\,kcal/mol$, Perry and Green (1984)).

- Constant liquid holdup and negligible vapour holdup on trays: This eliminates the specification of detailed tray hydrodynamics and flow characteristics that are usually not available during the preliminary design screening stage. Nevertheless, this feature disposes of the common negligible tray liquid holdup assumption.

- Rigorous thermodynamic models: This disposes of the assumption of constant relative volatility through the use of liquid and vapour densities, viscosities, enthalpies and fugacities.

In order to limit the size of the model to allow for solution within reasonable computational time and to eliminate the need to obtain commonly unavailable correlation parameters, certain assumptions have been retained. These include 100% tray efficiency, total condensation, no entrainment effects, no downcomer dynamics, adiabatic operation, phase equilibrium and perfect mixing. However, these assumptions can easily be eliminated where relevant information and correlation parameters are available. The resulting model equations for the distillation column is outlined in Appendix A.1.

3.3 Membrane Modelling

The behaviour of a membrane module is characterised by three sub-models, two which describe the flow on either side of the membrane and a third model which describes the separation properties of the membrane and its porous support. Similar to the approach of Marriott et al. (2001), all sub-models used here are developed from rigorous dynamic mass and energy balances which makes the models usable for any membrane separation. The main model features include:

- Multi-component systems: This allows for multi-component systems to be considered when investigating multi-component hybrid distillation/membrane processes.
- Non-isothermal flow: This feature considers the temperature variations within the membrane module. It is required where significant temperature changes occur, such as that in pervaporation membranes, as the permeation flux is highly dependent on these variations.
- Rigorous thermodynamic models: This disposes of the assumption of constant physical properties that can otherwise have a large impact on the model accuracy when significant temperature, pressure or concentration changes occur.
- Two-dimensional flow patterns: This allows for concentration variations perpendicular to the bulk flow direction to be investigated. Furthermore, the assumption of one-dimensional plug flow is eliminated.

Based on the above principles, models that describe the flow patterns inside hollow-fibre membrane modules are now presented. Model equations are given in Appendix A.2.

3.3.1 Hollow-Fibre Module

A hollow-fibre module consists of a large number of membrane fibres (typically of the order of 10^5) assembled together in a module as illustrated in Figure 3.1. The unit feed

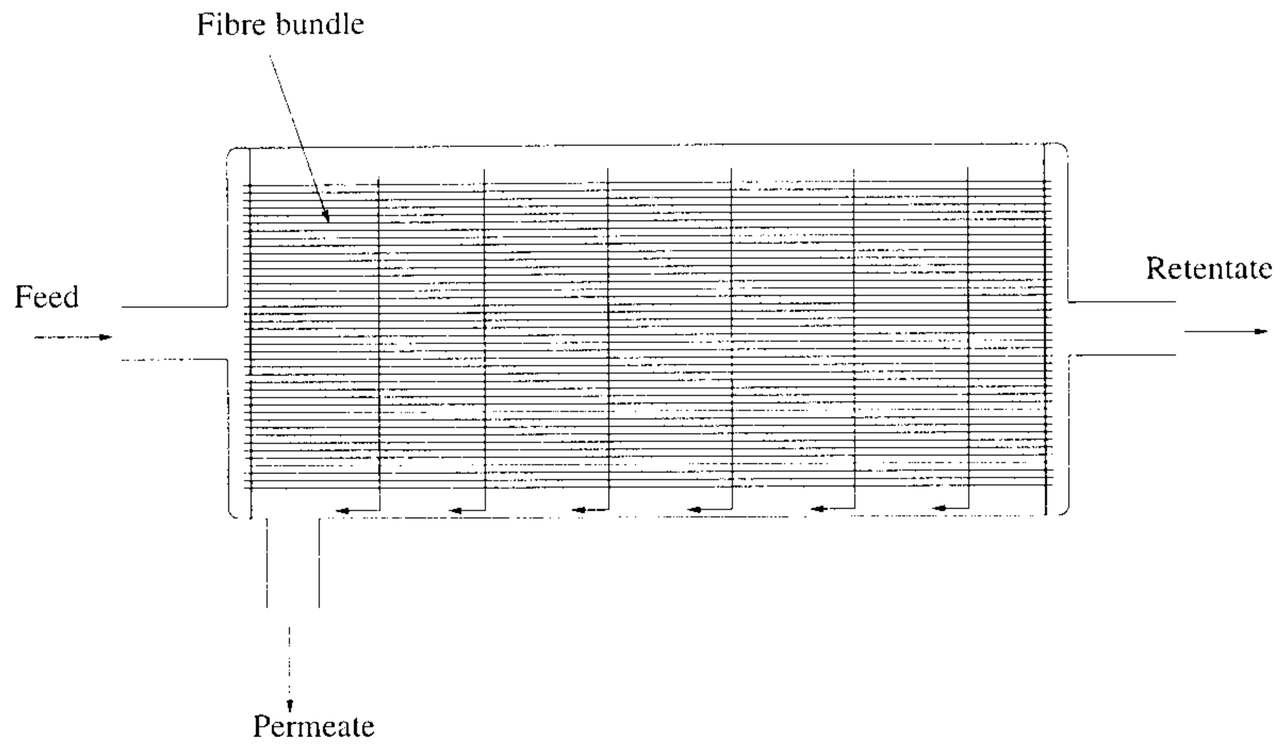

Figure 3.1: Hollow-fibre module

can be introduced to the inside of the fibre (known as fibre feed pattern) and the permeate collected on the shell side. Alternatively the feed can be introduced to the shell side of the membrane fibres (known as shell feed pattern) and the permeate flows inside the fibres. The permeate can either be drawn counter-currently (see Figure 3.1) or co-currently (see Figure A.10 in Appendix A.2) to the direction of the feed with the former being generally more effective due to the improved mixing in the shell.

Fibre Flow Sub-Model

A two-dimensional sub-model that considers liquid or gas flow inside the fibres of a hollow-fibre module has been developed. The model yields axial and radial variations in concentration and temperature through the dynamic mass and energy balances considered (Appendix A.2.2).

It is assumed that all fibres within the hollow-fibre module are of identical specifications and properties and can be modelled as a thin horizontal pipe of a uniform diameter. If the effects of fibre variability need to be investigated, a similar approach to that of Lemanski and Lipscomb (2000) can be adopted. Radial and axial variations in velocity and pressure are not considered but can easily be included through a momentum balance similar to those of the mass and energy balances.

Shell Flow Sub-Model

A similar two-dimensional sub-model to the fibre flow sub-model has been developed from dynamic mass and energy balances to describe the flow on the module shell side (Appendix A.2.2). The model yields both axial and radial variations in concentration and temperature. To limit the size of the model, no variations in radial or axial pressure and velocity are considered.

Reduced Membrane Models

Where models are considered for process optimisation, the axial and radial variations inside the fibre or indeed the shell have little significance, *i.e.* only the total mass and energy balances need to be considered. Therefore, the fibre and shell flow sub-models are reduced to only predict the total changes in membrane properties. In order to determine the level of confidence in the reduced models, it is necessary that comparison to the full 2-D model is made. This will also help establish the relative gain in computational efficiency and the loss in modelling accuracy. A comparison study between the two models developed, similar models (Marriott and Sørensen, 2003a) and experimental data (Tsuyumoto et al., 1997) revealed a good agreement between the reduced 1-D model and the other data. The reduced membrane model is therefore used to conduct the optimisation studies in this thesis (the equations of this model are shown in Appendix A.2.3).

3.4 Model Solution

The dynamic models described above consist of a set of differential and algebraic equations (DAE). These DAEs can either be solved through implicit or explicit numerical integration techniques. Implicit techniques have been found to be better suited than explicit ones (Boston et al., 1980) in solving systems where integration stiffness is experienced as that exhibited by the distillation and membrane models developed. The process modelling software gPROMS (PSE, 2005) employed in this work, provides a convenient platform

to solve the DAEs using an implicit integration method. The gPROMS integration is performed through the backward differentiation formulae (BDF) methods (Gear, 1971) where the order of integration and time step is varied automatically to ensure that user defined tolerance is met while taking the longest possible integration time step within the specified integration time horizon. Model physical properties are provided by an external software, *Multiflash* (Infochem, 2005), that is interfaced to the gPROMS simulation.

3.5 Optimisation Strategy

The simultaneous considerations of optimal configuration, design and operation in batch separation processes translates into the simultaneous consideration of binary, discrete and continuous variables which will give rise to complex mixed integer dynamic optimisation (MIDO) problems (Chapters 4). The solution of MIDO[1] problems is not a trivial task and there is much ongoing research in developing practical solution algorithms. Quesada and Grossmann (1992) proposed a branch-and-bound (BB) algorithm where the discrete variables are relaxed into continuous ones for the solution of the MIDO problem. Other algorithms reported in literature are all based on decomposing the optimisation problem into smaller sub-problems. One approach is to discretise the system into a finite-dimensional mixed integer nonlinear programming (MINLP) problem using techniques such as orthogonal collocation on finite elements (Avraam et al. (1999); Viswanathan and Grossmann (1990) and Mohideen et al. (1996)). Bansal et al. (2003) reports that the resulting MINLP from this discretisation can often be very large even for relatively small problems. The other approach is to decompose the problem into a series of primal problems (typically dynamic optimisation problems) where the discrete variables are fixed, and a master MILP is constructed. Different variations of this method include outer-approximation (OA) (Duran and Grossmann, 1986), OA/augmented-penalty (OA/AP) (Sharif et al., 1998) and Generalised Benders Decomposition (GBD) (Geoffrion, 1972). Bansal et al. (2003) proposed an algorithm based on the (GBD) where the MIDO problem is decomposed into primal,

[1] The general form of the dynamic optimisation problem is outlined in Appendix B

dynamic optimisation and master, mixed-integer linear programming sub-problems.

When the simultaneous optimal configuration, design and operation of steady-state separation processes is considered (Chapters 5), the MIDO problem described above is reduced to an MINLP optimisation problem. MINLP optimisation problems also present solution challenges. Conventional MINLP solution methods consider a sequence of non-linear programming (NLP) sub-problems solved using a gradient-based approach. One method is exhaustive search by enumeration of all possible integer values to result in a set of NLP sub-problems. The best optimal solution of the NLPs is the solution of the MINLP optimisation problem. Another method is the branch-and-bound algorithm where the integer variables are relaxed to continuous ones resulting in a relaxed NLP. The relaxed NLP is then solved to obtain a lower bound on the problem. The values of the integer variables are fixed using a branching method. The branch is terminated when all of the integer variables at a given obtained integer value or the current upper bound, has been exceeded. The search is terminated when all branches are terminated. Details of other techniques such as the outer-approximation (Duran and Grossmann, 1986), OA/augmented-penalty (OA/AP) (Sharif et al., 1998) and generalised Benders decomposition (GBD) (Geoffrion, 1972) are found in the relevant references.

The aforementioned conventional deterministic mathematical programming approaches used to solve the MINLP problem, and consequently the MIDO problem, require gradient information for the NLP problem solution. This makes these methods less attractive when problems with highly nonlinear functions, stiff models and complex search spaces are considered, such as that of the simultaneous optimisation of configuration, design and operation of hybrid separation processes. Furthermore, these methods perform a local search and hence (depending on the initial guesses) are more likely to converge to sub-optimal solutions. Also, great difficulties can be encountered by gradient-based methods due to systems discontinuities and the methods can be computationally expensive for large problems as they require derivatives information (Androulakis and Venkatasubramanian, 1991).

The consideration of multi-objective mixed integer dynamic optimisation (MO-MIDO) problems for the optimal configuration, design and operation of hybrid separation systems (Chapter 6) is only effectively solvable through an evolutionary algorithm, such as genetic algorithm (GA). This is because the final solution, *i.e.* the Pareto front, will normally represent tradeoffs in the optimisation problem considered between two or more conflicting objective functions (*e.g.* revenue versus costs) and therefore, not a single final solution, but rather a range of solutions is found. Using a single objective optimisation method would entail solving the optimisation problem n times to obtain n points on the Pareto front. As GA naturally produce a population of solutions, only a single run, as opposed to many, is required in determining the final solution.

In this thesis, the use of a stochastic genetic algorithm method to solve the mixed integer dynamic optimisation problem (MIDO) (Chapters 4), the mixed integer non-linear programming optimisation problem (MINLP) (Chapter 5) and the multi-objective mixed integer dynamic optimisation problem (MO-MIDO) (Chapter 6) is considered. The application of genetic algorithm to the optimal design of chemical engineering systems has been explored only in a limited number of cases and has not previously been considered for the optimal configuration, design and operation of hybrid separation systems. Genetic algorithm is generally slower than gradient-based solution techniques in terms of computational time when used for solving simple optimisation problems. However, GA potentially offer a number of advantages over conventional methods:

- Discontinuity can easily be handled as derivative information is not required
- Global search is performed and initial guesses are less relevant and the solution therefore less likely to be trapped in local optima
- A range of solutions are returned at the end of the run which is particularly useful when exploring tradeoffs
- Binary, integer and continuous variables are easily considered

Similar to the gradient-based methods, GA, nevertheless, has some disadvantages:

- The inherent need for a population of solutions may translate into a relatively higher computational cost in terms of function evaluations (GA operators require minimal computational effort). It is clearly possible to use a population size of one but this will diminish much of the GA evolutionary capabilities.
- The *optimality* of the final solution is dependent on the convergence settings and the tuning of a number of parameters (see Appendix C). These settings typically reflect trade-offs between accuracy and computational time depending on the purpose of the optimisation studies.

3.6 Genetic Algorithm

Genetic algorithm (GA) is a class of evolutionary algorithms. Genetic algorithm was first introduced by Holland (1962) as a general model of adaptive computer processes, but subsequently has largely been adopted as a stochastic optimisation method. The GA is inspired by the natural genetic process, and thus candidate solutions are encoded as genomes that contain a set of genes representing the decision variables analogous to the DNA in a natural organism.

Genome Coding

The set of decision variables representing a solution to the optimisation problem considered are translated into genes to form the solution *genome*. Where the optimisation of a batch operation process is considered (Chapters 4 and 6), the operational decision variables u_o are parameterised in a piecewise-constant manner within the batch time intervals t_i such that the operational variable u_{o,t_i} represent its value at the relevant batch time interval t_i, where the total batch time is $t_f = \sum t_i$ (Eq. 3.1).

$$\{u_{d,1}, \ldots, u_{d,j}, \underbrace{u_{o,t_i}, \ldots, u_{o,t_f}, t_i, \ldots, t_f}_{\text{parameterised}}\} \tag{3.1}$$

and u_d represents the time invariant design and configurational parameters. The parameterisation is clearly not required in case of a steady state optimisation problem (Chapter 5) and time invariant operational parameters are considered instead. Each gene has its own bounding range and can represent a discrete, continuous or logical decision variable which is particularly helpful where configurational, design and operational decision variables are considered simultaneously (Chapters 4, 5 and 6).

Fitness

The overall algorithm is driven by the *fitness* of the candidate solutions which is determined by a problem-specific objective function. The fitness also determines the survival of each candidate solution from one genetic generation to the next, and hence the progression of the optimisation procedure towards convergence.

The GA is typically initialised with a population of genomes with random genes from within the search space instead of a single guess or genome. The populations are then manipulated through the use of three genetic operators (selection, crossover and mutation) to direct the evolution of the algorithm towards the final population.

Simple GA

A simple GA (Goldberg, 1989) can be described through the procedure outlined in Figure 3.2. The initial population of size N_{pop}, is firstly created at random representing N_{pop} variations of configuration, design and operational variables. The population fitnesses are then evaluated based on the values of the objective function and its constraints. The genetic operators are applied to the evaluated generation to create the next generation. The algorithm continues to evolve until a termination condition is met.

Steady State GA

A steady state genetic algorithm (Syswerda, 1989) utilises overlapping populations as shown in Figure 3.3. Firstly, an initial population of a specified size N_{pop}, is generated

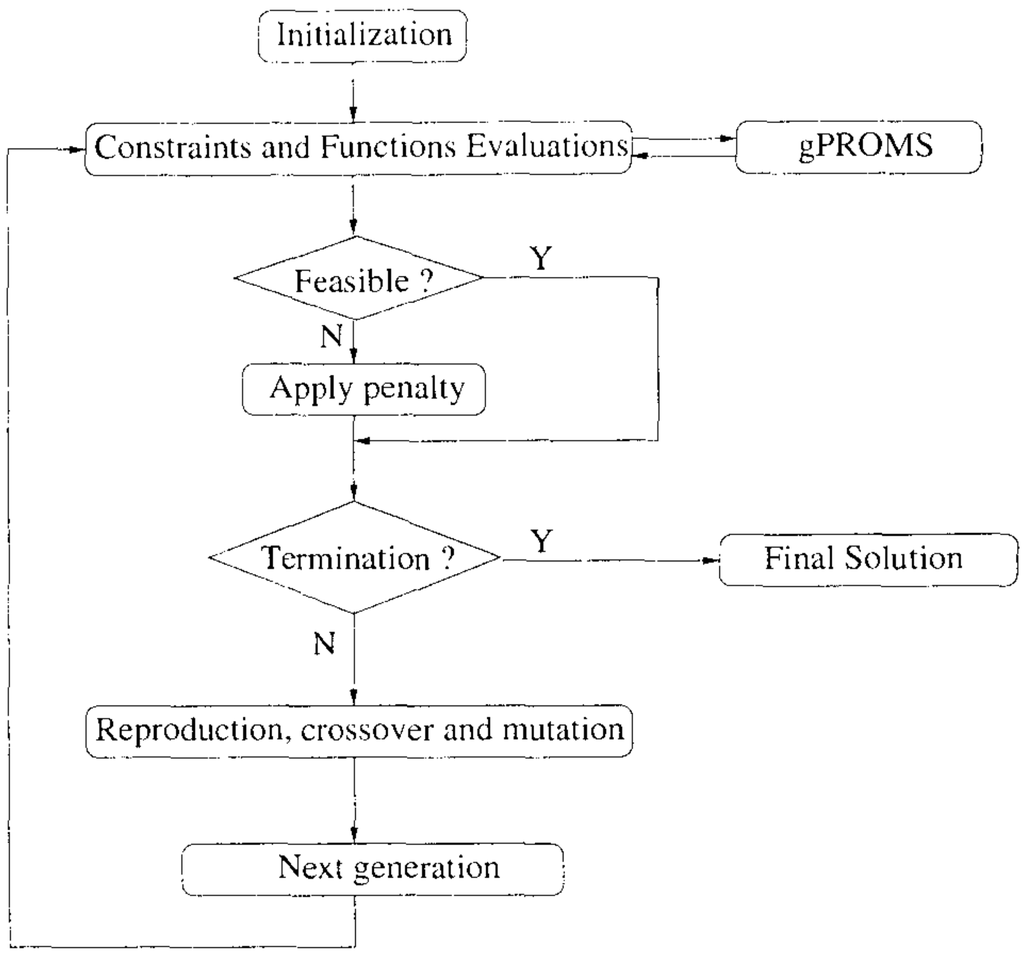

Figure 3.2: Simple GA

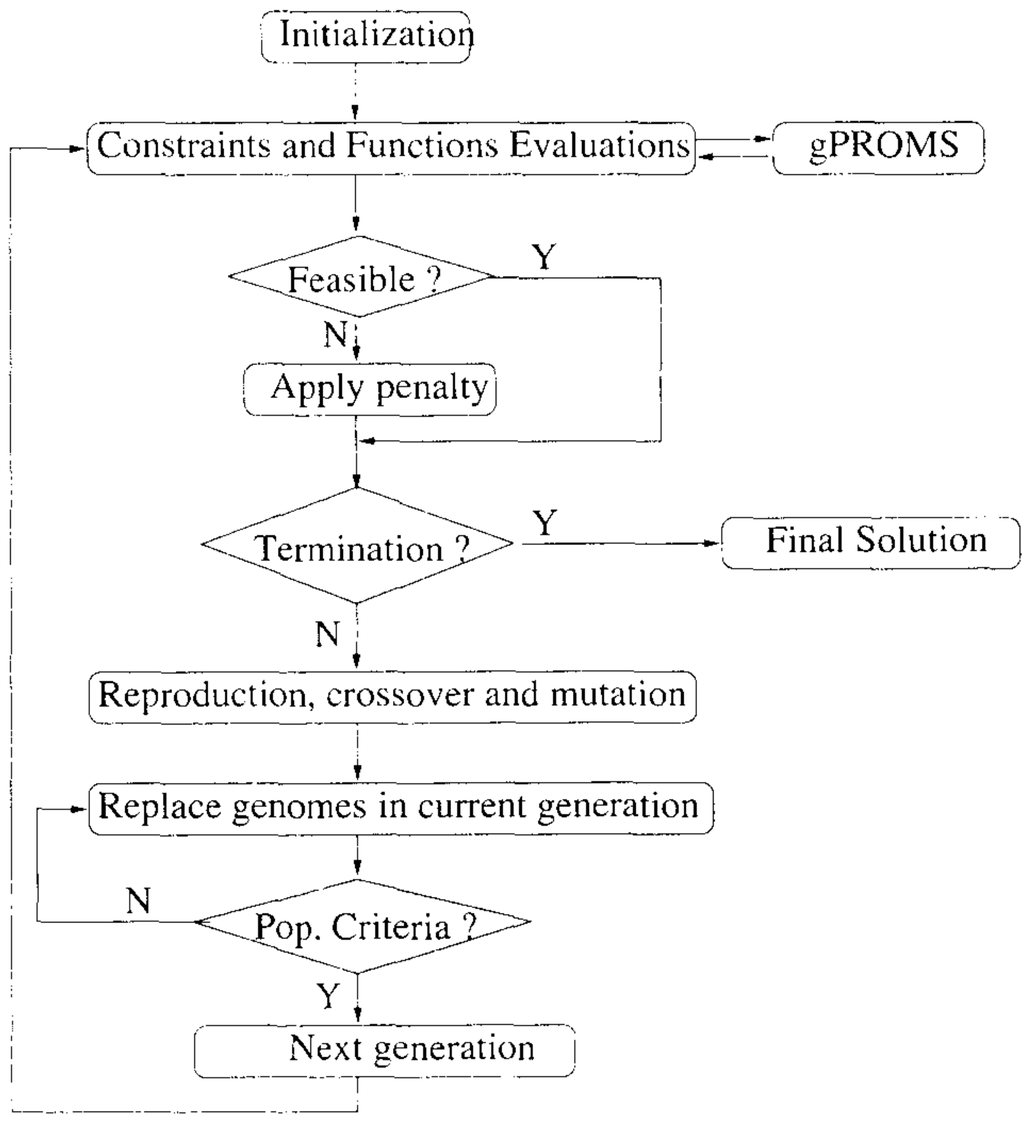

Figure 3.3: Steady State GA

randomly. Then, in each generation, the fitness of each genome is evaluated based on the objective function value and constraints. Based on the fitness function of each genome, the algorithm creates a new set of temporary genomes via the three genetic operators, *i.e.* selection, crossover and mutation, and adds these to the previous population. At the same time, the algorithm removes the weaker genomes in order to return the population to its original size. The percentage of population overlap specified, P_{ss}, governs the number of new genomes to be created in each generation and is known as the "population criterion". The new genomes may or may not be promoted to the next generation, depending on whether they are better or weaker than the rest in the temporary population. This allows the retention of fitter genomes for use in the next generation as well as provides the opportunity to discard new genomes that are weaker than those of the parents' generation. This is done by simply ranking the genomes according to their objective function values.

3.6.1 Constraints Handling and Solution Infeasibility

The optimisation problems considered in this work, like most other problems within separation system optimisation, are constrained by the final product purities and recoveries. The genome obtained as the final result of the GA evolution must necessarily be feasible, that is, satisfy all constraints considered. A mechanism is required to check the feasibility of the evaluated objective value. A method of hard (absolute) constraint handling is required when considering the separation of difficult mixtures. This will ensure that solutions that fail to tackle the difficult separation regions are not preferred to those that satisfy the constraints but resulted in lower objective values (see Appendix C).

In the optimisations considered in this work, the purity and recoveries of the final products (x_{i,t_f} and m_{i,t_f}), are checked against the constraints, ($x_i^{\min}$ and $m_i^{\min}$), respectively. If a solution represented by the genome falls short of these requirements, a corrected objective function is then assigned using a *penalty function* depending on the amount of constraint

violations experienced such that:

$$\kappa_i = \begin{cases} \left[1 - \frac{c_i^{\min} - c_i(t_f)}{c_i^{\min}}\right] & \text{if} \quad c_i(t_f) < c_i^{\min} \qquad c = [x_i, m_i] \quad \& \quad \forall\, i = 1, .., n_c \\ 1 & \text{otherwise} \end{cases}$$

$$f = \begin{cases} \Omega & \text{when} \quad \text{feasible} \\ \prod_{i=1}^{n_c} \kappa_i & \text{when} \quad \Omega \geq 0 \quad \text{(profit and infeasible)} \\ \Omega\,(2 - \prod_{i=1}^{n_c} \kappa_i) & \text{when} \quad \Omega < 0 \quad \text{(loss and infeasible)} \end{cases} \tag{3.2}$$

where κ_i denotes the penalty function for each of the n_c constraints, Ω is the original objective function value and f is the the corrected objective value. Note that the penalty function and the terms *profit* and *loss* of the objective function are concerned with the optimisation problems considered in Chapter 4 and 5 where the ultimate objective is to maximise the economic performance index and a solution genome may return a negative value (*i.e.* loss). A variant of this penalty function is considered for the *minimisation* problem outlined in Chapter 6.

It should be noted that the genomes may represent unrealistic or impractical solutions especially when the bounds set for the design and operational variables are generous. For instance, the maximum bounds on the boilup rate may cause the reboiler to run dry during the objective function evaluation and thus will stop the simulation due to the infeasibility of the solution values chosen. In such a case, a very low or high fitness, depending on whether the objective is to minimise or maximise the objective function, is automatically assigned to the genome so that the probability of it being promoted to the next generation is less than those with feasible, or indeed, better infeasible solutions.

Fitness Scaling

Solution set or genome fitness is a measure of the merit of that genome and it is proportional to the value of the objective function achievable by the genome. Fitness scaling

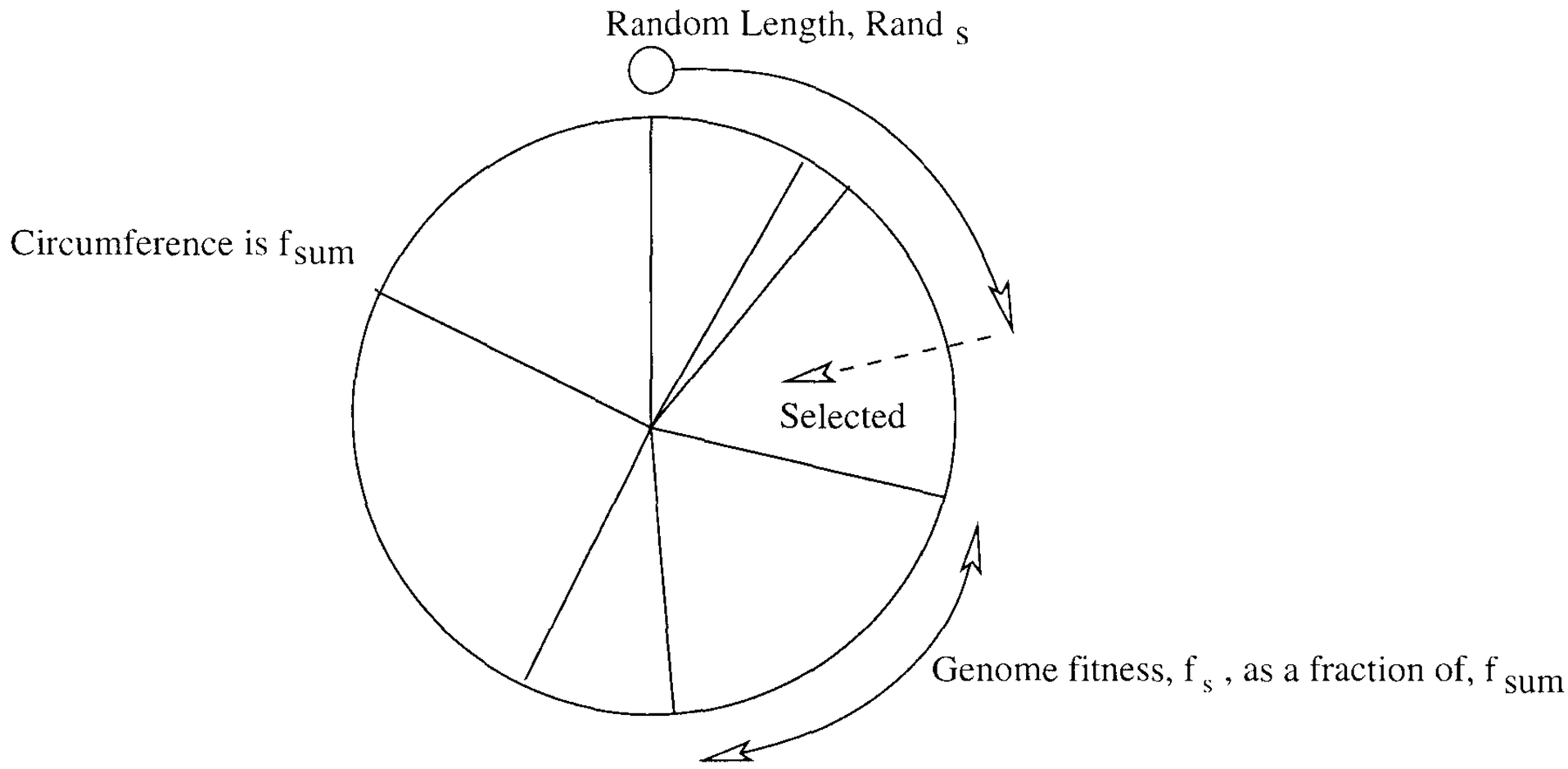

Figure 3.4: Roulette wheel selection

may be required to compensate for the slow convergence during the later stages of the algorithm where the difference between the best genome and the worst or the mean is not large (*e.g.* profit of 12.30 and 12.29 million). The algorithm needs to differentiate between these numerical differences for evolution to continue towards the global optimal. A sigma truncation scaling technique (Coley, 1999) is utilised in this work to overcome both premature convergence and the slow finishing difficulties. Fitness scaling works by pivoting the fitness of the population members about the average population fitness value using the population standard deviation. The scaling of the fitness score for each genome is therefore given by:

$$f_s = \max\left[f - \left(f_{ave} - \varrho f_\sigma\right), 0\right] \tag{3.3}$$

where f_s the scaled fitness, f is the corrected objective value of the genome (Eq. 3.2), f_{ave} is the average corrected objective value of the population, ϱ is the sigma multiplier ($1 \leq \varrho \leq 3$; typically 2) and f_σ is the population standard deviation. The fitness value, f_s, is then utilised by the genetic algorithm selection operator as detailed next.

Selection

The selection operator is used to generate offsprings from current genomes. In order to maximise the chance of selecting good genomes at the expense of worse ones, a fitness based selection criterion, such as roulette wheel and tournament selection, is adopted.

In a roulette wheel procedure (Figure 3.4), the probability of individual selection is proportional to its fraction of the sum-of-fitnesses ($f_{sum} = \sum f_s$) of the whole population. The slot of which a particular genome occupies within the roulette wheel is defined as:

$$\text{width of slot} = \frac{2\pi \times f_s}{f_{sum}} \tag{3.4}$$

For every parent selection step, the roulette wheel is spun and where the ball lands, that individual is selected for reproduction in the new generation. The position of the ball landing is determined through the following steps:

1. Choose a random number $Rand_s \in \{0, f_{sum}\}$
2. Add fitness, one at a time, until $f_{sum} \geq Rand_s$
3. The genome whose fitness was last added before $f_{sum} \geq Rand_s$ is the selected genome.
4. Repeat to select the second parent genome.

The parent selection is repeated until enough offspring has been produced to fill the next genetic generation. Because of the stochastic nature of this selection, there is no guarantee that a good genome will be selected for crossover, there is, however, a higher chance of their selection as they occupy a bigger proportion in the wheel.

An alternative to roulette wheel selection is tournament selection (Goldberg and Deb, 1991). In tournament selection, genomes are chosen to enter a tournament pool of size T_s through the roulette wheel method described above. From the tournament pool, the best are then chosen for mating. For instance if $T_s = 4$, then the best two genomes will

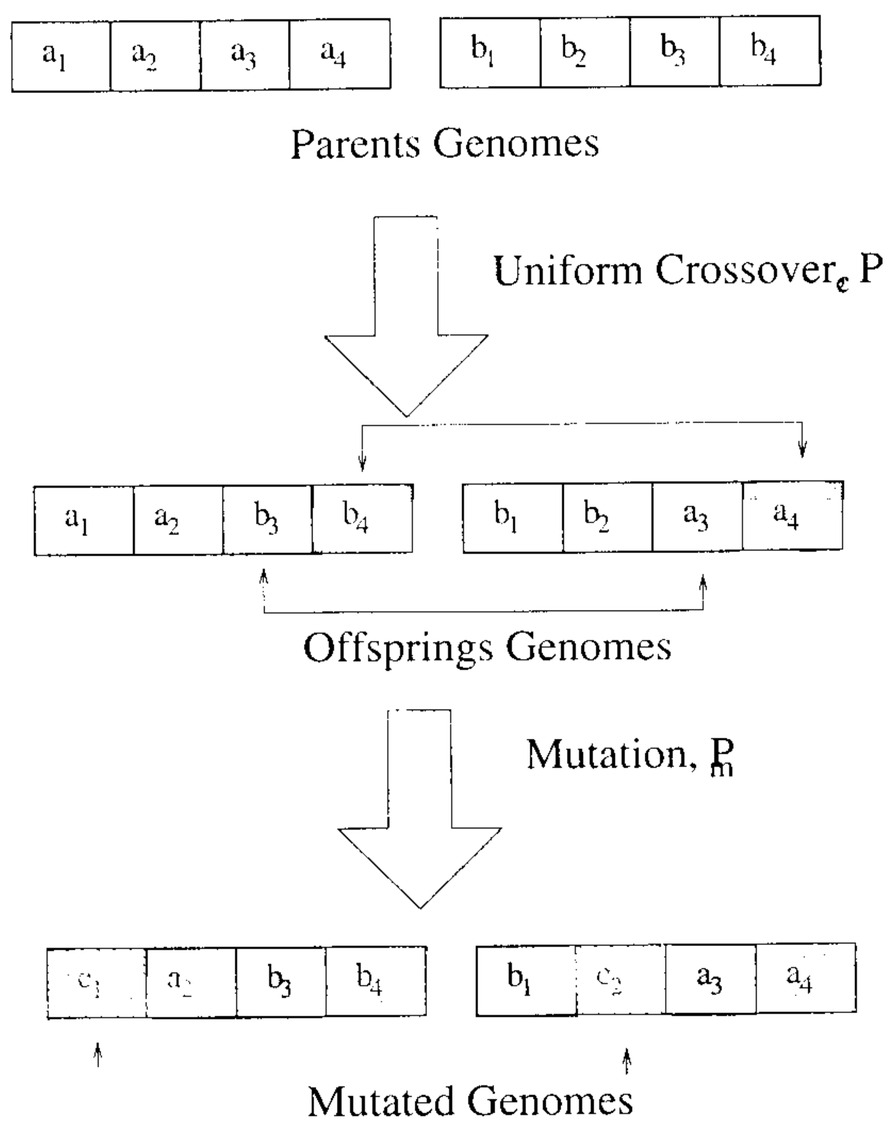

Figure 3.5: Uniform crossover and mutation operators

be selected as parents. This is repeated until enough offsprings have been produced to fill the next generation.

Crossover

After selection, the genes of selected parents are then combined using the crossover operator. The probability of crossover P_c determines the amount of genetic material to be exchanged in order to generate the offsprings. For each pair of genes, a random number $Rand_c \in \{0, 1\}$ is generated. If $Rand_c \leq P_c$, the genes are exchanged, otherwise the pair proceed without crossover. Uniform crossover preserve the structure of the genome, allowing the genetic material exchange to occur only between the same gene positions (see Figure 3.5). This is required where the genes hold variables of different relevance in the problem domain (*e.g.* number of trays, reflux ratio, ... etc).

Mutation

The mutation operator is used to introduce new genetic material into the offsprings' genomes (see Figure 3.5). Offspring genomes undergo Gaussian type mutation with a probability of P_m. For a randomly generated number $Rand_m \in \{0, 1\}$, the gene is mutated if $Rand_m \leq P_m$ using a Gaussian function around the current value, otherwise the gene is not mutated. In case the mutated gene results in a value outside the original gene's bounding range, the mutated gene value is reset to the violated bound. Rounding to the nearest integer is applied to discrete genes.

Elitism

The fitness-proportional selection methods outlined in the previous sections do not guarantee the selection of any particular genome, including the fittest. The retention of best solutions (known as elite genomes) is termed elitism. In a steady state GA framework, as used in Chapters 4 and 5, this is accounted for by the generation overlap percentage P_{ss}. In the simple GA framework used in Chapter 6, the elitism size e_s is defined to copy the best e_s genomes in the current generation to the next genetic generation.

Termination Criteria

During the sequential evolution from one generation to the next, the fitness of the best genome and the average fitness of the population in each generation increase towards the global optimum. The GA will continue evolving until there is no longer a diversity in the population, *i.e.* the best and average are the same. There are a number of ways to terminate the algorithm. One of the criteria is termination when a specified number of generations has been generated and tested. Other methods, such as termination based on the best genome, average genome or combination of the two can be used. The effects of two termination criteria. number of generation and best genome convergence is discussed in Appendix C.

3.6.2 Implementation

The GA frameworks used in this work are implemented in a C++ programme based on the genetic algorithm library GALib (Wall, 1999). Function evaluations are performed using the gPROMS gSERVER (PSE, 2005) which solves the process models for the particular genomes initialised by the genetic algorithm programme. The value of the objective function along with its constraint values are then passed back to the genetic algorithm programme for assessment. gPROMS also uses *Multiflash* (Infochem, 2005) to estimate the model thermodynamics states.

3.6.3 Parameter Tuning

The choice of the genetic algorithm parameters can have a considerable effect on the efficiency and accuracy of the algorithm. The parameters influence the solution quality and the speed of convergence as they govern the algorithm evolution in using previous generation knowledge and exploring new unknown areas in the search space. The parameters concerned with the GA performance as presented above are: the population size in each generation, N_{pop}, the population overlap (steady state GA), P_{ss}, the mutation rate, P_m, the crossover rate, P_c, the implemented penalty function and the termination criteria. In this work, a comprehensive sensitivity analysis was performed as outlined in Appendix C to investigate the effect of these parameters on the performance of the algorithm used in the optimisation of the hybrid distillation/membrane systems.

3.7 Summary

In this chapter, the dynamic modelling of distillation and membrane processes were presented, followed by the approach used for simulation and optimisation of the hybrid separation systems studied in this thesis. The stochastic genetic algorithm framework applied were then detailed.

Chapter 4

Optimal Synthesis of Batch Separation Processes

In this chapter, a procedure for the optimal determination of process synthesis and design for batch separation of mixtures that are difficult to separate by conventional batch distillation is presented. The procedure allows the determination, from available process alternatives, of the optimal batch process, its configuration and its design in order to perform a given separation duty. In this work, batch distillation, batch pervaporation and batch hybrid distillation/pervaporation processes are considered as process alternatives.

Since a batch process is inherently dynamic, and the configurational decisions are integer in nature, the overall problem is formulated as a mixed integer dynamic optimisation (MIDO) programme. The optimisation strategy takes into account an overall economic index that encompasses capital investment, operating costs and production revenues. Furthermore, rigorous mathematical models developed from first principles for distillation and pervaporation are used.

Case studies for the separation of acetone-water mixtures of different feed specifications and batch sizes are presented and it is found that batch hybrid distillation/pervaporation is the optimal synthesis solution in most cases.

4.1 Introduction

Distillation is the most commonly used technique for separating liquid mixtures within the chemical industries despite being an energy and capital intensive process. Many mixtures commonly encountered in the fine chemical and pharmaceutical industries are, however, difficult or impossible to separate by normal distillation due to azeotropic behaviour, tangent pinch or low relative volatilities. Pervaporation has been hailed as an alternative to distillation for such mixtures as the separation mechanism is different, relying on differences in solubility and diffusivity between the components in the mixture and not vapour-liquid equilibrium as in distillation. Pervaporation is still in general a more costly process than distillation; however, for some separations, the costs are comparable or in favour of pervaporation. Recently, hybrid processes have been proposed where a distillation column unit and a pervaporation unit are integrated into one process (Lipnizki et al., 1999). In such a process, the shortcomings of one method are outweighed by the benefits of the other, allowing for significant savings in terms of energy consumption and cost. As discussed in Chapter 2, Guerreri (1992) and Van Hoof et al. (2004) reported up to 60% reduction in energy consumption in their studies of separation of azeotropic mixtures using hybrid systems compared to distillation alone.

The two units can be integrated in different ways; the pervaporation unit can be positioned before the column, after the column or fully integrated. One example of a fully integrated system is to position the pervaporation unit after the column reflux drum outlet and recycle the unit retentate stream back to an appropriate location in the column. Further examples of how the two units can be integrated were discussed in chapter 1.

Most separations within the fine chemical or pharmaceutical industries are run batch-wise. The optimal design and operation of batch distillation columns has received considerable interest in recent years, particularly in terms of novel column configurations such as inverted, middle vessel and multivessel column configurations ((Hasebe et al., 1995, 1997), Hilmen et al. (1997), Furlonge et al. (1999) and (Low and Sørensen, 2002, 2003)). Adding a pervaporation unit to the system, either before, after or fully integrated, adds complexity to the system but also more degrees of freedom which, if properly chosen, can further

increase the profitability of the system, particularly for difficult separations such as that of azeotropic mixtures.

The design engineer is faced with a difficult task: to determine not only the best design and operation of the separation process, but also which separation technique to use and, if considering a hybrid system, how the two units should be combined. The objective of this work is thus to propose an optimal batch process synthesis procedure that allows the simultaneous determination of the optimal process type (distillation, pervaporation or hybrid), as well as its configuration, design and operation for a given separation duty. The procedure can be extended to any number of separation process alternatives, but the discussion in this work will be limited to batch distillation, batch pervaporation and batch hybrid distillation processes.

In the next section, the batch separation synthesis problem is presented, followed by the objective function formulation and the optimisation problem definition. The mathematical models used in this study are then given together with an overview of the optimisation strategy. Finally, the batch separation process synthesis problem and its solution strategy are applied to a case study which considers the separation of a tangent-pinch mixture of acetone and water.

4.2 The Batch Separation Synthesis Problem

4.2.1 Superstructure

The optimal synthesis of the batch separation process superstructure is presented next. The superstructure incorporates three separation processes: batch distillation, batch pervaporation and hybrid batch distillation/pervaporation processes. The superstructure proposed here is shown in Figure 4.1 and it allows not only for the most economical process to be selected, but also to simultaneously determine its optimal operation and design in order to carry out the required separation duty optimally.

The configuration decision of the superstructure is mainly characterised by the location of the feed and product withdrawal streams. The column reboiler acts as the feed tank. Material can either flow to the membrane unit or to the distillation column or to both. If the flow is to the distillation column, it can either be directed to the bottom of the column section or be distributed to the trays. If the reboiler vapour boilup is zero, there is no flow to the distillation column and the liquid flow rate from the reboiler to the membrane unit is optimised. The configuration in this case will either be a batch pervaporation or a pre-distillation hybrid. If the retentate is recycled back to the feed tank, and the vapour boilup is zero, the configuration is that of a batch pervaporation unit and the distillation column does not exist.

If there is no withdrawal from the column, including from the reboiler or the reflux drum, to the membrane unit, the configuration is that of a batch distillation column and the membrane unit does not exist. Otherwise, if the boilup is non-zero and there is withdrawal from the column, including the reboiler or the reflux drum, to the membrane unit, the configuration is that of a hybrid process.

The pervaporation membrane separation stage used in this superstructure, as shown in Figures 4.2, consists of a number of identical membrane modules (N_m) connected in parallel where the membrane stage feed stream is assumed to be distributed evenly between the membrane modules and therefore a single mathematical model can be used to describe the modules. This method, proposed by Marriott and Sørensen (2003b), was found to reduce the computational time significantly.

A rigorous distillation column tray model is employed and will be described in detail next. Each tray is modelled to accommodate three extra potential streams in addition to the regular vapour and liquid inlets/outlets to the neighbouring trays (see Figure 4.3). The first stream is the reboiler vapour inlet stream (dotted lines in Figures 4.1 and 4.3) allows for the optimisation of the number of trays through a Special Ordered Set 1 (SOS1) whereby only one out of N options can be selected as suggested by Viswanathan and Grossmann (1993). They stated that their suggested MINLP model for the selection of the optimal number of trays can be improved by introducing SOS1 methods, although no

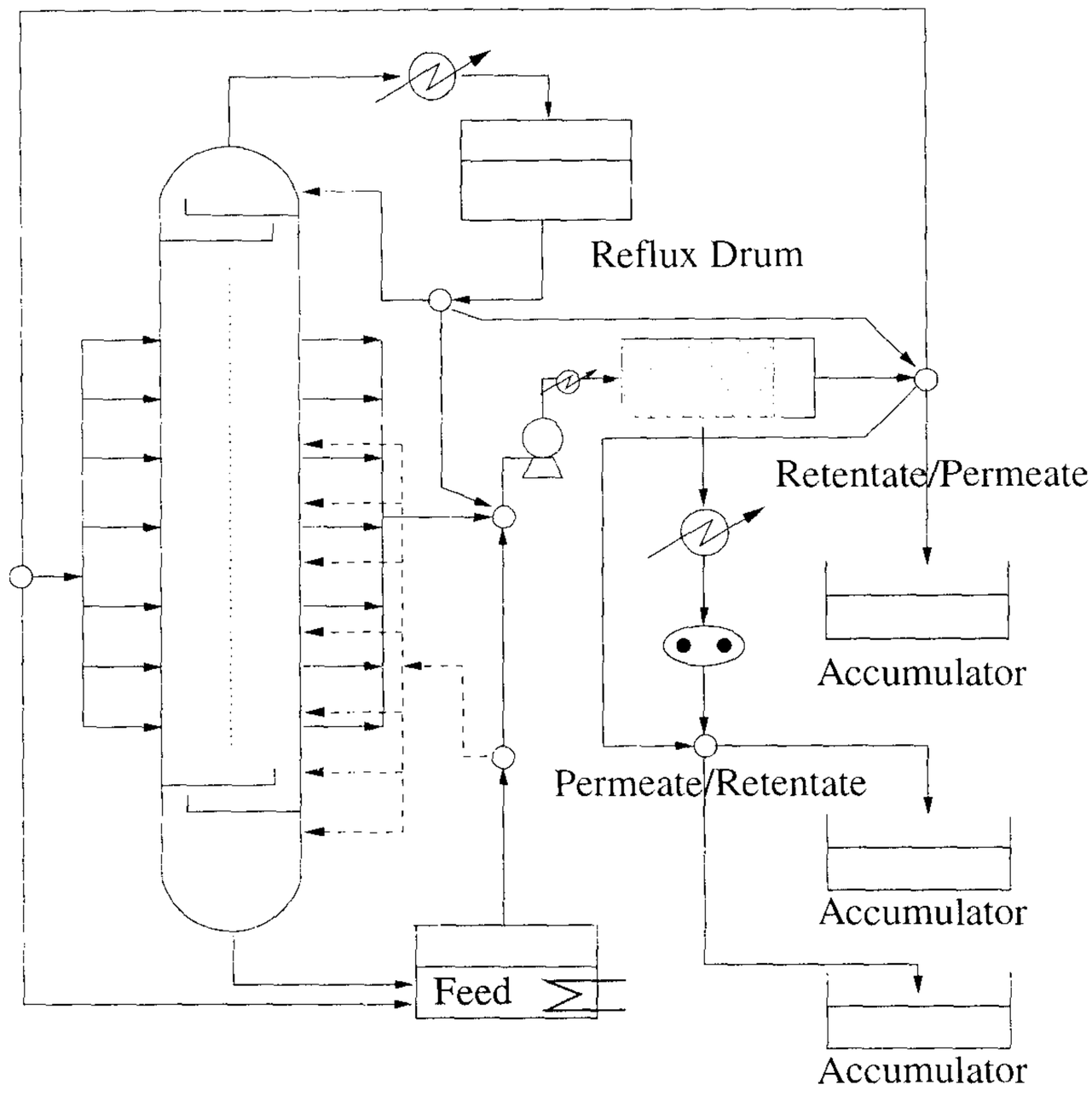

Figure 4.1: Batch separation processes synthesis superstructure

results to support this were presented. The second extra stream in Figure 4.3 is a side draw stream to the pervaporation unit in a hybrid configuration if the tray is selected as a membrane feed tray. The third extra stream is an inlet stream from the pervaporation unit in a hybrid configuration if the tray is selected as a retentate recycle tray. Only one membrane feed tray and one membrane retentate recycle tray is allowed to be selected along the column, however, both of these streams are allowed to exist in the same tray (although this might not be a very practical option). In this work, the SOS1 method is implemented using distribution and collection node models to optimise the location of the various streams within the process superstructure (equations of node models are detailed in Appendix A.4).

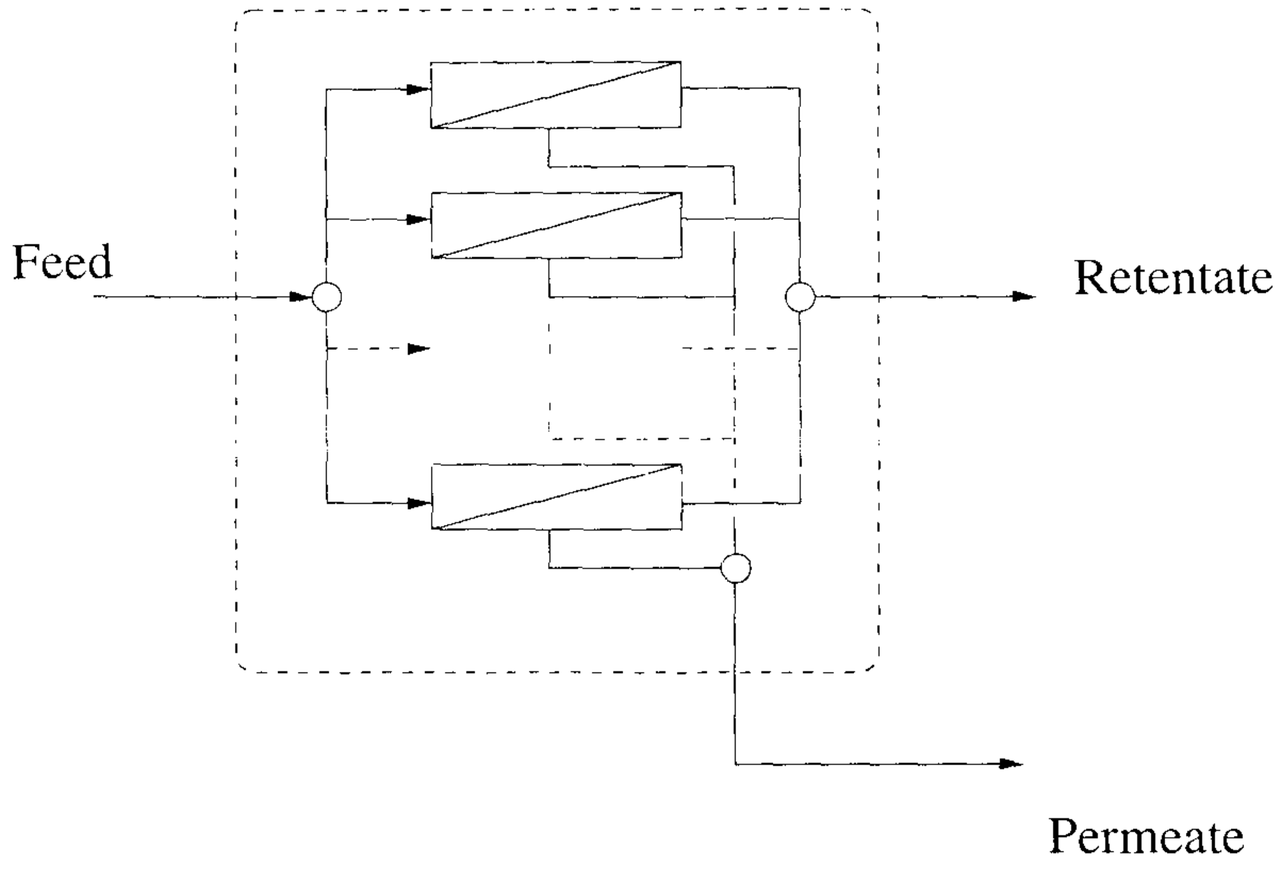

Figure 4.2: Pervaporation membrane separation stage

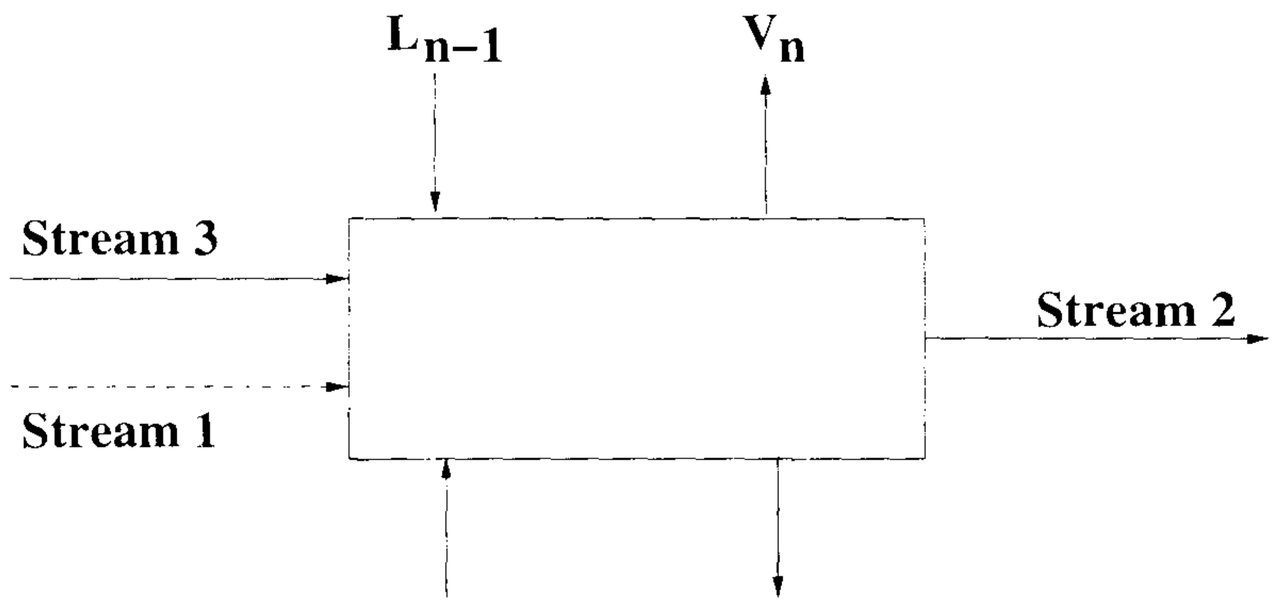

Figure 4.3: Superstructure tray model

4.2.2 Problem Definition

The objective of batch separation process synthesis is to determine the optimal separation process which results in the most economical benefit when processing a given separation task. To achieve this objective, the optimal configuration, design and operation must be considered simultaneously based on an objective function that encapsulates capital investment, operating costs and production revenues.

There is a trade-off between capital investment in terms of equipment and performance on the one hand, and between operational decisions and performance on the other. When considering a batch distillation column for instance, it is possible to design the column with a low number of trays operating at high reflux ratio, or alternatively, design the column with more trays and operating at lower reflux ratio and still achieve the same separation requirements. The decision will, however, clearly have an impact on the profitability of the process. The synthesis problem is further complicated when the process is designed for multiple separation duties. This is commonly the case in industry as batch processes are utilised as multi-purpose units because of their flexibility in accommodating changes in separation duty (Low and Sørensen, 2004). For such cases, the optimal product synthesis tends to be biased toward the separation duties that are performed more frequently than others. High product recovery generally leads to longer batch times than does low recovery. However, high recovery operation generally incurs higher operating costs and thus the balance between revenue and operating costs must be considered.

4.2.3 Objective Function

The optimal design and operation of a batch separation process, as it is considered in this work, is determined as the most economical process design and corresponding operating policy that will satisfy all specified separation requirements and constraints. The performance index used takes into account the chosen process configuration, batch processing time, batch product yields and energy consumption such that:

$$\textit{Performance Index} = f(\textit{Configuration, Batch time, Product yield, Energy consumption}) \tag{4.1}$$

The index above can be translated into an economic model of capital cost (annualised), sales revenue and operating costs. For the simultaneous optimisation of configuration, design and operation using a process superstructure, the optimal solution will be a trade-off between lower capital and operating costs against higher production revenue, thus the objective function must be formulated to reflect these trade-offs. The performance index for the optimal configuration, design and operation of batch separation systems as used in this study is an overall profitability function encapsulating all mentioned costs and revenues and is given by:

$$P_A = \left[\frac{\sum_{i=1}^{N_c} C_i m_i - C_{feed} m_f}{t_f + t_s}\right] \times T_A - AOC_k - ACC_k \qquad k = c, m, hyb \qquad (4.2)$$

where C_i and C_{feed} represent the unit costs of product i and feed, respectively. m_i and m_f are the quantities of on-specification product i and of feed, respectively. T_A represent the total available time for production per annum. t_f and t_s denote the processing time and the setup time of the process, respectively. The annualised capital and investments costs are represented by AOC_k and ACC_k where k is the unit index (distillation, membrane or hybrid). The derivations of these costing indices are detailed in Appendix D and will be outlined later in this chapter.

If the calculated objective function value P_A is for an infeasible solution, a penalty function procedure is applied as follow:

$$\kappa_i = \begin{cases} \left[1 - \frac{c_i^{\min} - c_i(t_f)}{c_i^{\min}}\right] & \text{if} \quad c_i(t_f) < c_i^{\min} \qquad c = [x_i, m_i] \quad \& \quad \forall\, i = 1, .., n_c \\ 1 & \text{otherwise} \end{cases}$$

$$f = \begin{cases} P_A & \text{when} \quad \text{feasible} \\ \prod_{i=1}^{n_c} \kappa_i & \text{when} \quad P_A \geq 0 \quad \text{(profit and infeasible)} \\ P_A \left(2 - \prod_{i=1}^{n_c} \kappa_i\right) & \text{when} \quad P_A < 0 \quad \text{(loss and infeasible)} \end{cases} \qquad (4.3)$$

where κ_i denotes the penalty function for each of the n_c constraints, P_A is the original objective function (Eq. 4.2) value and f is the corrected objective value. The terms *profit* and *loss* reflect the value of the economic performance index, P_A where a genome may return a positive (*i.e.* profit) or negative value (*i.e.* loss). The penalty function applied here is based on absolute constraints handling which was found to be better in terms of constraints satisfaction than soft constraint methods. A comparison between the two methods can be found in Appendix C.

Distillation Costs

The annualised capital costs for a distillation column, ACC_c, is found using the Guthrie's correlation from values of a reference case distillation column as discussed by Longsdon et al. (1990). These costs are then updated with an update factor (UF) assuming a similar trend as of the ACE (Association of Cost Engineering, IChemE (1988)) index between 1975 and 1985. The update factor is then estimated to bring the batch distillation column costs presented by Longsdon et al. (1990) from 1990 cost values to 2005 cost values allowing for fair comparison with recently obtained pervaporation membrane costing data. The resulting column costs were verified against data provided by Sulzer (2005) and were found to agree with current column costs. The annualised capital cost is therefore given by:

$$ACC_c = UF \times \left(K_1 N_t^{0.802} V^{0.533} + K_2 V^{0.65}\right) \tag{4.4}$$

The main contributions to the operating costs are assumed to be the reboiler heating and condenser cooling duties. The operating costs, AOC_c, for the batch distillation column is therefore given by:

$$AOC_c = (C_{ut,reb} \times Q_{reb} + C_{ut,c,cond} \times Q_{c,cond}) \times \left(\frac{T_A}{t_s + t_f}\right) \tag{4.5}$$

where $C_{ut,i}$ represents the utility cost of unit i. Q_{reb} and $Q_{c,cond}$ represent the total reboiler heating and condenser cooling duties, respectively.

Membrane Costs

The annualised capital cost for the batch membrane process is also correlated using the Guthrie's correlation from values of a reference case including pumps and heaters (Sulzer, 2005) such that:

$$ACC_m = ACC_{m,RC} \times \left(\frac{A_m}{A_{m,RC}} \times \frac{F_m}{F_{m,RC}} \times \frac{F_p}{F_{p,RC}} \right)^{0.3} \tag{4.6}$$

where $ACC_{m,RC}$ is the annualised capital costs of the reference case, A_m and $A_{m,RC}$. represent the membrane area of the system and that of the reference case, respectively. F_m and $F_{m,RC}$ represent the feed flowrate to the membrane system and that of the reference case, respectively. F_p and $F_{p,RC}$ represent the permeate flowrate of the membrane system and that of the reference case, respectively. Membrane stage flowrate, membrane area and permeate flowrate are the main parameters affecting membrane system performance and are hence included in the cost equation for comparison with the reference case. The scale exponent is estimated to be 0.3, the lowest recommended value (IChemE, 1988) for accurate prediction of batch pervaporation capital costs. The feed tank heater and a permeate side cooler, in addition to the membrane feed pump and the permeate turbine, are considered to be the main contributions to the operating cost. The operating costs for the batch membrane process are therefore given by:

$$\begin{aligned} AOC_m \quad = \quad & (C_{ut,m,h} \times Q_{m,h} + C_{ut,m,cond} \times Q_{m,cond} \\ & + C_{ut,p} \times Q_{m,p} + C_{ut,t} \times Q_{m,t}) \times \left(\frac{T_A}{t_s + t_f} \right) \end{aligned} \tag{4.7}$$

$$Q_{m,p} = \frac{\nu_p}{\eta_p} \left(P_p^{out} - P_p^{in} \right) \tag{4.8}$$

$$Q_{m,t} = \frac{\nu_t}{\eta_t} \times P_t^{in} \ln \left(\frac{P_t^{out}}{P_t^{in}} \right) \tag{4.9}$$

where $C_{ut,i}$ represent cost of utilities of equipment i, $Q_{m,h}$ and $Q_{m,cond}$ represent the pervaporation unit total feed tank heat duty and permeate condenser cooling duty. $Q_{m,p}$

and $Q_{m,t}$ are the total energy load of the membrane unit feed pump and permeate vacuum turbine, respectively. T_A represents the total available time for operation per annum and t_s and t_f represent the process startup and batch time respectively. ν_i is the flowrate entering the ancillary equipment, i (pump, vacuum turbine) and η_i is the efficiency of the equipment i. P_i^{in} and P_i^{out} represent the pressure at the inlet and outlet of the relevant equipment, i, respectively.

Hybrid Process Costs

The annualised capital costs, ACC_{hyb}, and the operating costs, AOC_{hyb}, for the hybrid batch distillation column are the summation of the cost contributions of the constituent processes and are therefore given by:

$$ACC_{hyb} = ACC_c + ACC_m \tag{4.10}$$

$$AOC_{hyb} = AOC_c + AOC_m \tag{4.11}$$

4.2.4 Optimisation Problem Formulation

The objective of the synthesis procedure is to maximise the profitability defined by the objective function P_A (Eq. 4.2), subject to process type, process model equations and all separation duty constraints. The optimisation problem is therefore:
Given a mixture of amount m_f with number of components N_C to be separated, minimum product purities x_i^{min} , minimum product recoveries m_i^{min} , price structure of feed and products, C_{feed} and C_i and total production time available per annum T_A ; determine the optimum set of design variables u_d , and the optimum set of operation variables u_o , to achieve the maximum objective function value P_A (Eq. 4.2):

$$\max_{u_d, u_o} P_A \tag{4.12}$$

subject to:

$$f(\dot{x}(t), x(t), t, u_d, u_o(t)) = 0 \tag{4.13}$$

$$c_i(t_f) \geq c_i^{min} \quad where \quad c = [x, m] \quad and \qquad i = 1, .., N_C \tag{4.14}$$

$$u_d^{min} \leq u_d \leq u_d^{max} \tag{4.15}$$

$$u_o^{min}(t) \leq u_o(t) \leq u_o^{max}(t) \tag{4.16}$$

Equation 4.13 represents the mathematical process model of the batch separation process; where x is a vector of process state variables, and u_d and u_o denote the vectors of design and operating control variables, respectively. Equation 4.14 represents the product purity constraints imposed which must be satisfied at the end of the batch. Equations 4.15 and 4.16 represent the physical and optimisation bounds of the design and operating control variables, respectively.

In this work, the set of operating variables for the batch distillation process includes vapour boilup rate and column reflux ratio profile, *i.e.* $u_o^c = (V, R_C)$, both of which can vary as functions of time in the specified batch task intervals t_i where the total batch time $t_f = \sum t_i$. The vapour boilup rate can subsequently be used to determine the diameter of the column (*e.g.* using Guthrie's correlation, $D \propto \sqrt{V}$) as well as the reboiler and condenser heat loads. Design variables include the optimal number of trays N_t , *i.e.* $u_d^c = \{N_t\}$.

For the batch pervaporation process, the set of operating variables include retentate recycle ratio R_r, permeate pressure P_p, permeate offcut ratio R_p and feed tank heat load $Q_{m,h}$, *i.e.* $u_o^m = \{R_r, P_p, R_p, Q_{m,h}\}$, all of which can vary as functions of batch time. R_r is defined as the fraction of retentate recycled back to the column or the feed tank (*i.e.* $R_r = 1$ means all retentate is recycled and $R_r = 0$ means all flows to the retentate product accumulator). R_p is defined as the fraction of permeate to the offcut tank (*i.e.* $R_p = 1$ means all permeate flow to the offcut tank and $R_p = 0$ means all flows to the permeate product accumulator). The set of design variables include number of membrane modules N_m, *i.e.* $u_d^m = \{N_m\}$.

For the hybrid batch distillation process, the set of operating variables and design variables are a combination of the previous two processes with two additional design variable for

the membrane feed location (from the column) L_s and the retentate recycle location (back to the column) L_r.

4.2.5 Process Models

The models detailed in Chapter 3 are used to describe the batch distillation systems in this work. The model equations used to conduct the work in this chapter can be found in Appendix A. The model disposes of some of the common modelling assumptions, such as negligible tray holdup and constant molal overflow, that may otherwise have a significant impact on the optimal solution as demonstrated by Furlonge et al. (1999). The main features of the model are:

- Dynamic mass and fast energy balances to dispose of the usual assumption of negligible tray holdup and constant molal overflow, respectively.
- Rigorous thermodynamics through the use of liquid and vapour fugacities that are functions of temperature and pressure, to dispose of the common assumption of constant relative volatility.

The batch distillation model assumptions retained in this work include no entrainment effects, no downcomer dynamics, adiabatic column operation, phase equilibrium and perfect mixing.

The mathematical model used in this study to describe the performance of hollow fibre pervaporation membrane modules is the reduced membrane model described in Chapter 3 and Appendix A.2. The model features a 1-D plug flow pattern through the membrane fibres and module shell. Furthermore, dynamic mass and energy balances, as well as rigorous thermodynamics have been included. The membrane characterisation equations reflect the membrane type used and can easily be modified. Here, a pervaporation membrane described by Tsuyumoto et al. (1997) has been integrated. Concentration variation perpendicular to the bulk flow direction is neglected. Furthermore, concentration and temperature polarisation effect were not taken into account.

The mathematical model of batch hybrid distillation/pervaporation is a combination of the batch distillation and pervaporation models outlined above. The startup period of operation, *i.e.* from when the units (column and membrane module) are initially dry and cold feed is placed in the feed tank or the reboiler drum and the mixture is heated up to the boiling point, is not considered as this leads to an optimisation problem which is extremely difficult to solve due to discontinuities. This assumption was indicated by Sadomoto and Miyahara (1983) to be a reasonably accurate approximation for tray column operation. All accumulators are assumed to be empty initially. It should be noted that the approach outlined in the following can be used with models of any modelling complexity although the confidence in the results will depend on the accuracy of the models. The fidelity of the dynamic models used in this work is a compromise between accuracy and computation time. It is assumed that once the optimal solution has been obtained, a more accurate simulation model is used to verify that the optimal solution is indeed the best process alternative.

4.2.6 Solution Methodology

The simultaneous consideration of optimal design and operation of batch separation processes translates into an optimisation problem with both discrete (*e.g.* number of trays and number of membrane modules) and continuous variables (*e.g.* reflux and recycle ratios). Furthermore, the nonlinear dynamic models used here, as well as the nonlinear objective function defined earlier, transform the problem into a complex mixed integer dynamic optimisation (MIDO) problem. MIDO problems are difficult to solve using conventional optimisation techniques due to the high non-convexity and complex search space topography nature of these problems and the combination of integer and continuous variables, and there is much ongoing research on developing robust and practical solution algorithms (Chapter 3). The proposed batch separation superstructure is in this work solved using a steady state genetic algorithm (GA) optimisation framework as described in Chapter 3.

In this work, a given solution set consisting of all decision variables are coded in the genome as direct real and integer values instead of converted binary bits and mapping

coding which has been found to be less efficient (Coley, 1999). The initial population is created randomly. The objectives and constraints of each individual in this population are evaluated using the gPROMS simulation software (PSE, 2005). Solutions are assigned a fitness score based on the annual profitability of each genome as given by Eq. 4.2. A penalty function procedure is applied (Eq. 4.3) when necessary to encourage the GA to drive the population towards feasibility.

The GA procedure uses a roulette wheel selection scheme, replacement rate, P_{ss}, of 75%, crossover rate P_c, of 75%, mutation rate, P_m, of 10%, population size, N_{pop}, of 100 genomes, and a stopping criterion based on a maximum number of generations (typically 200 for 15,000 function evaluations). The GA parameter values used here are demonstrated to yield good results in the sensitivity studies outlined in Appendix C. The procedure has been implemented using the GALib genetic algorithm library (Wall, 1999).

4.3 Case Study

In this section, separations of acetone-water mixtures are presented to demonstrate the procedure outlined in the previous sections. The objective for each case is to determine the optimal configuration, design and operation of the most economically favourable process for the given separation task. Based on annual profit measures given by the objective function in Eq. 4.2, the outcome of the process superstructure is then verified by comparing the optimal process with the optimal design and operation of the other two process alternatives. Note that only a single pervaporation membrane separation stage is considered in this work although multistage processes are possible and may in some cases have higher economical potentials. The effects of feed specifications and batch size on the optimal solution are also investigated to determine if these factors have any impact on which process is the optimal. The assumption that all energy duties, Q_i, carry the same utility cost index, $C_{ut,i}$, have been made although different indices could have easily been used.

4.3.1 Base Case Description

The separation of a 70:30 mol% acetone-water mixture of 20,000 mol (approximately 9000 litres) batch size is considered first. The objective is to determine the most appropriate process for the separation of the mixture assuming product constraints on both products. Tables 4.1 and 4.2 summarise the unit specifications and operating conditions and the optimisation decision variable bounds used.

The batch distillation process operation is split into three intervals, a total reflux period followed by an acetone product collection period and an offcut period for water product purification remaining in the reboiler. The optimal solution will have an appropriate balance between the time intervals as well as determine the total batch time which is the sum of these intervals. For the batch pervaporation process, a polyion complex membrane type reported by Tsuyumoto et al. (1997) is assumed. The membrane preferentially permeates water and the module is constructed as a highly porous (75%) hollow-fibre bundle (Table 4.3). The membrane characterisation equations reported by Tsuyumoto et al. (1997) are used in the modelling of the pervaporation membrane modules described in the previous section.[1]

The batch pervaporation process operation is separated into three intervals, a water product collection, followed by a possible offcut period and a final acetone product dumping period (into the retentate product tank) when acetone reaches the required product purity. The hybrid distillation/pervaporation process operation is also separated into three task intervals, the first period is a total reflux period similar to the batch distillation process, followed by a second interval for water product collection, and the final interval for acetone product collection.

[1] Although Tsuyumoto et al. (1997) only described the pervaporative separation of an ethanol-water mixture, it is considered a reasonable assumption to use these equations to describe the separation of the acetone-water mixture as the objective of the case studies is to demonstrate the usability of the optimisation procedure and not to obtain an accurate solution for this particular mixture.

Property	Value
Feed composition, $x_{i,feed}$ $(molefrac.)$	
Acetone	0.70
Water	0.30
Batch size, m_f (mol)	20,000
Product purity specifications, $x_{i,f}$ $(molfrac.)$	≥ 0.97
Product recoveries, $M_{i,f}$	≥ 0.70
Tray/Condenser holdup (mol)	1.0/50.0
Column operating pressure, P (atm)	1.0
Available production time, T_A (hr)	7920
Batch setup time, t_s (min)	30
Cost, C_i $(\$/mol)$	
Acetone	0.606*
Water	0.0038*
Feed	0.150
Offcut	0.010
Utility $(\$/MJ)$	0.019**
K1	1500†
K2	180†
UF	4.31†

* Adopted from Mujtaba (1999), ** Adopted from Sinnott (1993),
† Adopted from Longsdon et al. (1990), ‡ Calculated from IChemE (1988)

Table 4.1: Unit specifications and operating conditions

Decision variable	Bounds
No. of distillation trays N_t	[1,30]
No. of membrane modules N_m	[1,10]
Retentate recycle tray L_r	[1,30]
Time $t_i, t_f(min)$	[0.01,1000]
Recycle ratios R_r, R_c, R_p	[0,1]
Column boilup rate $V(mol/s)$	[0.5,5.0]
Permeate pressure $P_p(Pa)$	[300,4000]
Membrane feed rate $F_{feed}(mol/s)$	[0.5,5.0]

Table 4.2: Optimisation variable bounds

Property	**Value**
Membrane material	Polyion complex
Support material	Polyacrylonitrile
Module radius, (m)	97.4×10^{-3}
Fibre inner radius, (m)	0.251×10^{-3}
Fibre outer radius, (m)	0.395×10^{-3}
Membrane thickness, (m)	0.015×10^{-3}
Fibre length, (m)	1.0
Number of fibres	3800

Table 4.3: Hollow fibre module specifications (Tsuyumoto et al., 1997)

4.3.2 Optimal Solution of Base Case

The optimum solution set for the base case problem outlined above is shown in Table 4.4 and Figure 4.4. A batch hybrid distillation/pervaporation process is found to be the most profitable processes alternative that meets all separation requirements for this case study (see Table 4.4), with an estimated profit of $19.024 million per annum.

	Design Variables	Operation Variables	Profit M$/yr
Hybrid	$u_d = \{N_t, N_m, L_s, L_r\}$	$u_o = \{t_f, t_i, R_c, R_r, R_p, P_p, V, F_m\}$	\$19.024
(Optimal)	$u_d = \{30, 2, 1, 5\}$	$u_o = \left\{104.5, \begin{bmatrix} 81.3 \\ 15.0 \\ 8.1 \end{bmatrix}, \begin{bmatrix} 1.0 \\ 0.99 \\ 0.99 \end{bmatrix}, \begin{bmatrix} 0.16 \\ 0.16 \\ 0.15 \end{bmatrix}, \begin{bmatrix} 0.0 \\ 0.0 \\ 0.0 \end{bmatrix}, 300, 4.94, 2.72\right\}$	
Distillation	$u_d = \{N_t\}$	$u_o = \{t_f, t_i, R_c, V\}$	\$17.770
(Fixed)	$u_d = \{30\}$	$u_o = \left\{117.8, \begin{bmatrix} 0.02 \\ 117.0 \\ 0.06 \end{bmatrix}, \begin{bmatrix} 0.75 \\ 0.57 \\ 0.71 \end{bmatrix}, 4.70\right\}$	
Pervaporation	$u_d = \{N_m\}$	$u_o = \{t_f, t_i, R_r, R_p, P_p, F_m\}$	\$2.185
(Fixed)	$u_d = \{8\}$	$u_o = \left\{857.5, \begin{bmatrix} 797.5 \\ 25.4 \\ 34.6 \end{bmatrix}, \begin{bmatrix} 0.99 \\ 0.37 \\ 0.27 \end{bmatrix}, \begin{bmatrix} 0.0 \\ 0.0 \\ 0.0 \end{bmatrix}, 300, 4.84\right\}$	

Table 4.4: Optimal solution sets for case study

The optimal superstructure solution, a hybrid of distillation and pervaporation, indicated the optimal number of trays and membrane modules to be 30 & 1, respectively. The optimal number of trays (30) is at the upper bound, however, the vapour load, 4.94 mol/s, is below the upper bound (5 mol/s). The optimal side-draw location was found to be from tray 1, *i.e* from the top of the column (2.72 mol/s). The optimal retentate recycle stream location was found to be at tray 5. The optimal batch time is found to be 104.53 *minutes* with interval split of 81.4, 15.0 and 8.2 *minutes*, respectively. The interval splits are, however, insignificant as the optimal column reflux ratio (R_C), retentate recycle ratio (R_r) and the permeate offcut ratio (R_p) remain almost constant (the reflux ratio is slightly reduced from 1.0 to 0.99 during the last two intervals and the retentate recycle ratio is only reduced from 0.16 to 0.15 during the last interval while the permeate offcut ratio remains constant). The optimal reboiler vapour load is found to be 4.94 mol/s and the optimal side-draw feed to the membrane unit from tray 1 is 2.72 mol/s. The membrane permeate side pressure is found to be at the lower bound of 300 Pa as expected, as the minimum permeate side pressure will allow for faster retentate stream purification and hence lower overall batch time. The permeate offcut ratio (R_p) is constant at 0.0 which means no off-cut is required. It is observed that for the optimal hybrid process, variations in reflux and retentate recycle ratios are very small with no variations in the permeate offcut. This indicate that a constant operation settings can be adopted with minimal losses.

The product purity profiles are shown in Figure 4.5. It can be noted that the acetone product purity reached the required specification (0.97 mol%) after approximately 30 *minutes*, whilst the water purity in the reboiler continued to increase until all the acetone product was collected in the top accumulator.

4.3.3 Comparison with Fixed Configurations

For comparison, when the process superstructure is fixed to optimise a batch distillation column configuration only, the optimum design results in an estimated annual profit of \$17.77 million which is 7.3% less than that of the optimal hybrid solution. When the process superstructure is fixed to optimise a batch pervaporation configuration only, the

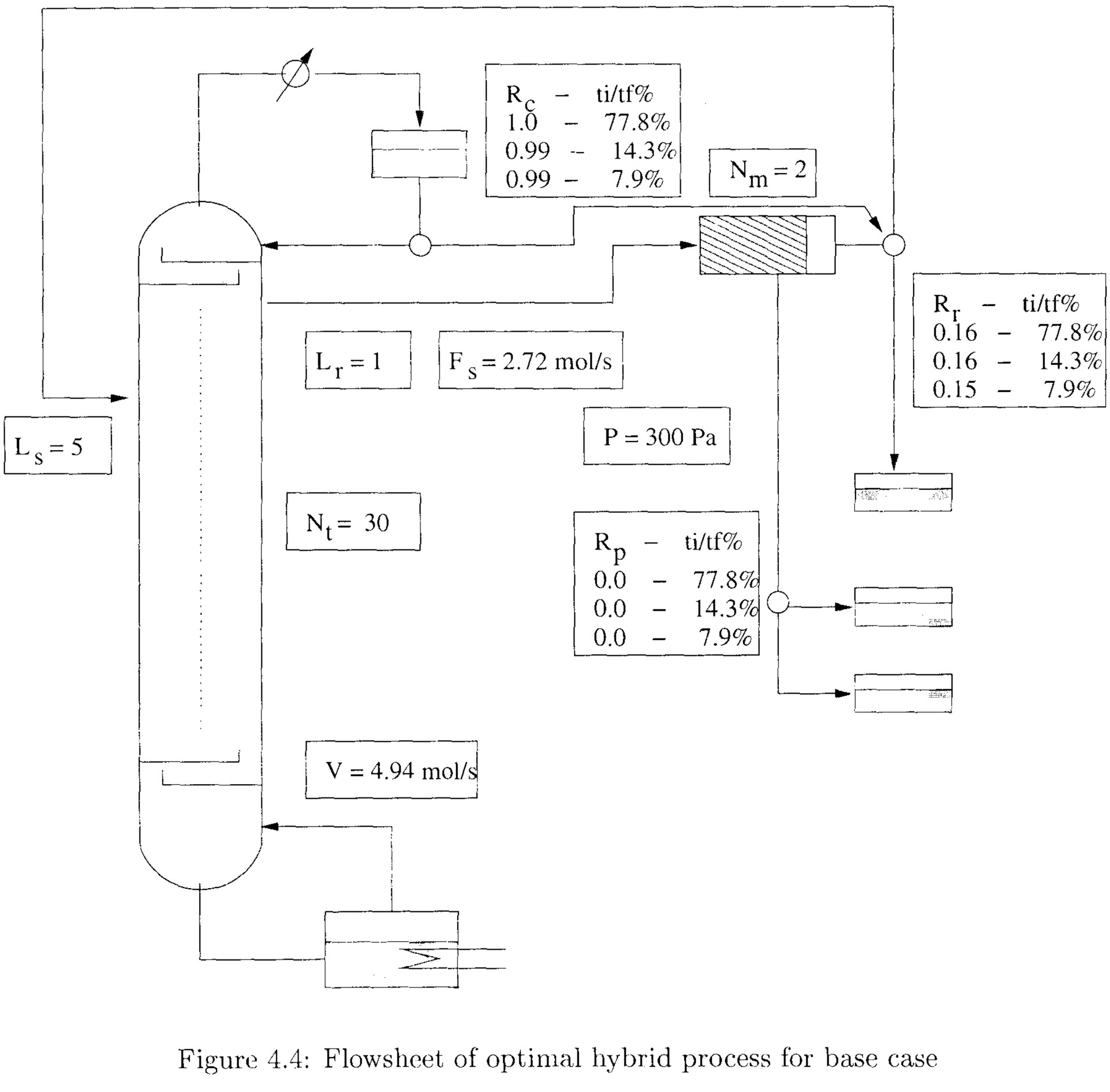

Figure 4.4: Flowsheet of optimal hybrid process for base case

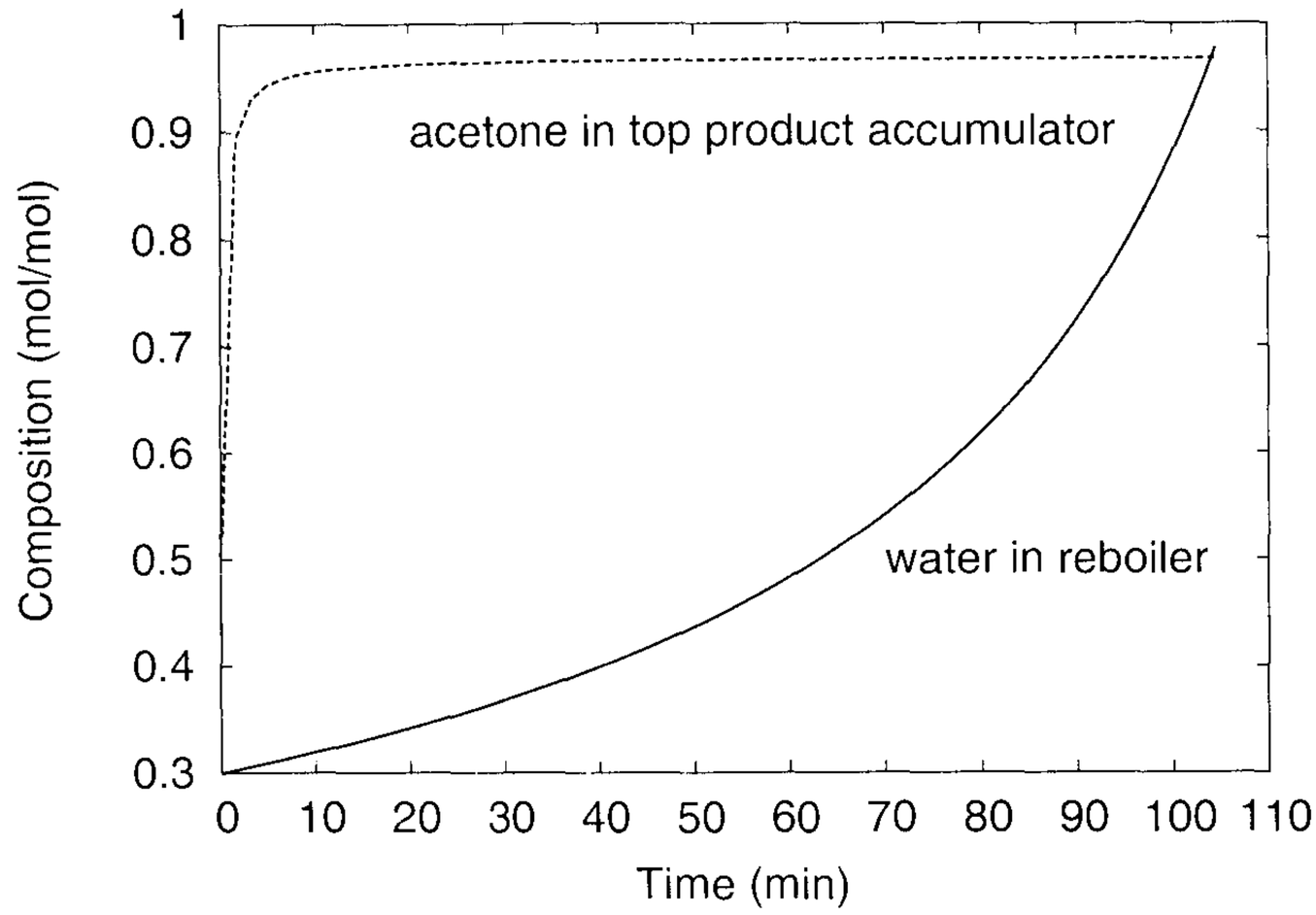

Figure 4.5: Product compositions in optimal hybrid (70:30 mol%, 20,000 mol feed)

optimal design and operation results in the least profitable alternative with an estimated annual profit of only \$2.185 million (88% less). This figure is significantly lower than that of the batch hybrid and distillation processes due to the long batch time required (857.5 min) for the pervaporation process, owing to the process scale as pervaporation membrane units are normally better suited to small scale processes.

Let's consider the designs in detail. In comparison, the optimal number of trays and the reboiler vapour load for a fixed batch distillation configuration are found to be 30 & 4.70 mol/s, respectively. The optimal number of trays is the same as that of the optimal configuration. The vapour load is, however, lower than that of the optimal configuration, indicating a smaller column diameter is preferred which results in lower capital and operation costs. The batch time is found to be 117.8 *minutes* with interval splits of 0.02, 117.0 & 0.06 *minutes* and corresponding constant reflux ratio values for these intervals of 0.75, 0.57 & 0.61, respectively. Note that the optimal total reflux period is found to be almost nonexistent (0.02 *minutes*) which is reasonable as the column was assumed to be at total reflux conditions initially.

The batch pervaporation process has an optimal number of 8 membrane modules. The batch time is significantly longer than that of the batch distillation and hybrid processes of 857.5 *minutes* with interval splits of 797.5, 25.4 & 34.6 *minutes*. The optimal retentate recycle ratio remained at 0.99 for the first interval (797.5 *minutes*) for the purification of the acetone product to the required purity. The recycled ratio is then reduced to 0.37 and 0.27 for the subsequent two intervals, respectively, to allowing for more product collection. The permeate pressure is found to be 300 Pa and the feed flowrate is 4.84 mol/s. As expected, the optimal permeate pressure is at its lower bound allowing for the maximum possible flux through the membrane and thus purification of the acetone retentate stream in the shortest possible time.

Comparing the optimal superstructure solution for the base case H,0.7 in Figure 4.6 with the optimal distillation and pervaporation solutions, D,0.7 and P,0.7, respectively, it was found that capital cost of the hybrid process (H,0.7) is the highest with the majority of the cost contributed by the distillation column. The pervaporation capital cost is the second highest and the distillation process capital cost is the lowest. This is in-line with the general assumption that membrane processes are more costly than distillation processes for large scale production ($20,000$ $mol/batch$). The operating cost of the hybrid process (H,0.7) is also the highest among the three processes with the major contribution from the distillation column accounting for almost two thirds of the total operating costs. The pervaporation process resulted in the lowest operating costs, almost half of that of the distillation process which had the second highest operating costs.

It should be noted that high performance equipment that is operating for high product recovery will cost more in terms of capital and operating costs. However, it will achieve more product revenue and result in shorter batch times. This tradeoff is implemented in the proposed procedure and for this case study, the optimal superstructure solution is biased toward higher product recoveries and shorter batch times instead of lower capital and operating costs.

Case	Feed Size (mol)	Feed Composition, (mol%) Acetone - Water	
A	20,000	[0.50,0.50]	
B	20,000	[0.70,0.30]	(Base Case)
C	20,000	[0.90,0.10]	
D	2,000	[0.90,0.10]	
E	200	[0.90,0.10]	

Table 4.5: Optimisation cases considered

4.3.4 Effects of Feed Composition on Optimal Synthesis

The results presented for the base case was for a 70-30 mol% mixture with a $20,000\,mol$ feed. In this section, the effect of the feed composition on the optimal synthesis is considered in order to investigate its impact on the optimal solution. The comparison studies are based on 20,000-mol feed of acetone-water mixture of various feed specifications as shown in Table 4.5 (cases A to C). All the feed mixtures are assumed to be of equal cost (0.15 \$/mol) and all other specifications and constraints are the same as in the base case and can be found in Tables 4.1 and 4.2.

The results in Table 4.6 and Figure 4.7 show the merit of the hybrid batch distillation/pervaporation process over the stand-alone processes. The hybrid distillation system was in all cases found to be more profitable than the other two and pervaporation was found to be the least profitable. This is mainly because pervaporation processes tend to have significantly longer batch time at this scale (20,000 mol). Distillation processes are expected to be economically favourable at lower acetone feed composition, as hydrophilic membrane processes are generally inefficient at high water content feed streams.

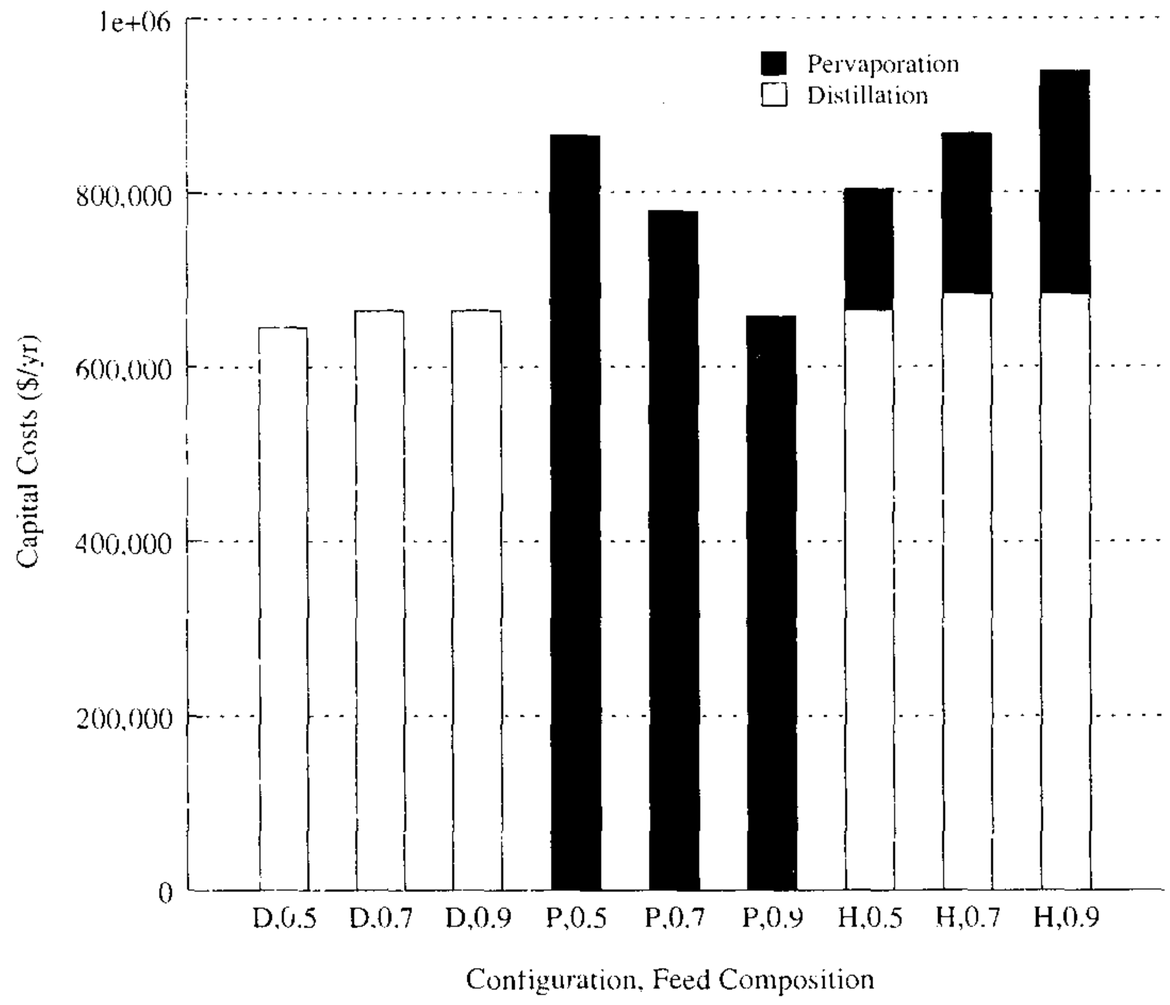

(a)

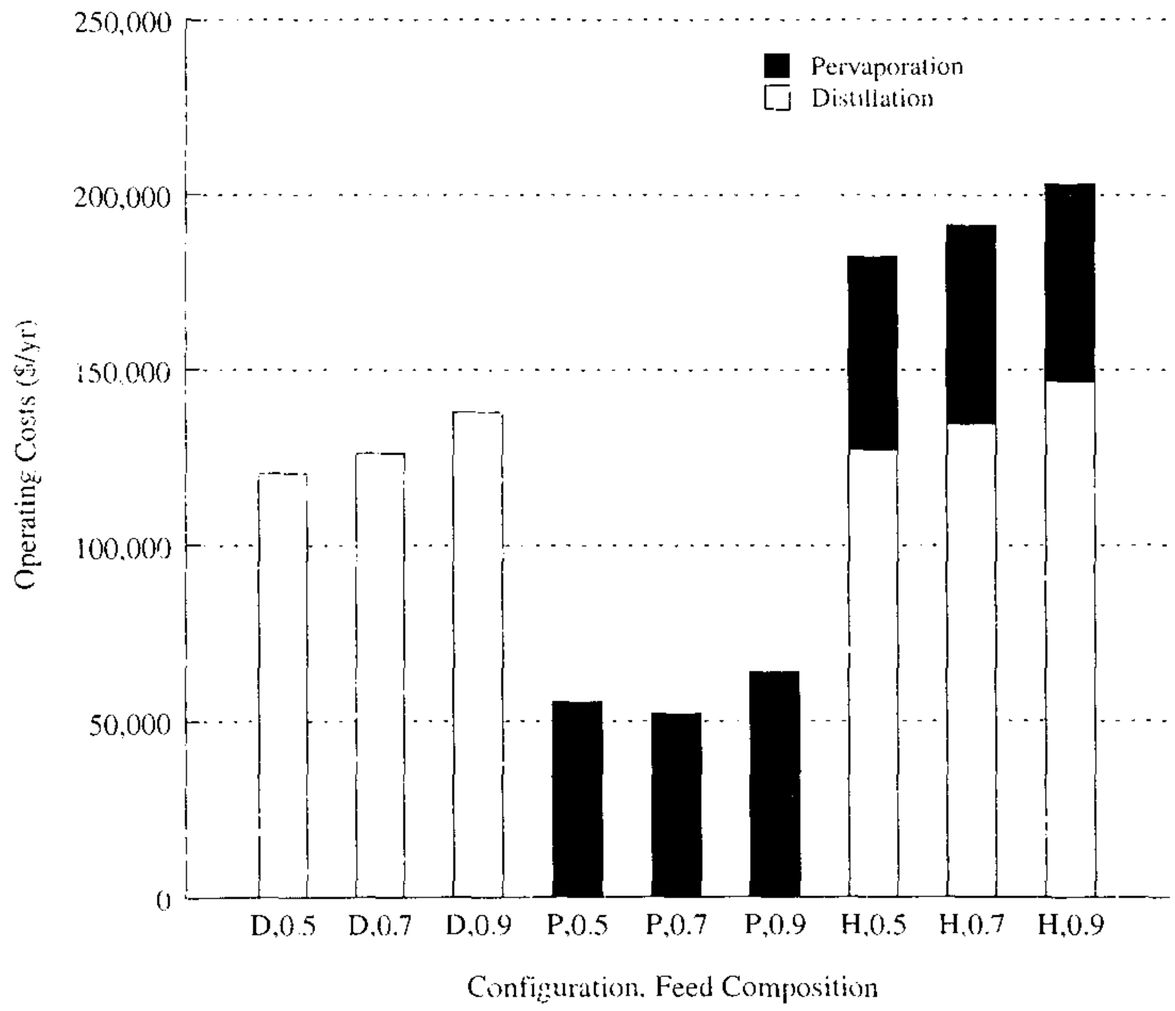

(b)

Figure 4.6: capital costs (a) and operating costs (b) as a function of acetone feed composition

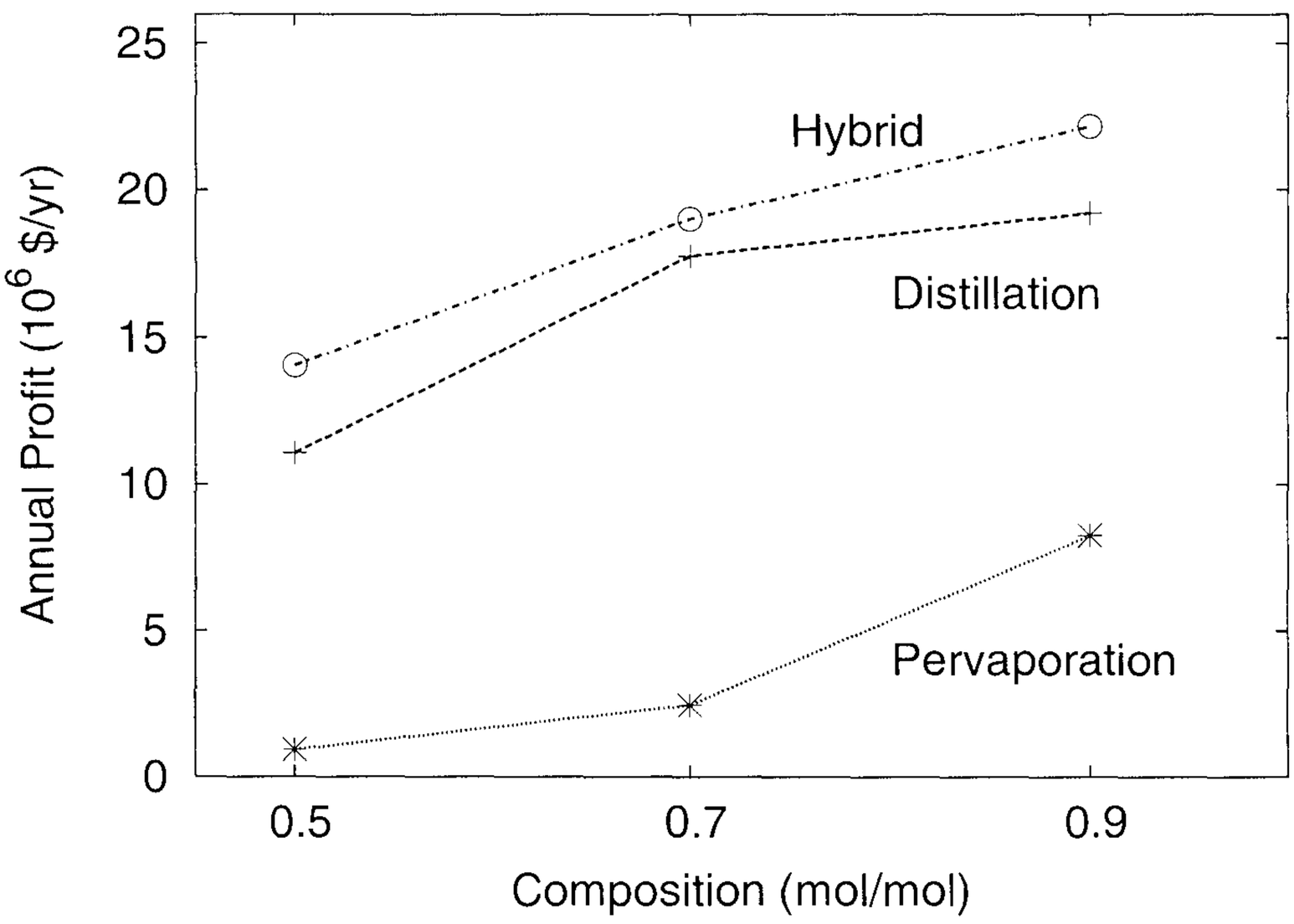

Figure 4.7: Profit versus feed concentrations for all processes (20,000 mol feed)

	Distillation			**Pervaporation**			**Hybrid**		
Case	A	B	C	A	B	C	A	B	C
Number of trays N_t	30	30	30	-	-	-	28	30	30
Number of modules N_m	-	-	-	9	8	10	1	2	3
Batch time, $t_f, (min)$	97.83	117.80	164.45	887.17	857.5	410.5	70.37	104.53	134.37
Permeate pressure, P, Pa	-	-	-	300	300	300	340	300	300
Vapour load, $V, (mol/s)$	4.46	4.70	4.70	-	-	-	4.99	4.94	4.94
Stage Feed $F_m(mol/s)$	-	-	-	4.94	4.84	5.0	2.40	2.72	2.97
Capital cost, ($/yr)	645,352	664,500	664,500	865,102	778,385	657,502	803,416	867,158	939,554
Operating cost, ($/yr)	120,540	126,275	137,976	55,542	52,236	64,074	182,534	191,419	203,207
Revenue, (M$/yr)	11.831	18.578	19.970	1.667	3.015	8.880	15.041	20.306	23.306
Annual Profit (M$/year),	11.065	17.770	19.168	0.747	2.185	8.158	14.055	19.024	22.163

Table 4.6: Optimal solution sets for cases A, B and C given in Table 4.5

The required number of distillation column trays in both the batch distillation and the hybrid distillation processes were consistently found to be close to, or on, the upper bound. The reboiler vapour load, however, did not, in all cases, hit the upper bound, indicating that bigger trays can be selected by the optimisation procedure if it results in a higher objective function value. The number of distillation column trays was extended to 50 for case A (Table 4.5) to investigate the effect of this on the optimal solution. The optimal superstructure solution was found to be a hybrid process with the optimal number of trays and the reboiler vapour load found to be 32 & 4.93 mol/s, respectively, compared to 30 & 4.94 mol/s with the optimal solutions obtained with upper N_C bound of 30. This configuration was, however, found to result in a sub-optimal solution with lower profit value ($15.51 million per annum) than the solution obtained with upper N_C bound of 30 ($19.024 million per annum). This is due to the fact that with higher bound for the N_C, the search solution space is further extended and hence it is made more difficult (and time consuming) to obtain the global solution and this was not taken into account in the solution.

In the hybrid configuration it is observed that the sidedraw flowrate increases as the hybrid becomes more dependant on the membrane stage, this is also apparent as more modules are used with decreased water content in the feed (1 for case A, 2 for case B & 3 for case C).

The batch processing time for the hybrid distillation system is generally less than those of the batch distillation and pervaporation processes, allowing for more batches to be processed per year in a 24-h production plant. The pervaporation processes have significantly longer batch time, resulting in a lower number of batches that can be processed in the available annual production time. This resulted in lower revenues and therefore a lower overall profitability. However, pervaporation processes are expected to out-perform distillation and hybrid processes at low, lab-size process scales as will indeed be discussed in the next section. The annual capital costs (see Figure 4.6) seem to have an increasing trend in batch distillation and hybrid configurations as the acetone feed concentration increases. However, for the pervaporation processes, the annual capital costs shows a decrease with

an increase in acetone feed purity, which is mainly because pervaporation with hydrophilic dense membranes have higher efficiency for lower water content in the feed.

4.3.5 Effects of Batch size on Optimal Synthesis

The effects of batch size is investigated at a feed concentration of 0.90 mol% acetone. Three different batch sizes of 200, 2,000 and 20,000 mol are explored (cases C, D and E in Table 4.5) and the results are given in Table 4.7 and Figure 4.8 (note the log scale). With a batch size of 200 mol, the superstructure has resulted in a pervaporation process as the optimal process to carry out the specified separation duty. At this batch size, an optimised hybrid configuration results in the least profitable operation. This conclusion does not hold, however, at batch sizes of 2,000 and 20,000 mol where the hybrid process is found to be the optimal process, with the pervaporation process the least profitable option and the distillation process second best. It is therefore concluded that pervaporation processes are more suited to small, rather than medium or large scale, separations. A capital and operating cost comparison (see Figure 4.9) indicates a consistent decrease, as expected, in costs as batch size decreases.

It is interesting to note that a hybrid process always seem to perform better than a pure batch distillation process for these cases (C-E). This is because the hybrid process resulted in lower batch times than distillation in cases C & D, hence more batches can be performed in the annual available time T_A and therefore higher annual revenue and consequently profit (Eq. 4.2) can be achieved. For case E, the hybrid process has resulted in lower energy consumption, hence in lower operating costs and therefore higher overall profitability than batch distillation alone.

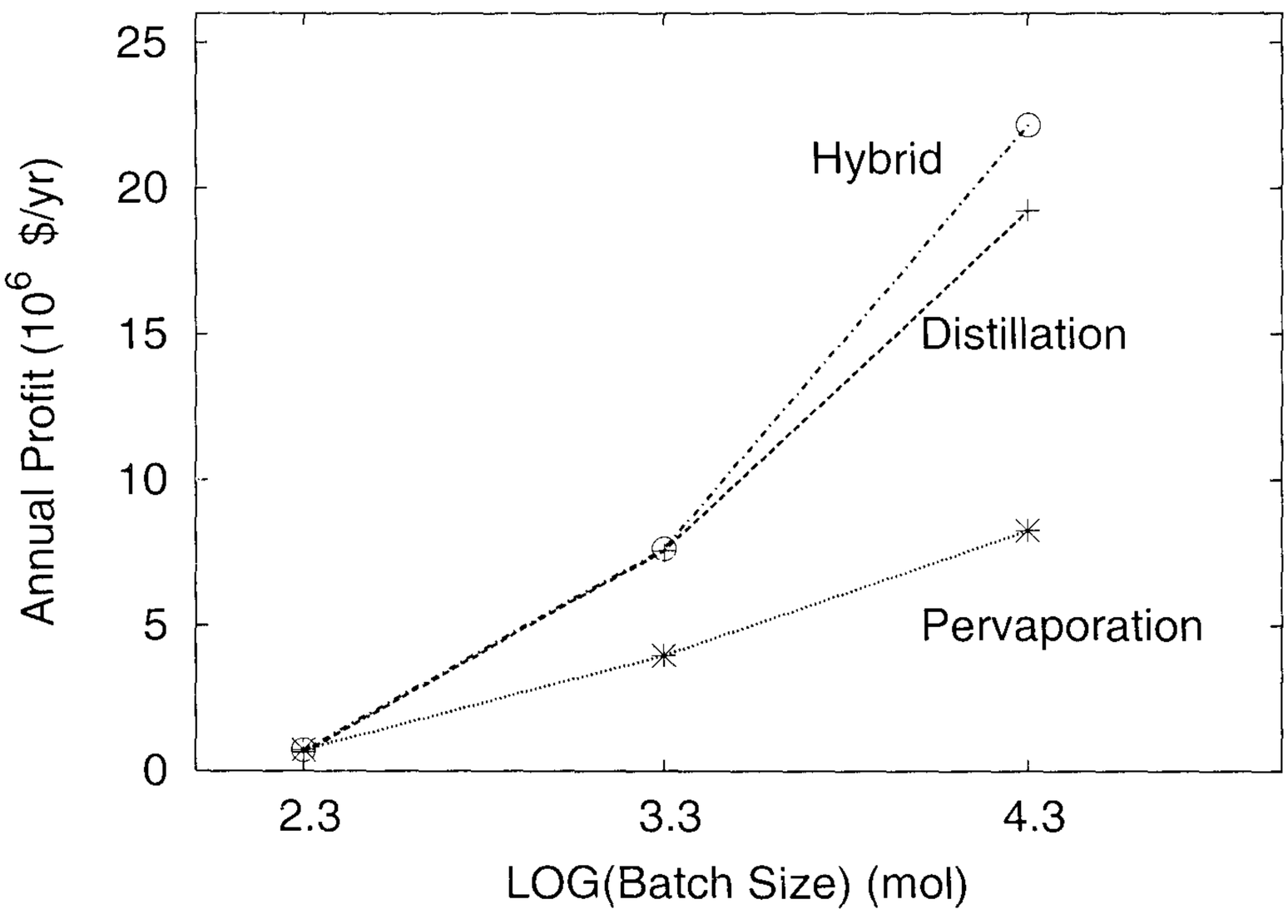

Figure 4.8: Profit versus scale for all processes (90 :10 mol% feed)

	Distillation			**Pervaporation**			**Hybrid**		
Case	C	D	E	C	D	E	C	D	E
Number of trays N_t	30	28	23	-	-	-	30	30	19
Number of modules N_m	-	-	-	10	4	1	3	1	2
Batch time, $t_f, (min)$	164.45	16.73	4.67	410.5	58.17	11.50	134.37	16.00	5.85
Permeate pressure, P, Pa	-	-	-	300	300	300	300	370	710
Vapour load, $V, (mol/s)$	4.70	4.90	5.0	-	-	-	4.94	4.72	1.66
Stage Feed $F_m(mol/s)$	-	-	-	5.0	3.96	3.33	2.97	2.31	2.22
Capital cost, ($/yr)	664,500	657,769	476,118	657,502	325,939	180,853	939,554	736,045	323,751
Operating cost, ($/yr)	137,976	60,151	17,545	64,074	30,761	11,841	203,207	67,109	10,750
Revenue, (M$/yr)	19.970	8.303	1.134	8.880	4.315	0.924	23.306	8.430	1.049
Annual Profit (M$/year),	19.168	7.585	0.641	8.158	3.958	0.731	22.163	7.627	0.714

Table 4.7: Optimal solution sets for cases C, D and E given in Table 4.5

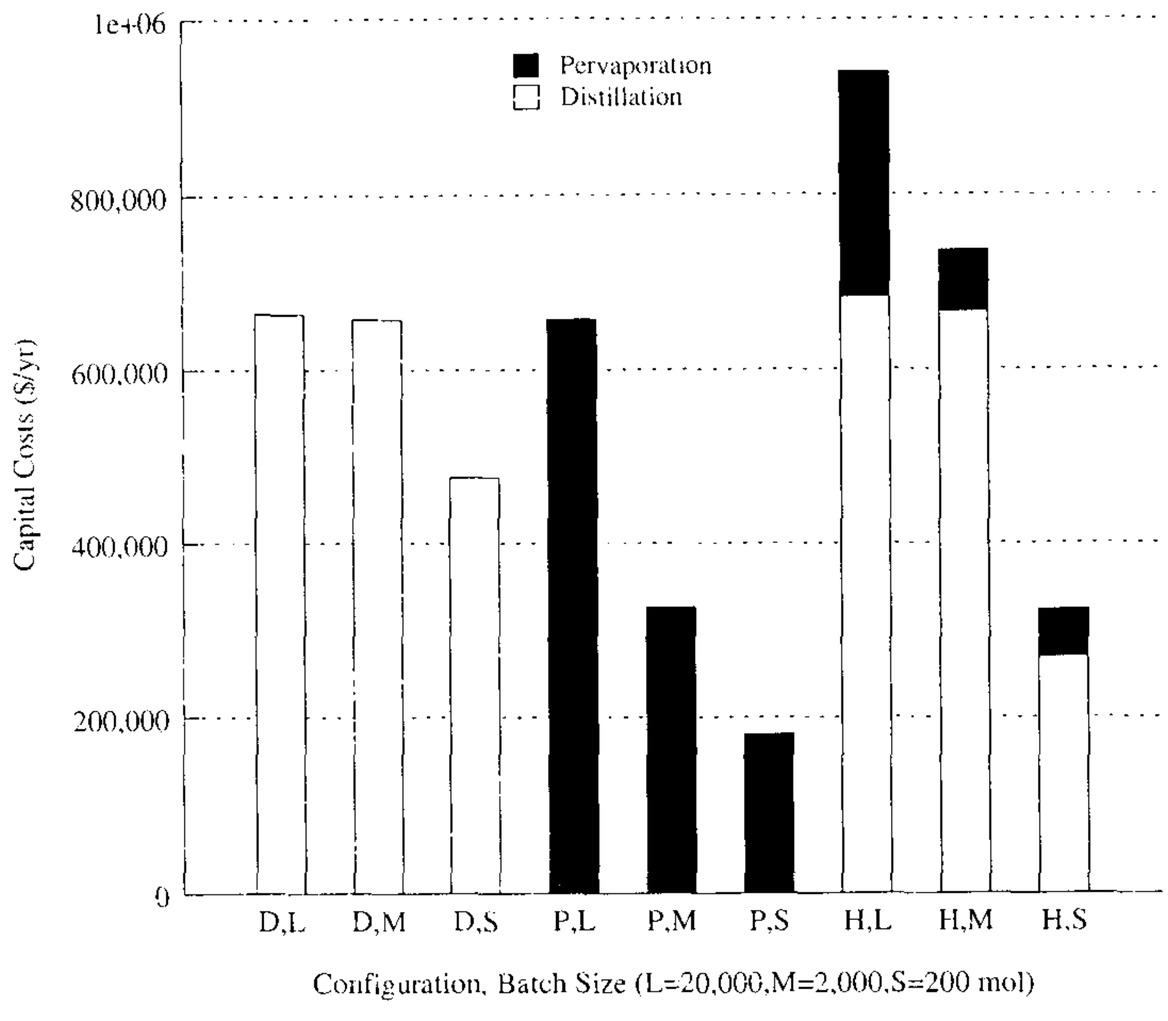

(a)

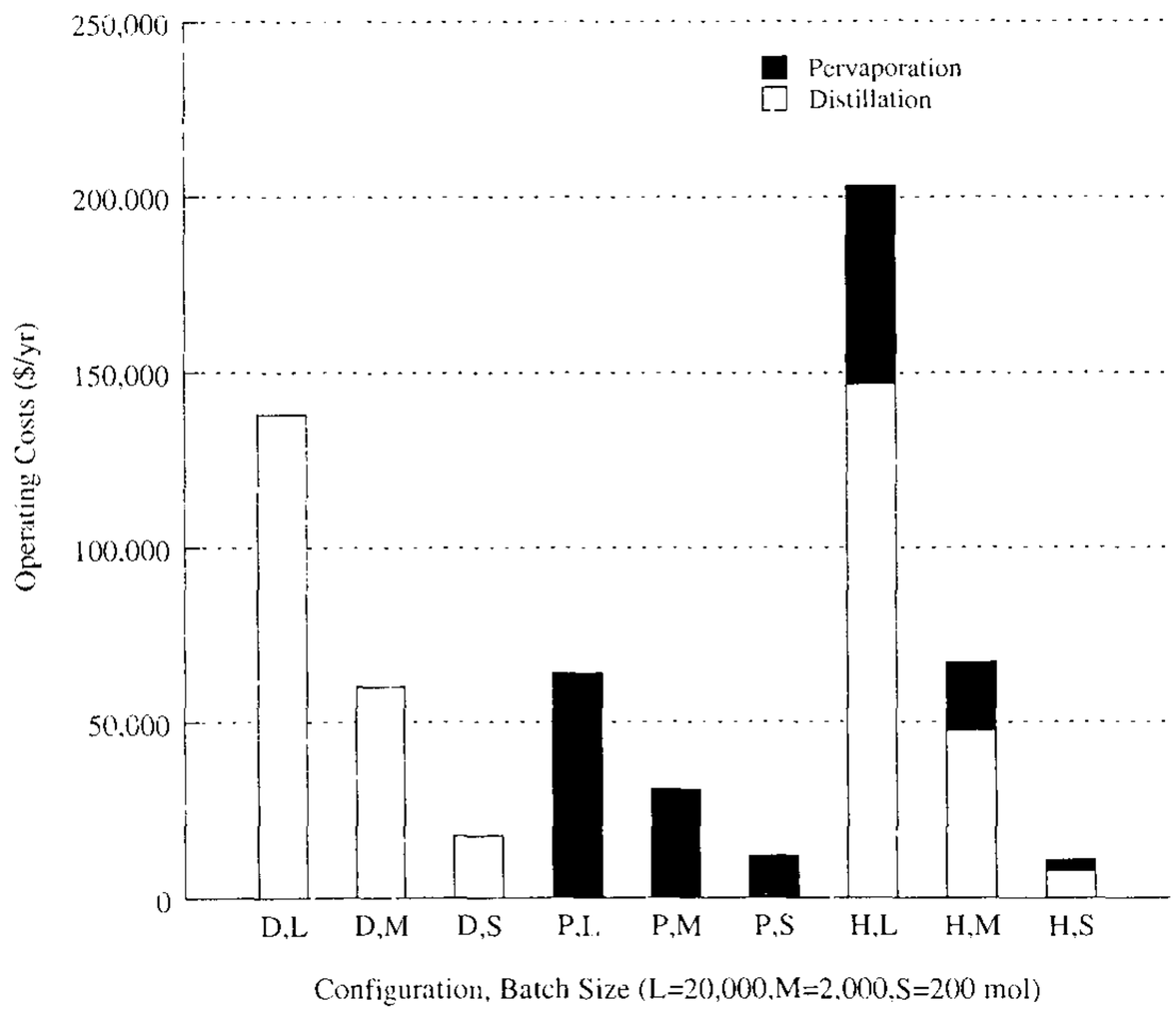

(b)

Figure 4.9: capital costs (a) and operating costs (b) as a function of batch size

4.4 Conclusions

In this work, the optimal synthesis of batch separation processes has been considered. The synthesis problem is solved through simultaneous consideration of optimal configuration, design and corresponding operating policy of all process alternatives through a process superstructure. The superstructure encompasses three different process alternatives, batch distillation, batch pervaporation and a hybrid of the two. Although other process alternatives can also be integrated into the superstructure, the complexity will greatly increase and accurate solution may become difficult to obtain.

The proposed objective function (Eq. 4.2) reflects the various trade-offs between design and operation decision variables versus production revenue as well as that of capital investments versus operating costs. An infinite feed availability and product demand has been assumed in this work. A supply and demand model can be integrated in the objective function where adequate information are available. This will reflect a more accurate representation of the number of batches than can be performed per year as well as the cost incurred and the revenue achieved from these batches. This will ultimately have an impact on the objective function and can consequently affect the optimal process selected by the synthesis procedure.

The separation of a mixture of acetone and water was used to demonstrate the procedure. The hybrid batch distillation/pervaporation configuration was found to be the optimal synthesis solution for most process scale separations, and distillation processes were second best. Pervaporation processes, however, were found to have significantly higher batch time which generally resulted in the least overall profitability.

The process scale was investigated at a fixed acetone feed composition of 0.90 mol%. Pervaporation processes were found to be most suitable at small scale, (200 mol) outperformed both distillation and hybrid processes at this scale. It is therefore concluded that batch pervaporation processes are most suited for small scale operations. For large scale separations, optimal hybrid configurations were found to be the most suitable for the case studies considered here.

Chapter 5

Optimal Synthesis of Continuous Separation Processes

This chapter considers the application of the proposed synthesis procedure proposed in Chapter 4 to the simultaneous optimisation of configuration, design and operation of continuous separation processes by considering all possible process structures. The discussion is limited to a hybrid distillation/pervaporation process and its comparison to a conventional distillation process only. The overall problem is formulated as a mixed integer non-linear programming optimisation (MINLP) problem. A case study for the separation of a tangent-pinch (acetone-water) mixture is presented and it is found that a fully integrated hybrid configuration is the optimal synthesis solution. Optimal hybrid processes can achieve significant savings in terms of annual capital costs (14%) and to a lesser extent 4% savings in operating costs, compared to an optimised conventional distillation process used to separate the same mixture.

5.1 Introduction

The optimal synthesis and optimisation of configuration, design, and operation of batch separation processes has been explored in chapter 4 of this thesis. In this chapter, the synthesis methodology is applied to *continuous* separation processes.

In the next section, the separation synthesis problem described in terms of a modified continuous process superstructure is presented, followed by the objective function formulation and optimisation problem definition. The mathematical models used in this study are then presented together with an overview of the optimisation strategy. Finally, the solution strategy is applied to a case study for the separation of a tangent-pinch mixture of acetone and water.

5.2 The Separation Synthesis Problem

5.2.1 Superstructure

The optimal synthesis of the superstructure as presented in Chapter 4 is modified to allow for continuous operation of the processes involved. The superstructure (see Figure 5.1) incorporates three separation processes: distillation, pervaporation and hybrid distillation/pervaporation processes and it is applied to a continuous operation mode. The discussion in this chapter, however, will be limited to the hybrid distillation/pervaporation process and its comparison with an optimised conventional distillation process, *i.e.* a continuous pervaporation plant is not considered.

Within the superstructure, the distillation column tray is modelled to accommodate for four extra potential streams in addition to the regular vapour and liquid inlet/outlet to the neighbouring trays. The first first stream is the reboiler vapour inlet stream (dotted lines in Figures 5.1) that allows for the optimisation of the number of trays. The second stream is the *feed stream* inlet, if the tray is selected as a distillation feed tray. The second is a side draw stream to the pervaporation unit in a hybrid configuration if the tray is

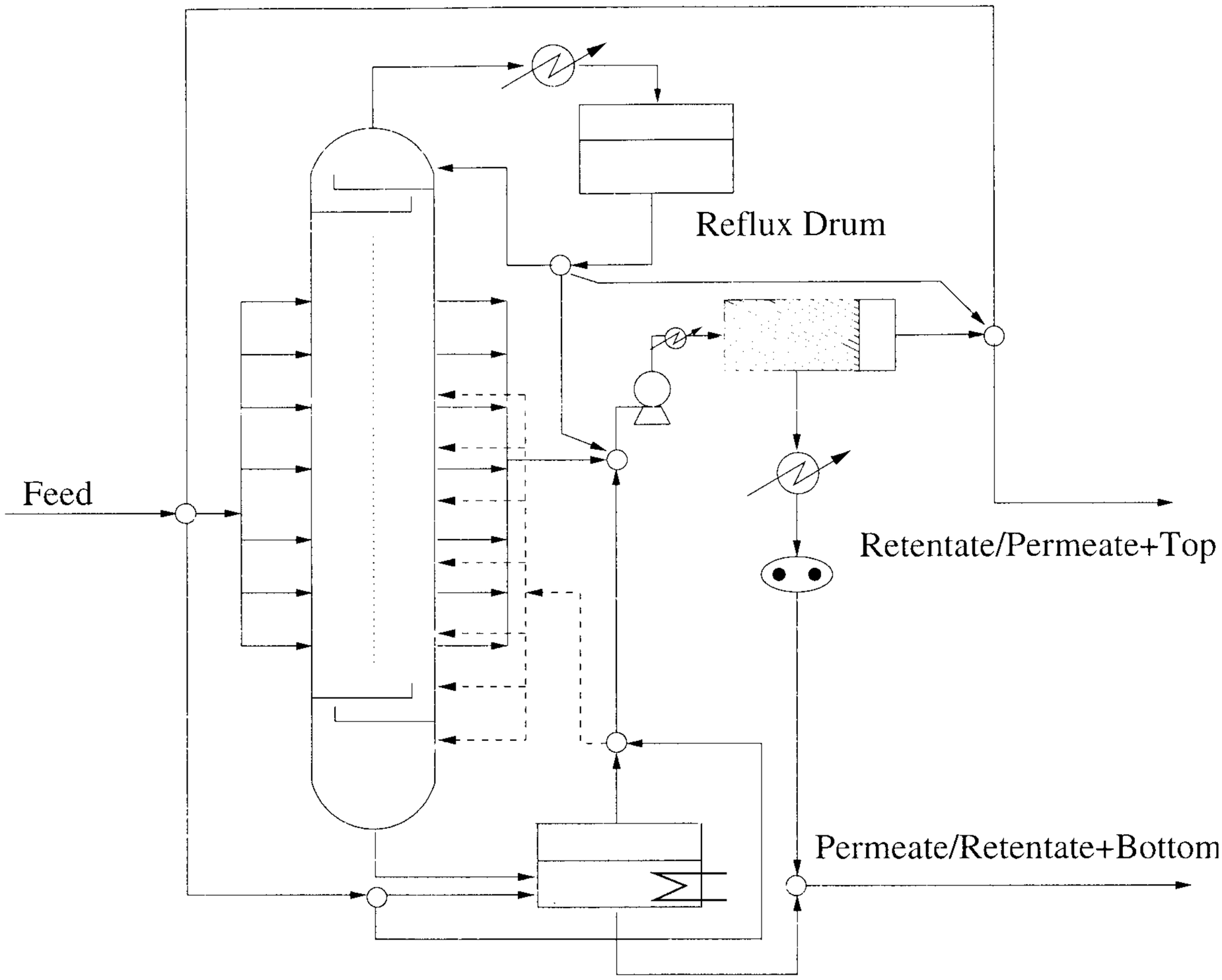

Figure 5.1: Separation processes synthesis superstructure

selected as a membrane feed tray. The third stream is an inlet stream from the pervaporation unit in a hybrid configuration if the tray is selected as a retentate recycle tray. In this work, SOS1 methods are implemented using distribution and collection node models to optimise the location of the various streams within the superstructure. The details of the mathematical equations for the distillation column, the membrane units and the node models are outlined in Appendix A.

5.2.2 Problem Definition

The objective of the synthesis procedure is to determine the optimal separation process which results in the most economical benefit when processing a given separation task. It is important that the optimal configuration, design and operation be considered simultaneously in order to result in the best available solution. The existence of trade-offs between capital investment, performance and operational decisions is evident as presented in full detail in chapter 4.

5.2.3 Objective Function

The optimal design and operation of continuous separation processes, as it is considered in this chapter, is determined as the most economical process design and corresponding operating policy that will satisfy all specified separation requirements and constraints. The optimal solution is a trade-off between capital and operating costs versus production revenue, and is reflected in the formulation of the objective function as shown below:

$$P_A = \sum_{i=1}^{N_c} C_i m_i - C_{feed} F_f - AOC_k - ACC_k \qquad k = c, m, hyb \tag{5.1}$$

Distillation Costs

The annualised capital costs for a distillation column ACC_c is given by:

$$ACC_c = UF \times \left(K_1 N_t^{0.802} V^{0.533} + K_2 V^{0.65} \right) \tag{5.2}$$

The main contributions to the operating costs are assumed to be the reboiler heating and condenser cooling duties. The operating costs AOC_c for the distillation column is therefore given by:

$$AOC_c = C_{ut,reb} \times Q_{reb} + C_{ut,cond} \times Q_{c,cond} \tag{5.3}$$

where $C_{ut,i}$ represents the cost of utility in unit i, Q_{reb} and $Q_{c,cond}$ represent the total annual consumption of energy by the reboiler heating and condenser cooling duties, respectively.

Membrane Costs

The annualised capital costs for the membrane unit ACC_m is given by:

$$ACC_m = ACC_{m,RC} \times \left(\frac{A_m}{A_{m,RC}} \times \frac{F_m}{F_{m,RC}} \times \frac{F_p}{F_{p,RC}} \right)^{0.3} \tag{5.4}$$

The feed tank heater and a permeate side cooler, in addition to the membrane feed pump and the permeate turbine, are considered to be the main contributions to the operating cost. The operating costs for the membrane process is therefore given by:

$$\begin{aligned} AOC_m &= (C_{ut,m,h} \times Q_{m,h} + C_{ut,m,cond} \times Q_{m,cond} \\ &\quad + C_{ut,p} \times Q_{m,p} + C_{ut,t} \times Q_{m,t}) \times \left(\frac{T_A}{t_s + t_f} \right) \end{aligned} \tag{5.5}$$

$$Q_{m,p} = \frac{\nu_p}{\eta_p} \left(P_p^{out} - P_p^{in} \right) \tag{5.6}$$

$$Q_{m,t} = \frac{\nu_t}{\eta_t} \times P_t^{in} \ln \left(\frac{P_t^{out}}{P_t^{in}} \right) \tag{5.7}$$

where $C_{ut,i}$ represent cost of utilities of equipment i. $Q_{m,h}$ and $Q_{m,cond}$ represent the pervaporation unit total feed tank heat duty and permeate condenser cooling duty. $Q_{m,p}$ and $Q_{m,t}$ are the total energy load of the membrane unit feed pump and permeate vacuum turbine, respectively. ν_i is the flowrate entering the ancillary equipment, i and η_i is the efficiency of the equipment i. P_i^{in} and P_i^{out} represent the pressure at the inlet and outlet of the relevant equipment, i, respectively. T_A represents the total available time for operation per annum and t_s and t_f represent the process startup and operating time respectively.

Hybrid Process Costs

The annualised capital costs ACC_{hyb} and operating costs AOC_{hyb} for the hybrid distillation column are the summation of the cost contributions of the constituent processes and are therefore given by:

$$ACC_{hyb} = ACC_c + ACC_m \tag{5.8}$$

$$AOC_{hyb} = AOC_c + AOC_m \tag{5.9}$$

5.2.4 Optimisation Problem Formulation

The objective of the synthesis procedure is to maximise the profitability defined by the objective function P_A (Eq. 5.1), subject to process type, process model equations and all separation duty constraints. The optimisation problem is therefore:

Given a feed flowrate F_f of a mixture containing a number of components N_C to be separated, minimum product purities x_i^{min}, minimum product recoveries m_i^{min}, price structure of feed and products, C_{feed} and C_i and a total production time available per annum T_A; determine the optimum set of design variables u_d , and the optimum set of operation variables u_o, to achieve the maximum objective function value P_A (Eq. 5.1):

$$\max_{u_d, u_o} P_A \tag{5.10}$$

subject to:

$$f(\dot{x}, x, u_d, u_o) = 0 \tag{5.11}$$

$$c_i(t_f) \geq c_i^{min} \quad where \quad c = [x, m] \quad and \quad i = 1, .., N_C \tag{5.12}$$

$$u_d^{min} \leq u_d \leq u_d^{max} \tag{5.13}$$

$$u_o^{min} \leq u_o \leq u_o^{max} \tag{5.14}$$

The set of operating variables for the distillation process is $u_o^c = (V, R_C)$, and the design variables set is $u_d^c = \{N_t, L_f\}$. The pervaporation process operating variables set is $u_o^m = \{R_r, P_p, Q_{m,h}\}$. R_r is defined as the fraction of retentate recycled back to the column or the feed stream (*i.e.* $R_r = 1$ means all retentate is recycled and $R_r = 0$ means all flows to the retentate product stream). The set of design variables for the pervaporation process is $u_d^m = \{N_m\}$.

For the hybrid distillation process, the set of operating variables and design variables are a combination of the previous two processes with two additional design variables for the membrane feed location (from the column) L_s and the retentate recycle location L_r (back to the column).

5.2.5 Process Models

The distillation column mathematical models and equations outlined in Appendix A are used to conduct the optimisation of continuous separation processes as described in section 5.2.4. The mathematical model used in this study to describe the performance of hollow fibre pervaporation membrane modules is also outlined in Appendix A.

The mathematical model of the hybrid distillation/pervaporation process is a combination of the distillation and pervaporation models outlined above. Models of various complexity, can be used with the approach outlined depending on the purpose of the optimisation. It should be noted, however, that the computational time required to solve these models and the accuracy of the results obtained, is influenced by the degree of modelling complexity used.

5.2.6 Solution Methodology

The simultaneous consideration of optimal configuration, design and operation of continuous hybrid distillation/pervaporation separation processes as outlined above, translates into an optimisation problem with both discrete (*e.g.* number of trays and number of membrane modules) and continuous variables (*e.g.* reflux and recycle ratios). Furthermore, the

non-linear dynamic models used here, as well as the non-linear objective function defined in Eq. 5.1, transform the problem into a complex mixed integer non-linear programming optimisation (MINLP) problem. The proposed separation superstructure in this chapter is solved using a steady state genetic algorithm (GA) optimisation framework that works through the genetic algorithm operators as detailed in Chapter 3.

The genetic parameter used are: a roulette wheel selection scheme, replacement rate, P_{ss}, of 75%, crossover rate, P_c, of 75%, mutation rate, P_m, of 10%, population size, N_{pop}, of 100 genomes, and a stopping criterion based on a maximum number of generations (typically 200 for 15,000 function evaluations). The GA parameter values used here are demonstrated to yield good results in the sensitivity analysis outlined in Appendix C.

5.3 Results and Discussion

The optimal process synthesis procedure developed in this work is demonstrated by considering the continuous separation of an equimolar tangent-pinch mixture of acetone and water. The separation process specifications are shown in Table 5.3.1. It is assumed that all energy duties, Q_i, carry the same utility cost index, $C_{ut,i}$, although different indices could have easily been used.

5.3.1 Optimal Solution

The optimum solution sets of the superstructure and that of a comparative distillation case are shown in Table 5.3.1. A fully integrated hybrid distillation/pervaporation process is found to be the optimal synthesis solution. The optimal number of trays (where tray 1 is the top tray of the distillation column) and membrane modules are found to be 18 & 1, respectively. The optimal feed stream location is found to be at tray 16 as expected for a tangent-pinch mixture where the separation is more difficult at the top of the column, and the unpure feed is directed to the bottom of the column. Optimal reflux and recycle ratios are found to be 0.92 and 0.23, respectively. Optimal reboiler vapour load is found to be 4.32 mol/s with optimal sidedraw flowrate of 2.72 mol/s. The optimal membrane inlet

heater temperature is found to be at its upper bound, 330 K, as expected, and permeate side pressure is 370 Pa. Optimal sidedraw location is found to be at tray 1, with optimal retentate return location to tray 5 of the hybrid column.

The optimal design and operation of the hybrid distillation/pervaporation is found to be the most profitable process alternative that meets all separation requirements for this case study (see Table 5.3.1), with an estimated profit of $22.85 M per annum. The optimum hybrid process is found to be of a comparable profit to the optimal distillation process. Only a 1.0% increase in profitably can be achieved with an optimised hybrid column (Table 5.3.1). It is noted, however, that the capital cost of the hybrid column (distillation and membrane) is considerably lower than that of the conventional distillation process where a 14% saving can be achieved. Similar savings, though not as large, in operating costs can be achieved where the hybrid process shows a 4% decrease compared to the optimal distillation process.

5.4 Conclusions

In this work, the optimal synthesis of continuous separation processes has been considered. The synthesis problem is solved through simultaneous consideration of optimal configuration, design and corresponding operating policy of all hybrid process alternatives described through a process superstructure. The optimal solution is then determined as the most economical process configuration, design and operation that achieves all separation requirements. The problem objective function reflects the various trade-offs between design and operation decision variables versus production revenue, as well as that of capital investments versus operating costs. A hybrid distillation/pervaporation configuration was found to be the optimal synthesis solution for the separation of the equimolar tangent-pinch acetone-water case considered, however, the hybrid process was only marginally more profitable than the conventional distillation process.

Property	**Value**
Feed composition, $x_{i,feed}$ $(molefrac.)$	
Acetone	0.50
Water	0.50
Feed rate, F_{feed} (mol/hr)	18,000
Product purity specifications, $x_{i,f}$ $(molfrac.)$	≥ 0.97
Product recoveries, $M_{i,f}$	≥ 0.70
Tray/Cond./Reboiler holdup (mol)	1/100/500
Column operating pressure, P (atm)	1.0
Available production time, T_A (hr)	7920
Cost, C_i $(\$/mol)$	
Acetone	0.606*
Water	0.0038*
Feed	0.150
Offcut	0.010
Utility $(\$/MJ)$	0.019**
K1	1500†
K2	180†
UF	4.31‡

* Adopted from Mujtaba (1999), ** Adopted from Sinnott (1993),
† Adopted from Longsdon et al. (1990), ‡ Calculated from IChemE (1988)

Table 5.1: Unit specifications and operating conditions

	Optimal Hybrid	**Optimal Distillation**
Design Variables	$u_d = \{N_t, N_m, , L_f, L_s, L_r\}$	$u_d = \{N_t, L_f\}$
	$u_d = \{18, 1, 16, 1, 5\}$	$u_d = \{23, 22\}$
Operation Variables	$u_o = \{R_c, R_r, P_p, V, F_m\}$	$u_o = \{R_c, V\}$
	$u_o = \{0.92, 0.23, 370, 4.32, 2.72\}$	$u_o = \{0.58, 4.50\}$
Revenue (M$/yr)	23.55	23.42
Capital Cost ($/yr)	503,000	572,000
Operating Costs ($/yr)	195,000	203,000
Profit (M$/yr)	22.85	22.64

Table 5.2: Optimal solution sets for case study

Chapter 6

Multi-Objective Optimisation of Batch Separation Processes

This chapter considers for the first time the simultaneous multi-objective optimisation of design and operation of batch distillation as well as of batch hybrid distillation/pervaporation processes. The overall problem is formulated as a multi-objective mixed integer dynamic optimisation (MO-MIDO) problem. The optimisation strategy comprises of different ranking procedures that allow the determination of the Pareto optimal set. A case study for the separation of a homogeneous tangent-pinch (acetone-water) binary mixture is presented for a dual-criteria optimisation case of minimising capital investment while at the same time minimising the energy consumption rate during the batch. It is found that the proposed distance ranking procedure yields the best Pareto optimal set when compared to other non-dominated sorting procedures. Furthermore, the distance ranking procedure was found to be further improved when used with an elitism operator.

6.1 Introduction

The performance of batch distillation and hybrid distillation/pervaporation processes depends on a number of different criterion that are often conflicting (*e.g.* revenue & cost). The effective optimisation of such systems therefore requires the consideration of multi-criteria approaches to accommodate for the multi-objective nature of the problem and to effectively evaluate and optimise the performance in order to meet the objectives. Although the optimisation of design and operation of distillation processes has been attempted before, this work is the *first* where the simultaneous multi-objective optimisation of design and operation of such processes is considered.

The existence of multiple performance measures in a problem results in a set of optimal solutions known as Pareto optimal solutions, instead of a single optimal solution (Deb et al., 2002). Solutions in the Pareto optimal set are all equivalent, therefore in the absence of user-defined decision making information, no solution can be said to be better than the other. The solutions in the Pareto optimal set can therefore to assist in the decision making process by highlighting the tradeoffs involved in the problem studied. Depending on which objective is regarded as more important than the other(s) (*e.g.* capital investment savings is favoured over energy savings), the decision will clearly have an impact of some extent on the other decision variables. Conventionally, multiple objectives are combined into a single objective function composed of the weighted sum of individual objectives, thereby allowing for solutions using existing single-objective optimisation techniques. Other methods suggest using one objective function at a time and combining the solution results of the different optimisation runs in order to obtain the Pareto optimal set (Dedieu et al., 2003).

The objective of this work is to propose a genetic-algorithm based multi-criteria optimisation procedure that allows the determination of the Pareto optimal set for multi-objective optimisation of design and operation of batch distillation processes. In the next section, a background to multi-objective optimisation is presented. The multi-criteria batch separation optimisation problem is then outlined followed by the objective functions formulation

and the optimisation problem definition. The mathematical models used in this study are then given together with an overview of the solution methodology employed. Finally, the multi-criteria batch separation process optimisation problem and its solution strategy are applied to a case study which considers the separation of a tangent-pinch mixture of acetone and water.

6.2 Multi-Objective Optimisation

Multi-objective optimisation is the simultaneous consideration of two or more objective functions that are completely or partially in conflict with each other. The *optimality* of such optimisations is largely defined through the Pareto optimality (Pareto, 1896) which is based on the Pareto dominance criteria as defined below.

Pareto Optimality

Assume minimisation of k objectives to be optimised simultaneously:

$$Minimise \quad \vec{f}(g_i) = (f_1(g_i), f_2(g_i), \ldots, f_k(g_i)) \quad \forall i, \ldots, N_{sol} \tag{6.1}$$

G is the feasible solution set space. A solution set $u \in G$ is said to dominate $v \in G$ (denoted by $u \prec v$) if and only if

$$\forall i \in \{1, \ldots, k\} : f_i(u) \leq f_i(v) \qquad \wedge$$

$$\exists j \in \{1, \ldots, k\} : f_j(u) < f_j(v) \tag{6.2}$$

For a given multi-objective optimisation problem $f(g)$, the Pareto optimal set (P^*) is defined as:

$$P^* := \left\{ g \in G \quad | \quad \neg \exists g' \in G \quad \vec{f}(g') \prec \vec{f}(g) \right\} \tag{6.3}$$

i.e. a solution set g is a member of the Pareto optimal set if there exists no other feasible solution set g' that dominates the set g.

For a given multi-objective optimisation problem $\vec{f}(g)$ and Pareto optimal set (P^*), the Pareto front (PF^*) is defined as:

$$PF^* := \left\{ \vec{f}(g) \quad | \quad g \in P^* \right\} \tag{6.4}$$

6.3 The Multi-Objective Batch Separation Problem

6.3.1 Problem Definition

The goal of multi-objective optimisation is generally to determine a range of different process alternatives to explore the trade-offs between two or more conflicting design and/or operational criteria. All optimal process alternatives will need to satisfy given constraints in meeting these criteria. To achieve this goal, it is important that all of these criteria be considered *simultaneously* through an effective multi-objective optimisation procedure.

In batch separation processes there is a trade-off between capital investment and energy consumption in terms of equipment sizing and performance. For instance, the design of high performance equipment will generally incur high capital investment but low operational and energy costs. Alternatively, low performance equipment, requiring less capital investment but more operational and energy costs, can be considered. Longer batch times required for high product recovery will also lead to higher energy consumptions than would low recovery. Thus the multi-criteria balance between capital investment and energy consumption must be considered.

6.3.2 Objective Functions

The problem of optimal design and operation of batch separation processes, as it is considered in this work, is to determine the Pareto optimal solution set that will satisfy all specified separation requirements and constraints. The multiple objectives to consider are; 1) the investment cost and 2) the energy consumption rate (energy duty) during the batch.

The investment cost is based on column costing by Longsdon et al. (1990) and membrane costing as detailed in Chapter 4 and Appendix D of this thesis:

$$f_1 = CC_i \quad where \quad i = [c, hyb] \tag{6.5}$$

$$CC_c = UF \times \frac{1}{CRF_c} \times \left(K_1 N_t^{0.802} V^{0.53} + K_2 V^{0.65} \right) \tag{6.6}$$

$$CC_{hyb} = CC_c + CC_m \tag{6.7}$$

where the membrane module investment costs CC_m is given by:

$$CC_m = \frac{1}{CRF_m} \times CC_{m,RC} \times \left(\frac{A_m}{A_{m,RC}} \times \frac{F_m}{F_{m,RC}} \times \frac{F_p}{F_{p,RC}} \right)^{0.3} \tag{6.8}$$

The energy consumption rate during the batch is given by;

$$f_2 = E_i \quad where \quad i = [c, hyb] \tag{6.9}$$

$$E_c = \frac{Q_{reb} + Q_{c,cond}}{t_f + t_s} \tag{6.10}$$

$$E_{hyb} = E_c + E_m \tag{6.11}$$

where the membrane module energy consumption E_m is given by:

$$E_m = \frac{Q_{m,h} + Q_{m,cond} + Q_{m,p} + Q_{m,t}}{t_f + t_s} \tag{6.12}$$

$$Q_{m,p} = \frac{\nu_p}{\eta_p} \left(P_p^{out} - P_p^{in} \right) \tag{6.13}$$

$$Q_{m,t} = \frac{\nu_t}{\eta_t} \times P_t^{in} \ln \left(\frac{P_t^{out}}{P_t^{in}} \right) \tag{6.14}$$

where Q_{reb} and $Q_{c,cond}$ are the total heat and cooling load of the reboiler and condenser, respectively. $Q_{m,h}$ and $Q_{m,cond}$ are the membrane heater and condenser heat and cooling

load respectively. The energy load of the membrane feed pump and permeate turbine are denoted $Q_{m,p}$ and $Q_{m,t}$, respectively. ν_i is the flowrate entering the ancillary equipment, i and η_i is the efficiency of the equipment i. P_i^{in} and P_i^{out} represent the pressure at the inlet and outlet of the relevant equipment, i, respectively. t_s and t_f represent the batch setup and batch time respectively.

The optimisation problem can then be stated:

Given a mixture m_{feed} with number of components N_c to be separated, minimum product purities x_i^{min}, minimum product recoveries m_i^{min}; determine the optimum set of design variables u_d, and the optimum set of operation variables u_o, to minimise the investment cost, CC_i, while at the same time minimising the energy consumption rate during the batch, E_i:

$$\min_{u_d,u_o} \quad [CC_i, E_i] \qquad i = [c, hyb] \tag{6.15}$$

subject to:

$$f(\dot{x}(t), x(t), t, u_d, u_o(t)) = 0 \tag{6.16}$$

$$c_i(t_f) \geq c_i^{min} \quad where \quad c = [x, m] \quad and \qquad i = 1, .., N_C \tag{6.17}$$

$$u_d^{min} \leq u_d \leq u_d^{max} \tag{6.18}$$

$$u_o^{min} \leq u_o \leq u_o^{max} \tag{6.19}$$

Equation 6.16 represents the mathematical model of the process; x is a vector of process state variables, u_d and u_o denote the vectors of design and operating control variables, respectively. Equation 6.17 represents the product purity and recoveries constraints imposed which must be satisfied at the end of the batch. Equations 6.18 and 6.19 represent the physical and optimisation bounds of the design and operating variables, respectively.

The set of design and operating optimisation decision variables for both batch distillation and batch hybrid processes are outlined in Table 6.1 below.

	Design Variables	Operation Variables
Distillation	$u_d = \{N_t\}$	$u_o = \{t_f, t_i, R_c, V\}$
Hybrid	$u_d = \{N_t, N_m, L_s, L_r\}$	$u_o = \{t_f, t_i, R_c, R_r, R_p, P_p, V, F_m\}$

Table 6.1: Optimisation variables considered

6.4 Process Models

The models detailed in Chapter 3 and its relevant equations found in Appendix A were implemented to describe the behaviour of the distillation and hybrid distillation/pervaporation processes considered in this work.

6.5 Solution Methodology

Simultaneous multi-objective consideration of optimal design and operation of batch separation processes translates into an optimisation problem with both discrete (e.g. number of trays) and continuous variables (e.g. reflux ratio). Furthermore, the non-linear dynamic models used here as well as the non-linear objective functions defined, transform the problem into a complex multi-objective mixed integer dynamic optimisation (MOMIDO) problem.

The solution of multi-objective optimisations, where the definition of optimality is different, requires different solution techniques than those adopted for *single* objective optimisation problems. There are a number of classical methods for solving these optimisations where single objective optimisation (often gradient-based) techniques are used (Deb, 2001). One of these methods is the so-called weighted sum methods where the objectives are pre-multiplied with user-supplied weights, (w_i), representing the relative significance of the objectives to each other to form a single objective function (*e.g.*, $\min a$, where $a = w_1 \times b + w_2 \times c + \ldots + w_i \times z$). The optimisation will then need to be repeated for different combinations of objective weights to obtain the Pareto optimal set. Although this method is rather easy to use, repeating the optimisation procedure many times may

not be a feasible option for large optimisation problems. Furthermore, setting an appropriate balance between the objectives to result in a full exploration of the desired range of trade-offs within the objectives space can be difficult, especially where a non-convex objective space is explored.

Haimes et al. (1971) proposed the ϵ-constraints method in order to alleviate the difficulties faced by the weighted sum in solving problems having non-convex objectives space. In this method all but one of the objectives are converted into constraints. However, user-defined limits to these constraints will need to be pre-defined.

These methods and other classical ones, such as the Benson Method (Benson, 1978) and the Goal Programming method (Ignizio (1978)), are limited by the fact that the single optimisation procedure will need to be repeated many times to obtain a range of solutions in the Pareto optimal set. It should also be noted that repeating the optimisation n times does not guarantee that all n solutions are non-dominated as defined by the Pareto optimality above. Classical multi-criteria optimisation methods can therefore be time consuming when employed to solve multi-objective optimisation problems.

Genetic algorithm has the advantage, over classical multi-criteria optimisation methods, by its nature to relay on the evolution of solution populations (Chapter 3) which, if properly exploited, can produce the Pareto optimal set in a single optimisation run. In GA, the genome fitness is the driving mechanism of the genetic evolution and hence a crucial parameter in determining the effectiveness and efficiency of a GA-based multi-criteria algorithm. Over the last decade, many suggestions have emerged for alternative definitions of the solution or *genome* fitnesses in order to equally emphasise all non-dominated solutions while simultaneously maintaining the diversity of the genetic populations (*e.g.* Srinivas and Deb (1994), Osyczka and Kundu (1995) and Deb et al. (2002)).

In this work, the use of different ranking-based fitness procedures is investigated when solving the multi-objective optimisation problem of the batch distillation and the hybrid separation processes.

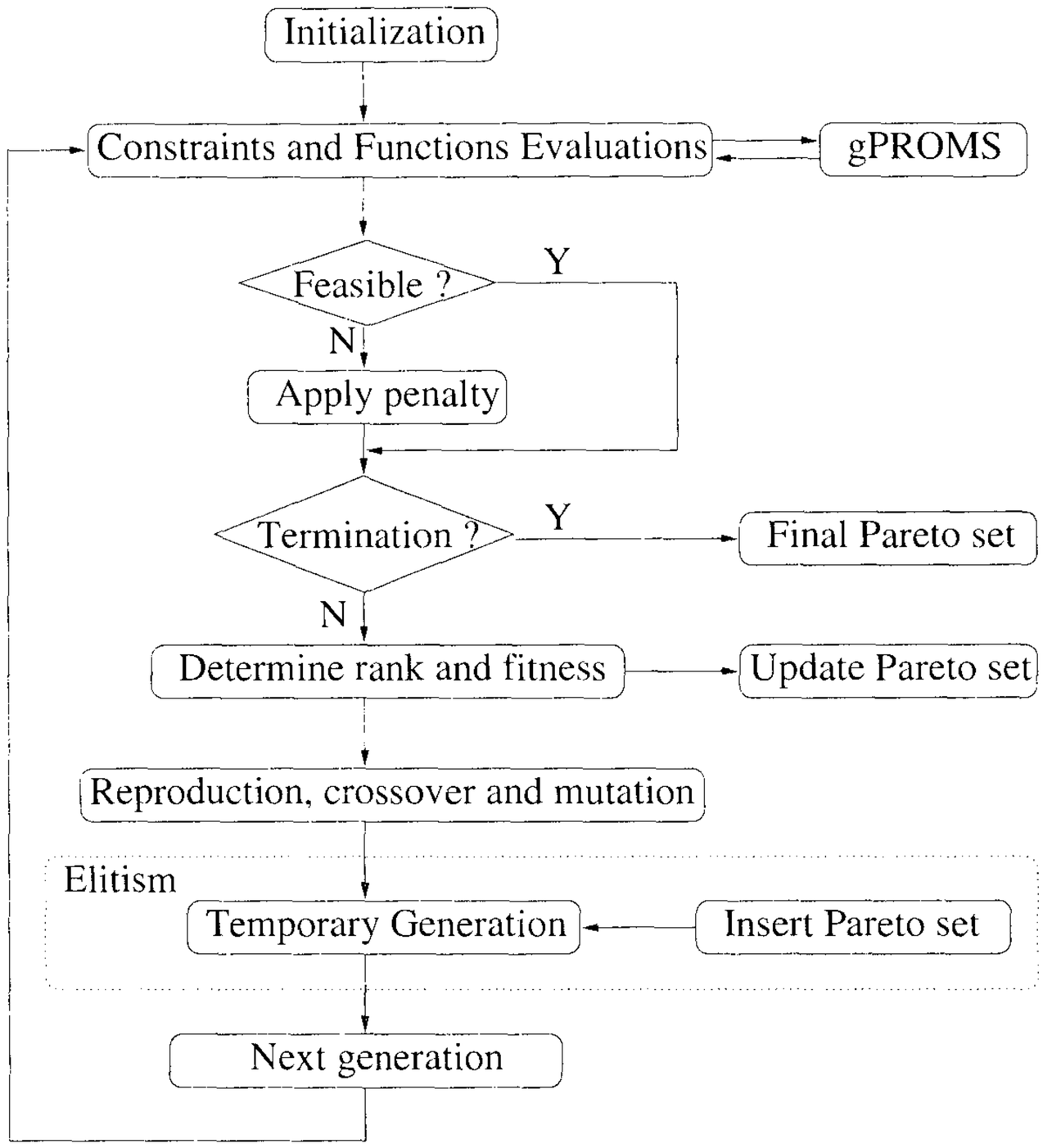

Figure 6.1: GA procedure

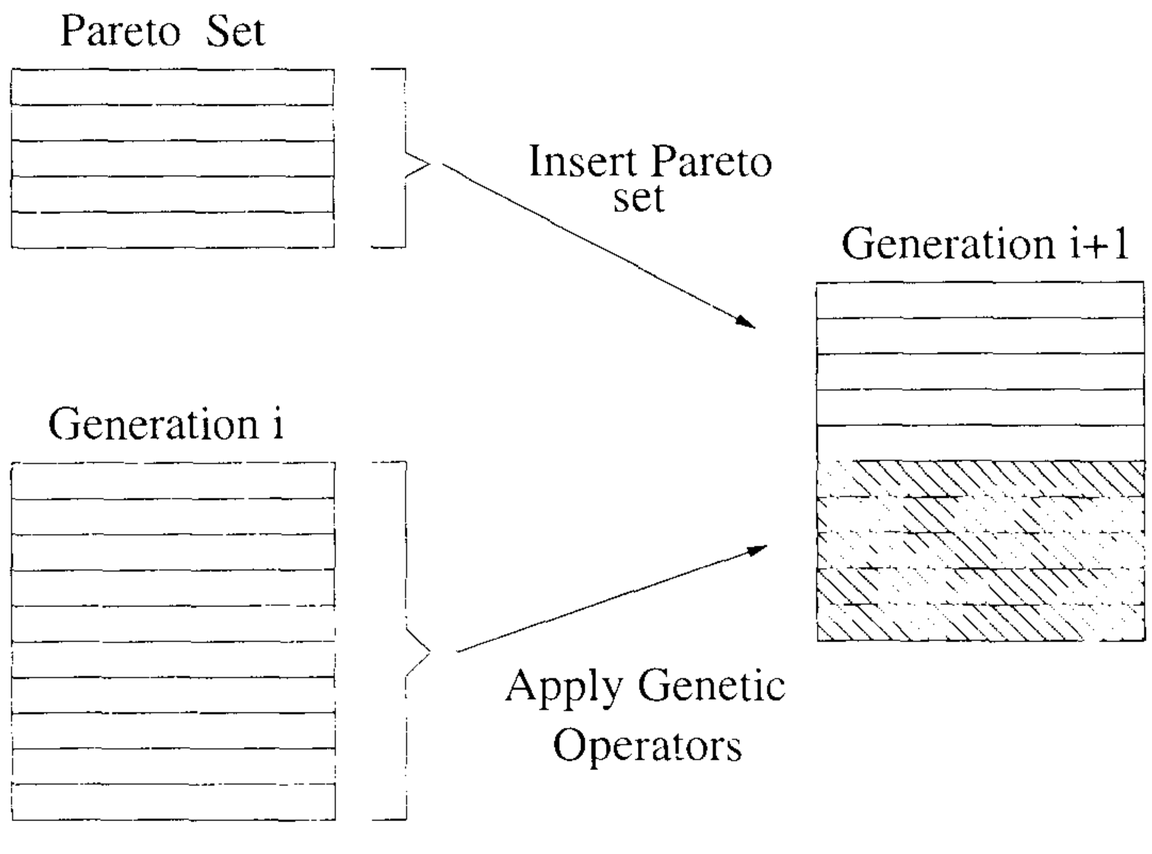

Figure 6.2: Elitism procedure

The proposed multi-criteria GA optimisation framework works through the following steps (see Figure 6.1):

1. Create a randomly generated initial population
2. Evaluate objective function and constrains of individuals in population
3. Rank the genomes (see Section 6.6) and calculate fitnesses
4. Reproduce, crossover, mutate and perform elitism (if desired) to obtain a new generation
5. Repeat steps 2-5 until a pre-set convergence criterion is met

Where elitism operator is implemented, elitism is performed as follows:

a. If population is infeasible, use elitism size of e_i to copy best solutions
b. If population is feasible, update the Pareto set and use elitism size of e_s given in Eq. 6.20 below, where S_{front} is the number of solution in the Pareto optimal set:

$$e_s = \max\left(e_i, S_{front}\right) \tag{6.20}$$

c. Apply genetic operators to current population to create $N_{pop} - e_s$ individuals (see Fig. 6.2)
d. Insert elite set of size e_s to the temporary generation created in step c above to create the next genetic generation (see Figure 6.2)

In this work, decision variables are represented in the genome as direct real values instead of converted binary bits and mapping which has been found to be less efficient (Coley, 1999). The initial population is created randomly. The objectives and constraints of each individual in this population are evaluated using the gPROMS simulation software (PSE, 2005). A penalty function procedure is applied (Eq. 6.22) to infeasible solutions with

the aim of minimising their occurrence in successive generations. Solutions are assigned a rank based on whether an individual is infeasible, dominated or non-dominated with respect to the rest of the population using the Pareto domination concept (Section 6.2) that defines dominated and non-dominated solutions. The ranking procedure, as detailed in the next section, rewards non-dominated solutions at the expense of others in order to encourage the GA to drive the population towards generations of successively better Pareto fronts. When the proposed elitism procedure is applied, the size of the elite set in infeasible populations e_i should be small ($e_i = 2$ was used here) in order to preserve the diversity of the genetic populations which will result in quicker population feasibility. This is also necessary to avoid premature and local optimality convergence of the algorithm.

The GA procedure is based on the total replacement population strategy of the simple GA framework as detailed in Chapter 3 and uses a tournament selection procedure (with a tournament size, T_s, of 2), crossover rate, P_c, of 75%, mutation rate, P_m, of 10%, population size, N_{pop}, of 100 genomes and a stopping criterion based on either 1) all population members are part of the Pareto front or 2) maximum number of generations (here 200 for 20,000 functions evaluations is used) has been exceeded. The procedure has been implemented using the GALib genetic algorithm library (Wall, 1999).

6.6 Ranking Procedure

As solution or *genome* ranking is crucial in the successful implementation of a multi-criteria GA, this work considers various ranking algorithms to investigate their effects on the solution quality. Ranking procedures consist of the classification of individuals into different categories based on the Pareto dominance criteria described in Section 6.2. The ranking of solutions is proportional to the fitness of genomes and should emphasise all non-dominated solutions equally while at the same time it maintains the diversity of the population by preferring these solutions to those they dominate. This will allow the non-dominated solution to equally progress towards the Pareto front while encouraging the dominated solutions to evolve, as their ranks and hence fitnesses are lower, into non-dominated ones. Srinivas

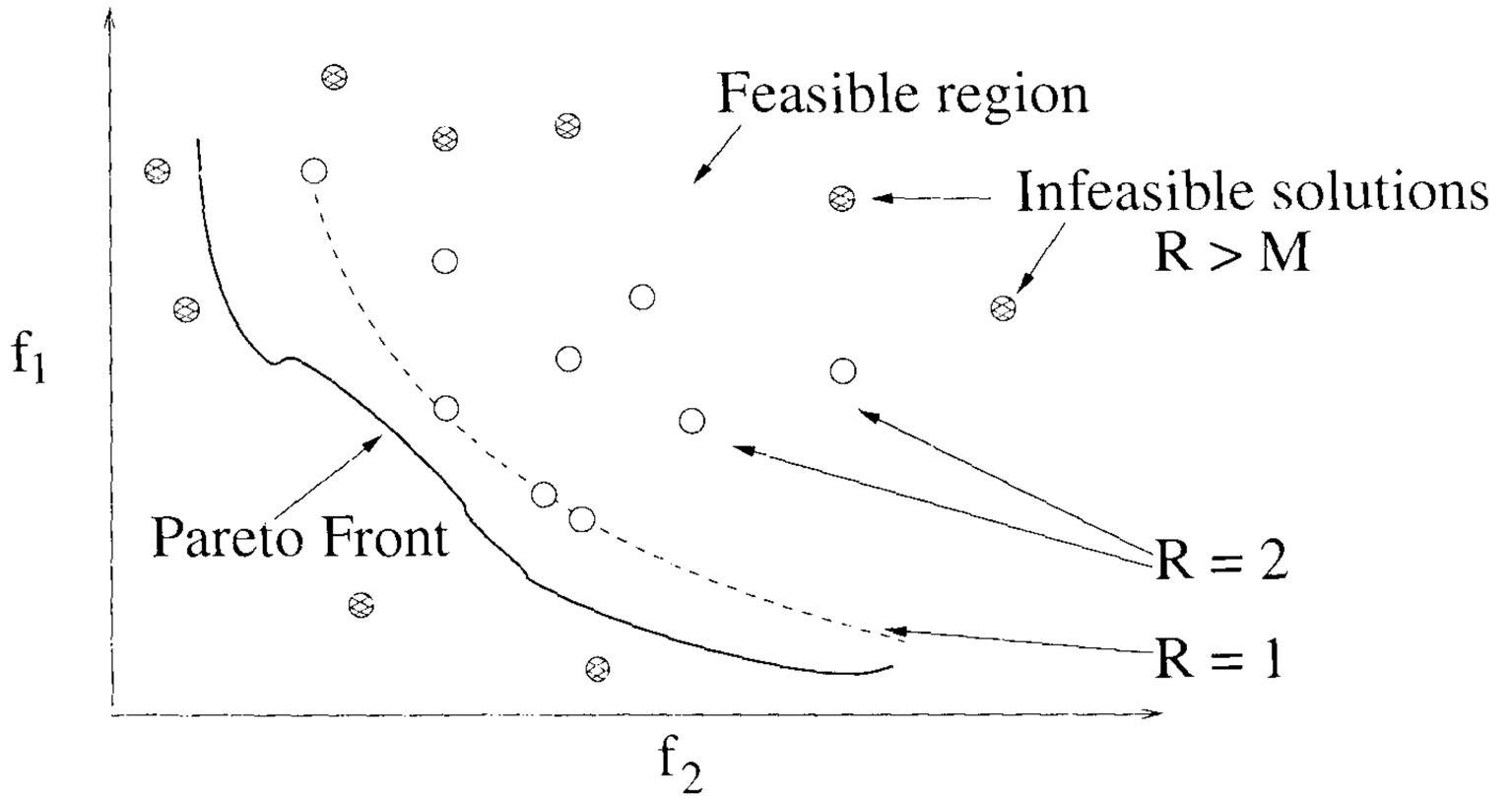

Figure 6.3: Single-front ranking

and Deb (1994) implemented the idea of non-dominated sorting (Goldberg, 1989) to rank solutions depending on their closeness to the real Pareto front. A reduced form of this ranking termed *single-front* ranking has been proposed and implemented in this work. The proposed single-front ranking is then compared to the multi-front ranking presented by Srinivas and Deb (1994). These procedures are also compared to a proposed geometrical-distance-based ranking method termed *distance ranking*. The following sections detail the ranking methods used in this work.

6.6.1 Single-Front Ranking (S-F)

The single-front ranking procedure classifies all non-dominated genomes into a single rank assigned 1 as shown in Figure 6.3. The rest of the dominated genomes within the feasible solution space are assigned a rank of 2. All other genomes outside the feasible region are assigned a large rank ($> M$) relative to the amount of constraints violated (Eq. 6.22). The aim of the optimisation is the minimisation of these ranks in order to obtain as many genomes of rank 1 as possible. The single-front procedure works through the following steps (see Figure 6.3):

1. All non-dominated individuals of the population are identified and assigned rank $R = 1$

2. All dominated individuals are assigned rank $R = 2$

3. All infeasible point are assigned a rank according to Eq. 6.22 where the minimum rank is M (M is a large number, typically 1×10^6).

$$R(g) = \begin{cases} 1 & \text{if solution is feasible and non-dominated} \\ 2 & \text{if solution is feasible but dominated} \\ \prod_{i=1}^{N_c} \kappa_i & \text{if solution is infeasible} \end{cases} \tag{6.21}$$

where κ_i is the penalty term defined as:

$$\kappa_i = \begin{cases} M \times \left[2 - \left(1 - \frac{c_i^{min} - c_i(t_f)}{c_i^{min}}\right)\right] & if \quad c_i(t_f) < c_i^{min} \qquad \forall i = 1, \ldots, N_c \\ M & otherwise \end{cases} \tag{6.22}$$

6.6.2 Multi-Front Ranking (M-F)

The multi-front ranking procedure (Srinivas and Deb, 1994), similarly to the single-front procedure, works through the ranking of the genomes within the feasible solutions space into fronts representing a particular class. In multi-front ranking, however, the genome rank is determined by whether it is dominated or not as well as if it dominates any other genomes in the population. *i.e.* If a genome A is dominated, another dominance check is preformed within all dominated genomes to see if the dominated genome A dominates any other genomes. The overall procedure identify all non-dominated individuals and assigns them a rank of 1 (Figure 6.4). These are then excluded from the next round of ranking where only dominated solutions are checked for their dominance with the rest of the population and assigned a rank 1+i (i is the round number for the domination check). The procedure is repeated until all genomes within the feasible space are given a rank. Non feasible solutions are penalised according to the constraints violation using equation

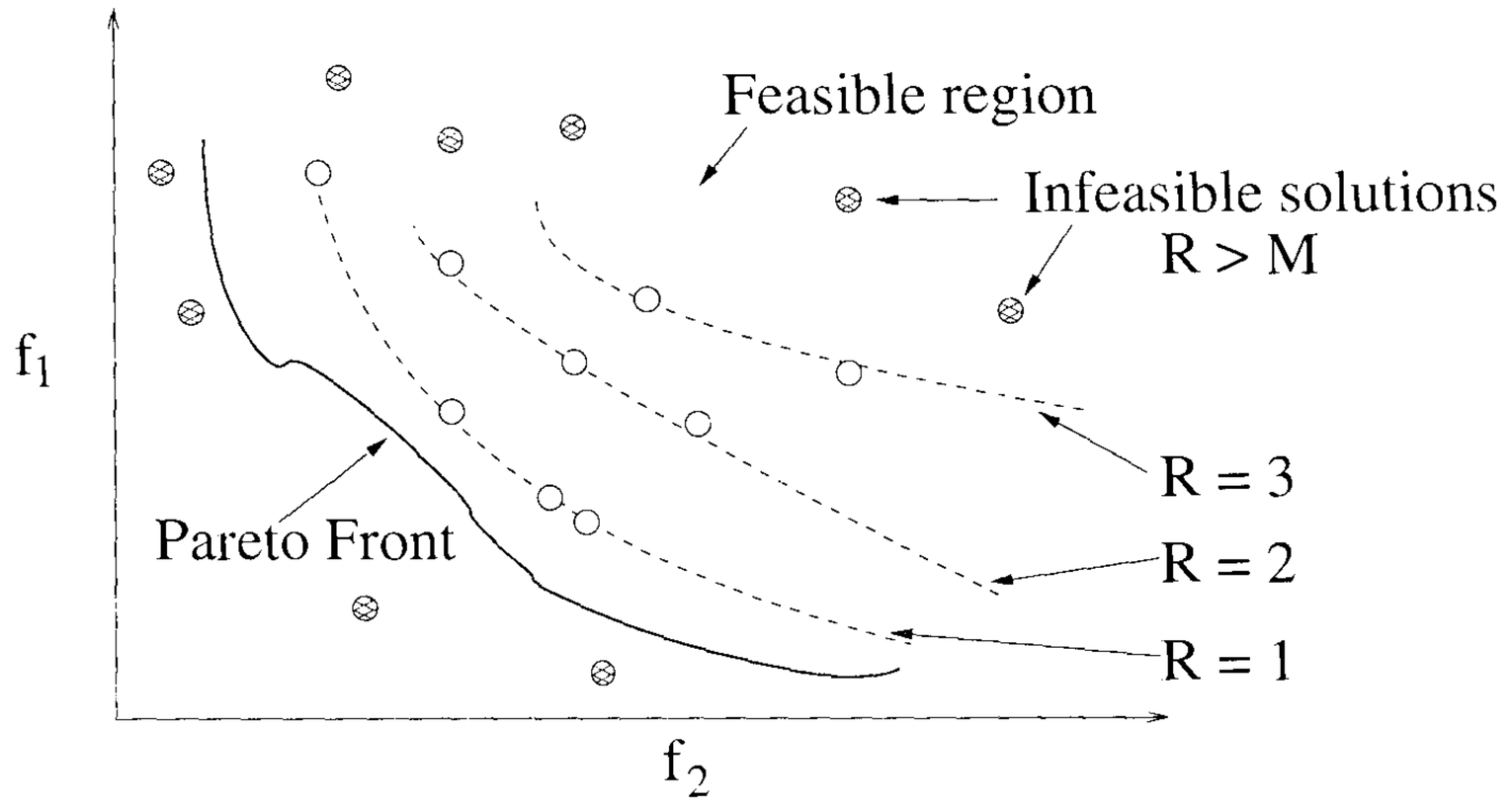

Figure 6.4: Multi-front ranking

6.22. In summary, the multi-front procedure works through the following steps (see Figure 6.4):

1. All non-dominated individuals of the populations are identified and assigned a rank $R = 1$

2. Within the dominated solutions found in previous step, identify all new non-dominated individuals and assign a rank of $R = 2$

3. Repeat step 2 until all individuals are ranked, giving the most inferior front (one that is dominated by all others) a rank equal to the number of fronts found, $R = N_{front}$

4. All infeasible point are assigned a rank according to Eq. 6.22 where the minimum rank is M

$$R(g) = \begin{cases} 1 & \text{if solution is feasible and non-dominated} \\ 2 & \text{if solution is feasible and dominated by 1 ONLY} \\ 3 & \text{if solution is feasible and dominated by 1 and 2} \\ . & ..... \\ N_{front} & \text{if solution is feasible but dominated by all} \\ \prod_{i=1}^{N_c} \kappa_i & \text{if solution is infeasible} \end{cases} \tag{6.23}$$

6.6.3 Distance Ranking and Elite Distance Ranking (D and D-E)

The proposed distance ranking procedure calculates the geometrical distance between the non-dominated solutions (Pareto optimal set) and the rest of the feasible solutions in the population. The aim of the procedure is to reward genomes that are on the Pareto optimal set by assigning them with a rank of zero (because they calculate the distance to themselves) and encourage other solutions based on how far they are from this optimal set (Eq. 6.24). The optimal set is checked for dominance in each new generation to include newly generated non-dominated solutions and discard of dominated ones. The genome distance to the Pareto optimal set works through the following steps:

1. all non-dominated individuals in the populations are identified
2. all individuals have their minimum distance to the Pareto front calculated, including points on the front itself
3. all infeasible point are assigned a distance according to Eq. 6.22 where the minimum distance is M

$$R(g) = \begin{cases} d_i & \text{if solution is feasible (Eq. 6.25)} \\ \prod_{i=1}^{N_c} \kappa_i & \text{if solution is infeasible} \end{cases} \tag{6.24}$$

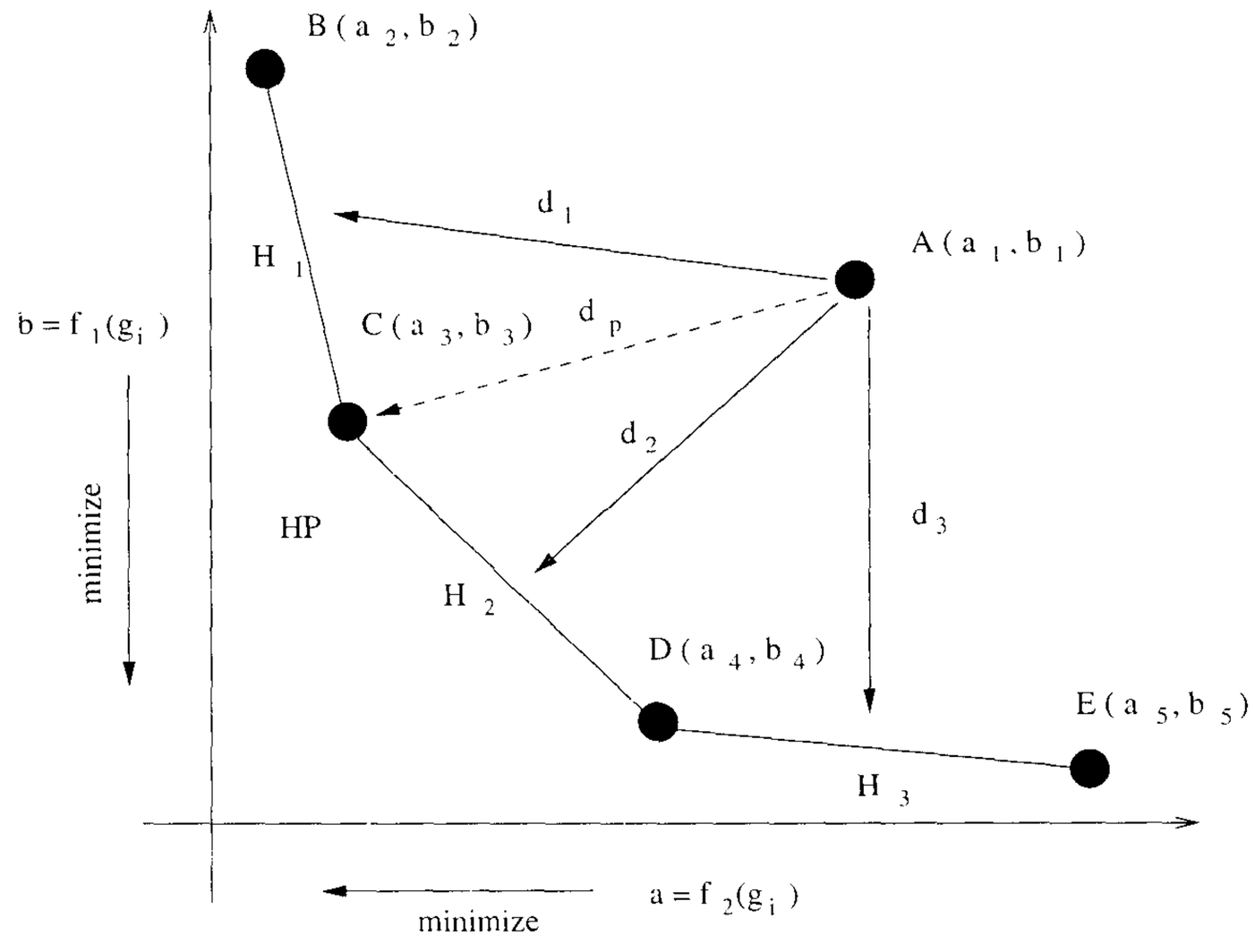

Figure 6.5: Fronts and Distances

where κ_i is the penalty term given in Eq. 6.22 and d_i is the distance between the solutions and the Pareto optimal set defined as:

$$d_i = \min_{j=1,\ldots,N_{seg}} d\left(\vec{f}(g_i), H_j\right) \qquad \forall i, \ldots, N_{sol} \tag{6.25}$$

where $d\left(\vec{f}(g_i), H_j\right)$ is the distance from the objectives vector $\vec{f}(g_i)$ to the hyperplane segment H_j. The segments H_j are part of the plane HP which is an $N_{obj} - 1$ dimensional hyperplane, in 2D, *i.e.* where only two objective functions are considered, HP is a line and its segments H_j are line segments as shown in Fig. 6.5. Details of how the segmentation is performed are given in the next section. In 2D, the distance d, of a given point(a_o, b_o) to a line segment represented by the line equation $Aa + Bb + C = 0$ is calculated as follows:

$$d = \frac{\mid Aa_o + Bb_o + C \mid}{\sqrt{A^2 + B^2}} \tag{6.26}$$

The distance calculation (Eq. 6.25) is repeated for all segments H_j and the minimum distance of these is then taken as the distance d_i for the solution set i.

However in the limiting case where the size of the front contains only one solution, *i.e* $S_{front} = 1$, the distance is then defined as the Euclidean distance between two points (see points A and C in Figure 6.5) and given by:

$$\mid S_{front} \mid = 1 \Rightarrow d\,(g_i) = \parallel \vec{f}(g_i) - \vec{f}(g^*) \parallel_2 \tag{6.27}$$

where $g^* \in P^*$ is the only solution on the front.

Front Segmentation

The hyperplane Pareto front HP is segmented for the purpose of calculating the distance of the objectives vector $\vec{f}(g_i)$ to the hyperplane segment H_j. Consider, without any loss of generality, the simultaneous minimisation of two objective function, $f_1(g)$ and $f_2(g)$. The values of these objective functions can be plotted in a two dimensional plot as shown in Fig. 6.5. The Pareto front found is represented in Fig. 6.5 as a line, HP, from point **B** to point **E** where a_i & b_i are the values of the two objectives for different points or solution sets. The points on the front are then sorted in descending order with respect to the first objective function ($f_1(g)$). Each two successive points on the sorted front are taken as a segment, H_j, of the front, HP, (*e.g.* points **B** & **C**). This procedure is then repeated for all points resulting in segments equal to $N_{seg} = N_{sol} - 1$, where N_{sol} are the number of solution or points on the Pareto front. The segments found are then used to calculate the distances as presented in the previous section.

6.7 Results and Discussion

The procedure has been applied using different ranking procedures to the bi-criteria optimisation problem of minimising capital investment (f_1) and minimising the energy consumption rate during the batch (f_2) for the separation of a tangent-pinch mixture of acetone and water. The batch distillation and hybrid distillation/pervaporation process specifications as studied in this chapter are shown in Table 6.2.

Property	**Value**
Feed composition, $x_{i,feed}$ $(molefrac.)$	
Acetone	0.70
Water	0.30
Batch size, M_{feed} (mol)	20,000
Product purity specifications, $x_{i,f}$ $(molfrac.)$	≥ 0.97
Product recoveries, $M_{i,f}$	≥ 0.70
Tray/Stage holdup (mol)	1.0/50.0
Column operating pressure, P (atm)	1.0
Available production time, T_A (hr)	7920
Batch setup time, t_s (min)	30
K1	1500†
K2	180†
UF	4.31‡
CRF_c	$\frac{1}{3}$†
CRF_m	$\frac{1}{3}$

† Adopted from Longsdon et al. (1990), ‡ Calculated from IChemE (1988)

Table 6.2: Case study specifications and operating conditions

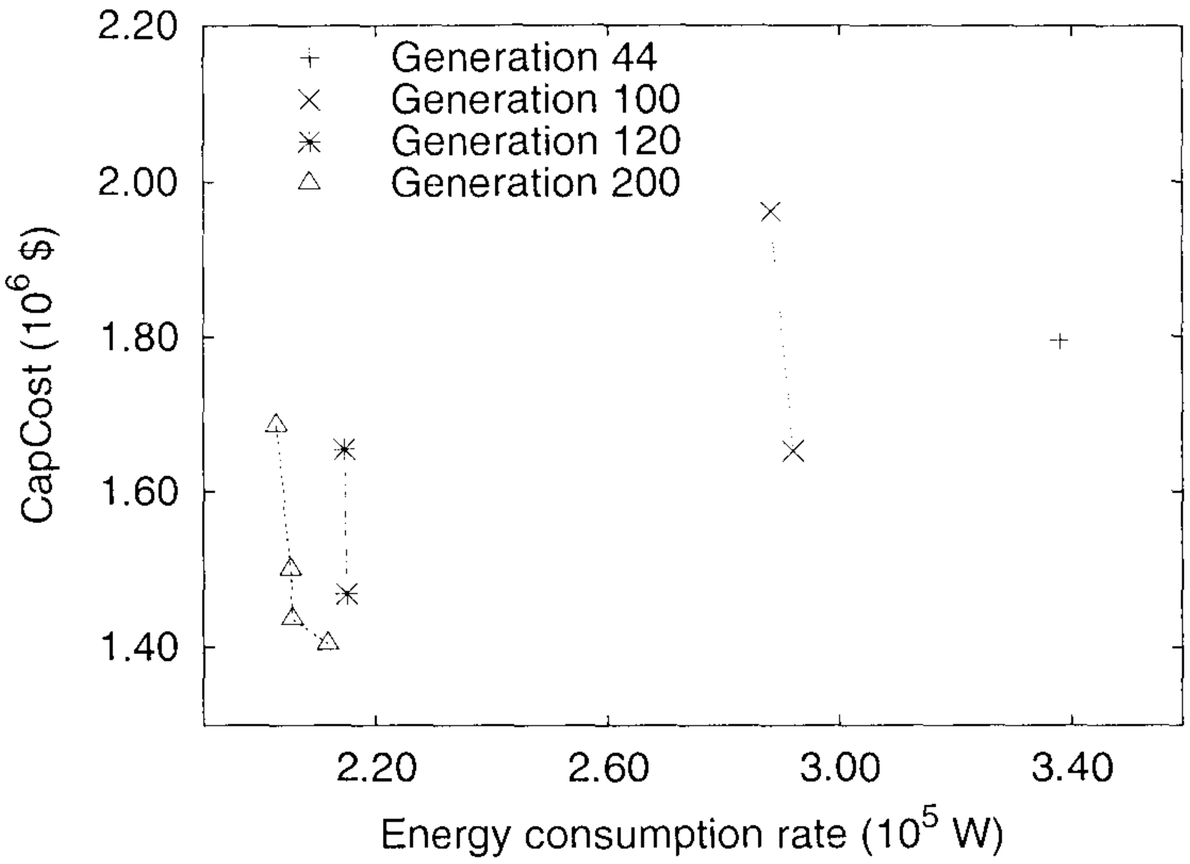

Figure 6.6: Distillation Evolution

6.7.1 Distillation

Figure 6.6 illustrates the evolution of the Pareto optimal set generated for the bi-criteria optimisation of a batch distillation process using the single-front ranking procedure (Eq. 6.21). It shows the generated non-dominated Pareto optimal sets in representative generations. It was found for this case that the population of the 44th genetic generation is the first generation to have produced a feasible Pareto set as all previous populations consisted solely of infeasible solutions. This illustrates the complexity of the simultaneous multi-objective optimisation of batch distillation processes in obtaining not only Pareto optimal solutions but merely feasible ones. The figure shows the progression of the Pareto front to the final population obtained after 200 generations, with the fastest convergence achieved between generations 100 and 120. The Pareto optimal set of generation 200 was found to contain four points compared to two in previous sample generations. This indicates the ability of the algorithm to obtain more inclusive optimal sets as the generation progresses.

Distillation Process Alternatives

The four points or process alternatives in the final front in Figure 6.6 are shown in Table 6.3. Process 1 represent the process with the maximum capital and minimum energy consumption rate, *i.e.* the top point on the final front in Figure 6.6. Process 4 represent the process with the minimum capital costs but maximum energy consumption rate as shown in Figure 6.6.

Table 6.3 shows that as the number of column trays decreases the process batch time as well as the reflux ratio at the end of the batch increases. This is due to the fact that when less trays are used the batch separation will take longer than does with more trays. As a result, the capital investment decreases when lesser trays are used and consequently causes the energy consumption rate to increase.

It is noted that the reboiler boilup remained constant (3.81 mol/s) in all process alternatives. This is an indication that for the same boilup rate, the process can be designed (number of trays) and operated (batch time, interval splits and reflux ratio) differently to obtain a range of solutions within the investigated trade-offs. The number of trays can therefore be identified as the main factor affecting the process capital investment and batch time, interval splits and reflux ratio are the main factors affecting the process energy consumption rates.

The flowsheet for process 1 and the product profiles are given in Figures 6.7 and 6.8, respectively. The reflux ratio for process 1 decreases during the offcut period in order to reduce the energy consumption while purging any off-specifications acetone from the reboiler to obtain the required water purity in the reboiler (Figure 6.8).

Process	Design Variables	Operation Variables	Objectives
	$u_d = \{N_t\}$	$u_o = \{t_f, t_i, R_c, V\}$	CC_c & E_c
1	$u_d = \{27\}$	$u_o = \left\{257.7, \begin{bmatrix} 0.93 \\ 256.7 \\ 0.07 \end{bmatrix}, \begin{bmatrix} 1.0 \\ 0.76 \\ 0.70 \end{bmatrix}, 3.81\right\}$	$\begin{bmatrix} CC_c \\ E_c \end{bmatrix} = \begin{bmatrix} 1.684 \times 10^6 \\ 0.203 \times 10^6 \end{bmatrix}$
2	$u_d = \{21\}$	$u_o = \left\{257.6, \begin{bmatrix} 0.50 \\ 256.7 \\ 0.40 \end{bmatrix}, \begin{bmatrix} 1.0 \\ 0.76 \\ 0.75 \end{bmatrix}, 3.81\right\}$	$\begin{bmatrix} CC_c \\ E_c \end{bmatrix} = \begin{bmatrix} 1.500 \times 10^6 \\ 0.205 \times 10^6 \end{bmatrix}$
3	$u_d = \{19\}$	$u_o = \left\{258.2, \begin{bmatrix} 1.08 \\ 256.7 \\ 0.42 \end{bmatrix}, \begin{bmatrix} 1.0 \\ 0.76 \\ 0.79 \end{bmatrix}, 3.81\right\}$	$\begin{bmatrix} CC_c \\ E_c \end{bmatrix} = \begin{bmatrix} 1.436 \times 10^6 \\ 0.206 \times 10^6 \end{bmatrix}$
4	$u_d = \{18\}$	$u_o = \left\{259.1, \begin{bmatrix} 1.45 \\ 256.7 \\ 0.95 \end{bmatrix}, \begin{bmatrix} 1.0 \\ 0.76 \\ 0.85 \end{bmatrix}, 3.81\right\}$	$\begin{bmatrix} CC_c \\ E_c \end{bmatrix} = \begin{bmatrix} 1.404 \times 10^6 \\ 0.212 \times 10^6 \end{bmatrix}$

Table 6.3: Optimal distillation process alternatives

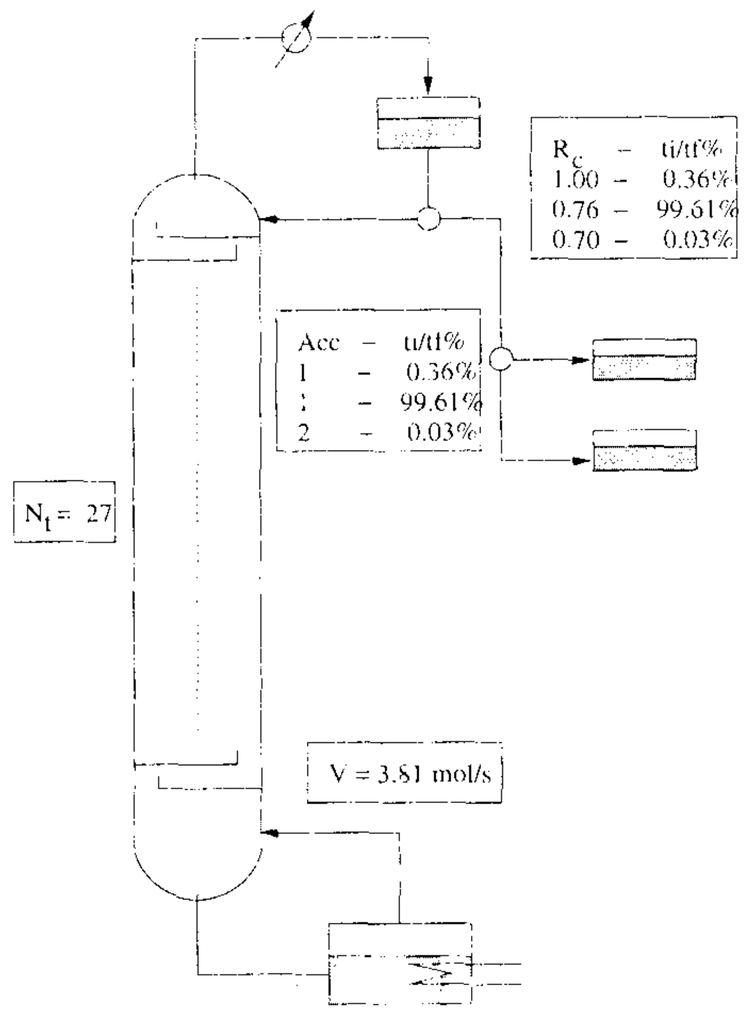

Figure 6.7: Flowsheet for distillation process 1

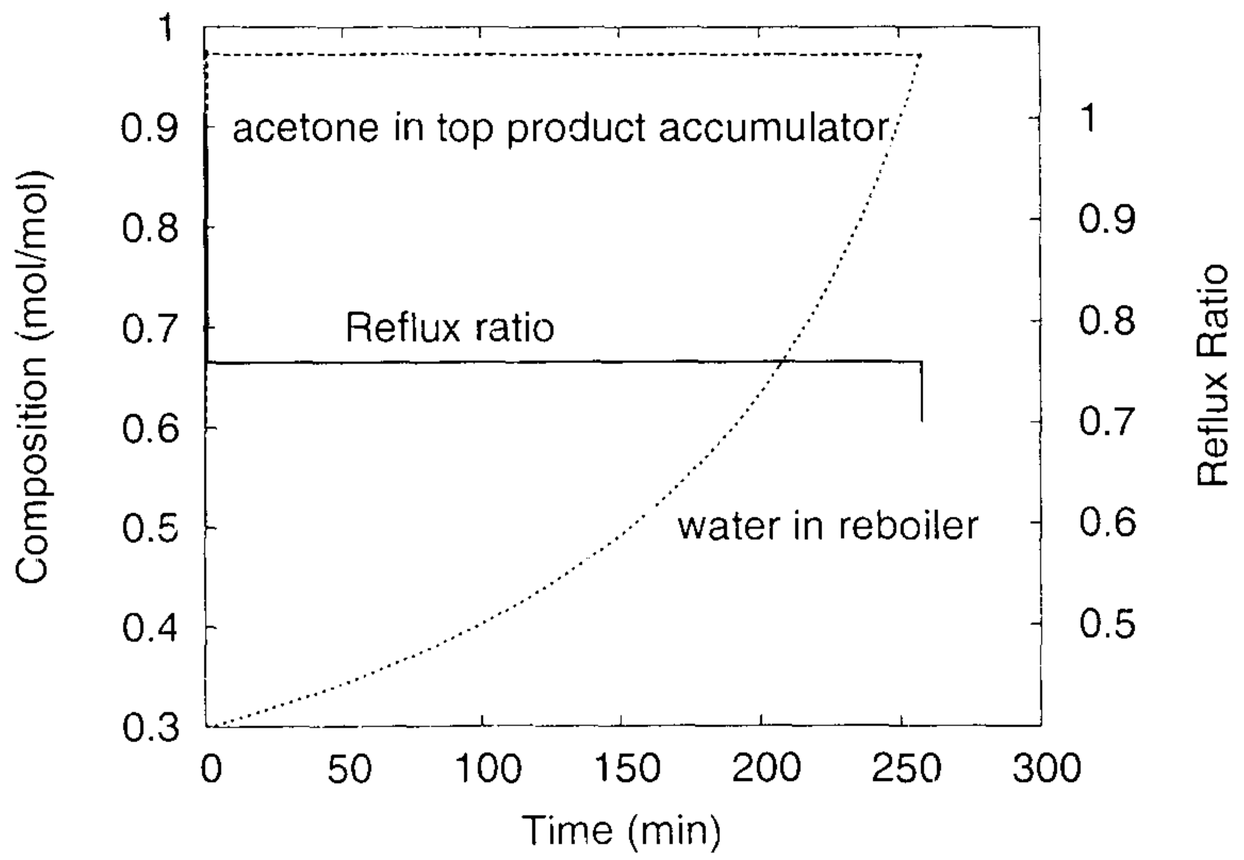

Figure 6.8: Product profile for distillation process 1

6.7.2 Hybrid Distillation/Pervaporation

Single- and Multi-Front Ranking

When the same ranking procedure (single-front) is applied to hybrid batch distillation/ pervaporation separation processes, it was found that the 43th generation was the first generation to have a feasible solution within its population, this has therefore resulted in a Pareto optimal set (Figure 6.9) containing only one non-dominated solution. Figure 6.9 also shows that the 100th generation optimal Pareto solutions did not include the non-dominated solution obtained in the 43th generation. This is due to the lack of an elitism operator which, if implemented as will be shown later, can avoid the loss of such solution through the genetic reproduction, crossover and mutation in successive generations. It is observed that the progression of the Pareto fronts to obtain the final front in generation 200 is slower than the batch distillation process optimisation (note the scale in Figures 6.6 and 6.9), which is owed to the presence of more decision variables (Table 6.1) in the hybrid case compared to the distillation case. The increase in the decision variables in the case of the hybrid process will result in a larger solution space which is harder to explore with the same number of maximum function evaluations (20,000).

Comparing the final optimal Pareto fronts obtained for the batch distillation and batch hybrid distillation/pervaporation process shown in Figure 6.10 using the single-front ranking procedure, it can be observed that hybrid processes have higher capital investment due to the existence of the membrane unit. However, the hybrid processes were found to have a lower energy consumption rate in one of the cases.

Figure 6.11 compares the different ranking procedures used in obtaining the Pareto optimal sets for the hybrid distillation/pervaporation processes. It shows that when using the multi-front ranking (M-F) procedure, the front is found to be of a reduced span compared to that of a single-front (S-F). The multi-front ranking, however, has resulted in lower capital investments values (f_1) for comparable energy consumption rates (f_2) compared to the Pareto front obtained by the single-front ranking procedure.

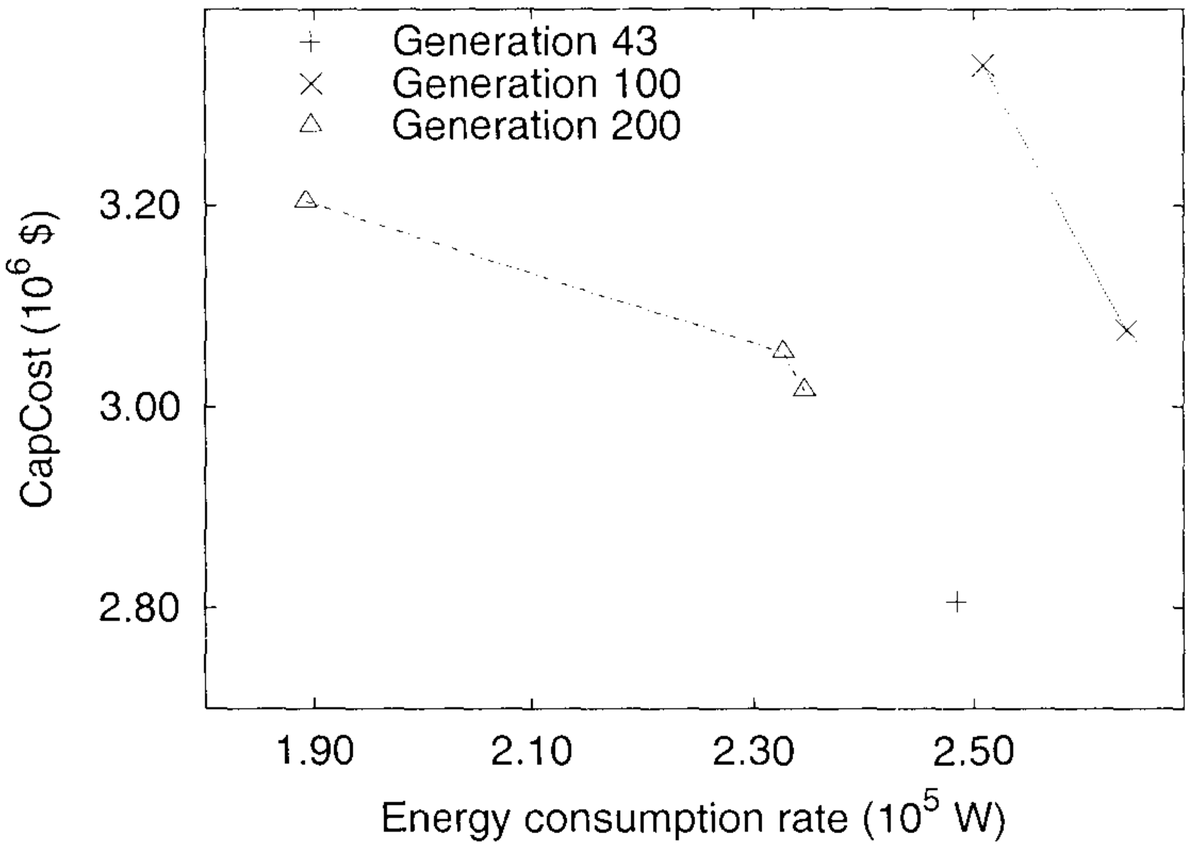

Figure 6.9: Hybrid Evolution

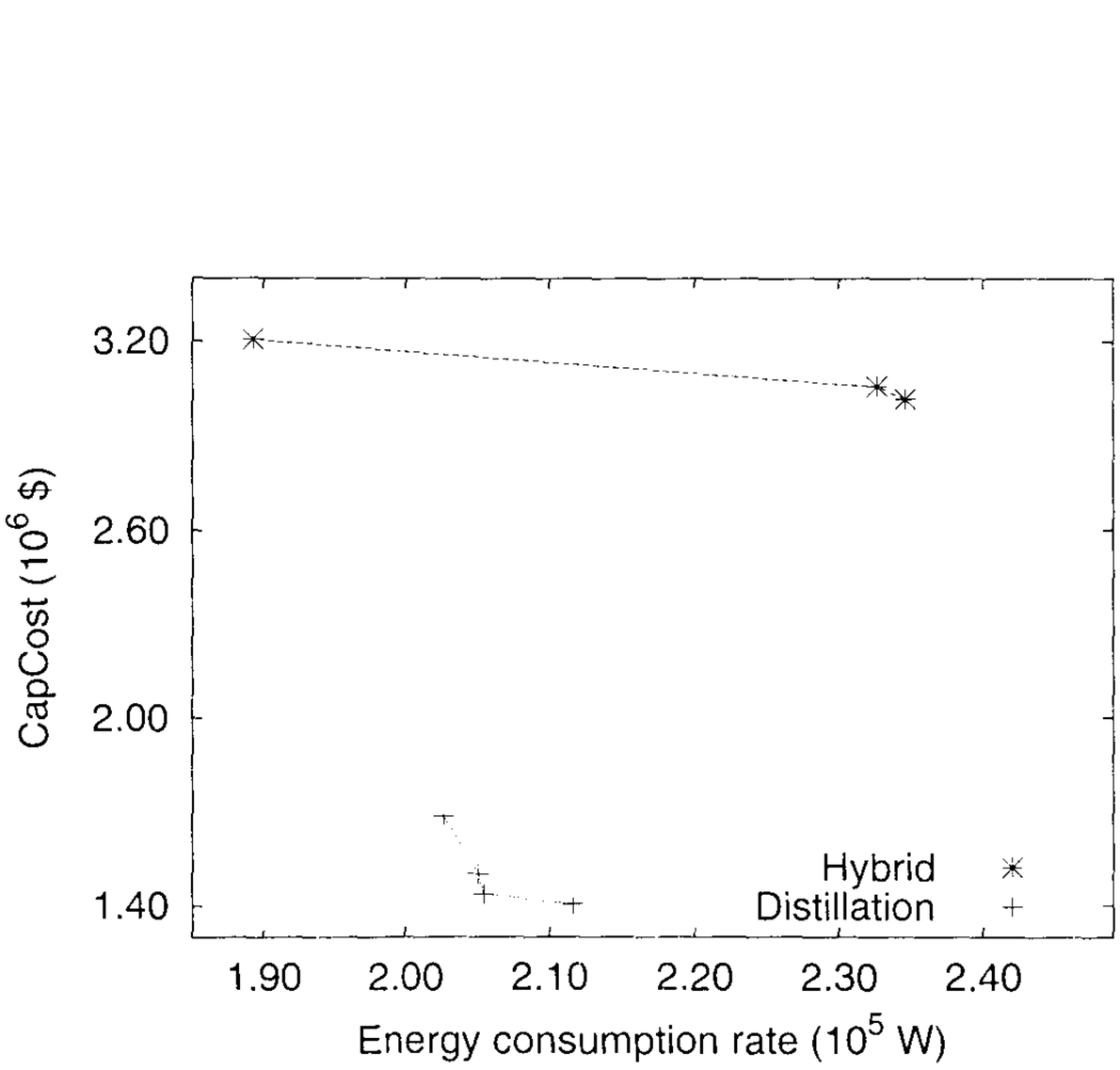

Figure 6.10: Distillation and Hybrid Single front ranking

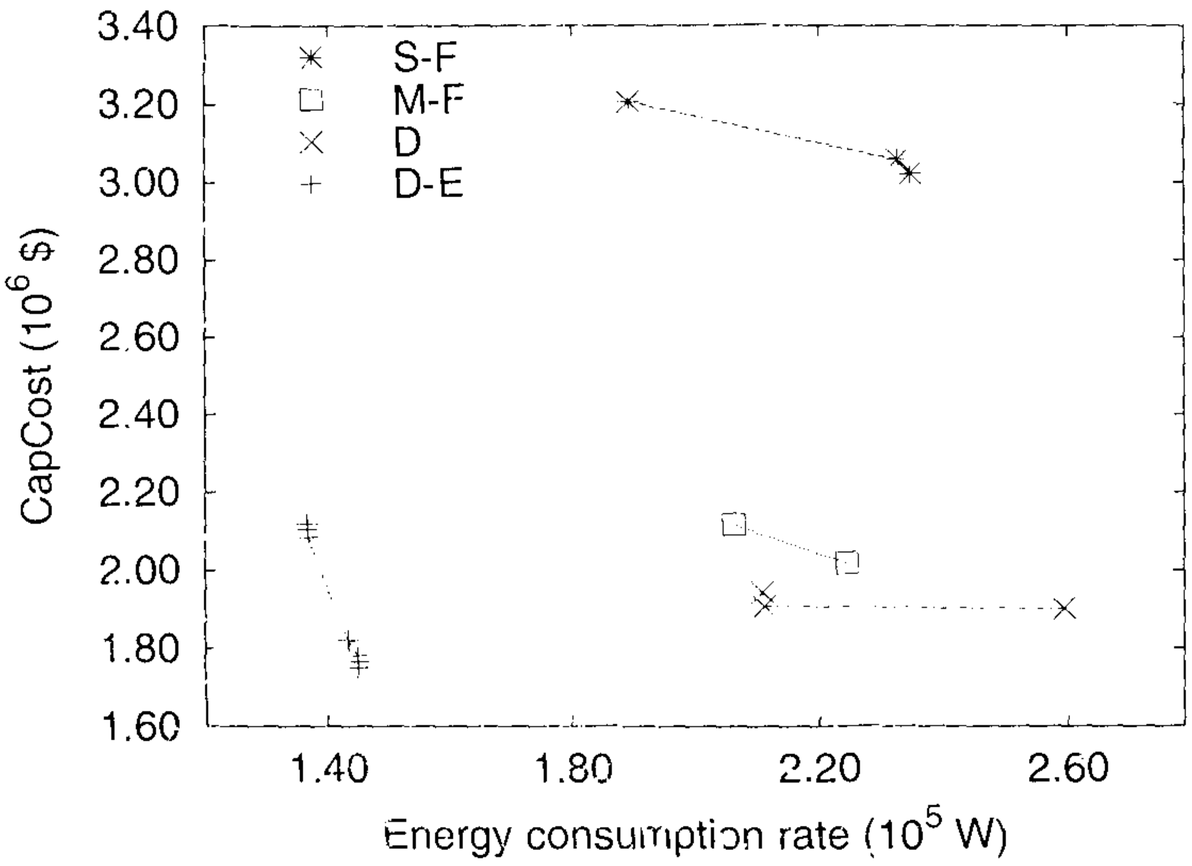

Figure 6.11: Ranking methods

Distance and Elite Distance Ranking

A further improvement to the multi-front (M-F) method over the single-front (S-F) is observed when using the distance (D) ranking procedure. The distance ranking resulted in comparable front span to that of the single-front procedure, the span was, however, more towards higher energy consumption rates for lower capital investments. If elitism is implemented in the distance (D-E) procedure it can be observed that an even better front is obtained as shown in Fig. 6.11. This is mainly because any dominated solutions found are retained through the elitism procedure for inclusion in successive generations.

Generation Feasibility and Final Front Size

The number of feasible solutions and final Pareto front sizes for the different methods are summarised in Table 6.4. It should be noted that the number of feasible solutions obtained for the pure distillation process (6793) was much more than that of the hybrid process (635) for the single-front procedure. This is because the increased number of optimisation variables for the hybrid process compared to distillation alone (see Table 6.1) as discussed. The first feasible solution occurrence and final front sizes are comparable for both processes

	Distillation				**Hybrid**			
Method	S-F	M-F	D	D-E	S-F	M-F	D	D-E
First feasible generation	44	-	-	-	43	38	36	25
Total feasible solutions	6793	-	-	-	635	525	1101	1686
Final front size S_{front}	4	-	-	-	3	2	3	7

Table 6.4: Results summary

in the case of the single-front ranking procedure. The elite distance ranking resulted in the earliest feasible solution occurrence (generation 25) and most generated feasible solutions (1686) as well as the largest front size (7) for the hybrid processes. It should be noted that the multi-front, distance and elite distance ranking procedures were not conducted for the pure distillation case because of the long computation time required to generate these results (typically 6 days on dual-P4-processor Dell Precision 380).

Hybrid Process Alternatives

Representative solutions of the front obtained with the elite distance (D-E) ranking for the hybrid process are shown in Table 6.5. Process 1 represents the process with the highest capital investment on the Pareto front and process 7 represents the process with the highest energy consumption. Process 4 is the point in the middle of the final Pareto front for the elite distance (D-E) ranking as shown in Figure 6.11. Within these processes it is noted that the batch time and the interval splits remained constant and no off-cuts were needed during the batch. This indicates that for these values different process alternatives are possible. Changes in number of trays and number of modules, as expected, have impact on the capital investment of the process. This is indicated by the difference between the processes design variables, u_o, and their effects on the capital investment as shown Table 6.5. Factors affecting the energy consumptions were identified as the permeate pressure column reflux and retentate recycle ratios.

Schematic of process 1 and product profiles and reflux/recycle ratios are shown in Figures 6.12 and 6.13, respectively. It is interesting to note from Figure 6.13 that the column reflux and the retentate recycle ratios move in opposite directions. This indicates a change in separation and collection roles between the membrane unit and distillation column during the batch. Due to the low retentate recycle ratio at the beginning of the batch, the majority of the light component is collected through the membrane retentate stream, however, as the batch progresses, the retentate recycle ratio increases and the column reflux ratio decreases to allow more of the light component collection through the top of the column. This is caused by the fact that as top product stream becomes purer in the lighter component more products can be withdrawn from the top of the column at lower reflux ratio which will result in lower energy consumption rate. The decrease in column reflux causes an increase in the retentate recycle ratio to obtain an even purer products in order to maintain the light component purity in the top product accumulator.

Process	Design Variables	Operation Variables	Objectives
	$u_d = \{N_t, N_m, L_s, L_r\}$	$u_o = \{t_f, t_i, R_c, R_r, R_p, P_p, V, F_m\}$	CC_{hyb} & E_{hyb}
1	$u_d = \{48, 1, 9, 15\}$	$u_o = \left\{185.36, \begin{bmatrix} 44.18 \\ 138.5 \\ 2.68 \end{bmatrix}, \begin{bmatrix} 0.86 \\ 0.64 \\ 0.71 \end{bmatrix}, \begin{bmatrix} 0.62 \\ 0.95 \\ 0.60 \end{bmatrix}, \begin{bmatrix} 0.0 \\ 0.0 \\ 0.0 \end{bmatrix}, 880, 3.0, 2.66\right\}$	$\begin{bmatrix} CC_{hyb} \\ E_{hyb} \end{bmatrix} = \begin{bmatrix} 2.117 \times 10^6 \\ 0.137 \times 10^6 \end{bmatrix}$
4	$u_d = \{33, 4, 4, 7\}$	$u_o = \left\{185.36, \begin{bmatrix} 44.18 \\ 138.5 \\ 2.68 \end{bmatrix}, \begin{bmatrix} 0.86 \\ 0.64 \\ 0.77 \end{bmatrix}, \begin{bmatrix} 0.62 \\ 0.95 \\ 0.58 \end{bmatrix}, \begin{bmatrix} 0.0 \\ 0.0 \\ 0.0 \end{bmatrix}, 540, 3.0, 2.66\right\}$	$\begin{bmatrix} CC_{hyb} \\ E_{hyb} \end{bmatrix} = \begin{bmatrix} 1.819 \times 10^6 \\ 0.143 \times 10^6 \end{bmatrix}$
7	$u_d = \{33, 1, 8, 9\}$	$u_o = \left\{185.36, \begin{bmatrix} 44.18 \\ 138.5 \\ 2.68 \end{bmatrix}, \begin{bmatrix} 0.86 \\ 0.64 \\ 0.77 \end{bmatrix}, \begin{bmatrix} 0.62 \\ 0.95 \\ 0.60 \end{bmatrix}, \begin{bmatrix} 0.0 \\ 0.0 \\ 0.0 \end{bmatrix}, 650, 3.0, 2.66\right\}$	$\begin{bmatrix} CC_{hyb} \\ E_{hyb} \end{bmatrix} = \begin{bmatrix} 1.750 \times 10^6 \\ 0.145 \times 10^6 \end{bmatrix}$

Table 6.5: Optimal hybrid process alternatives

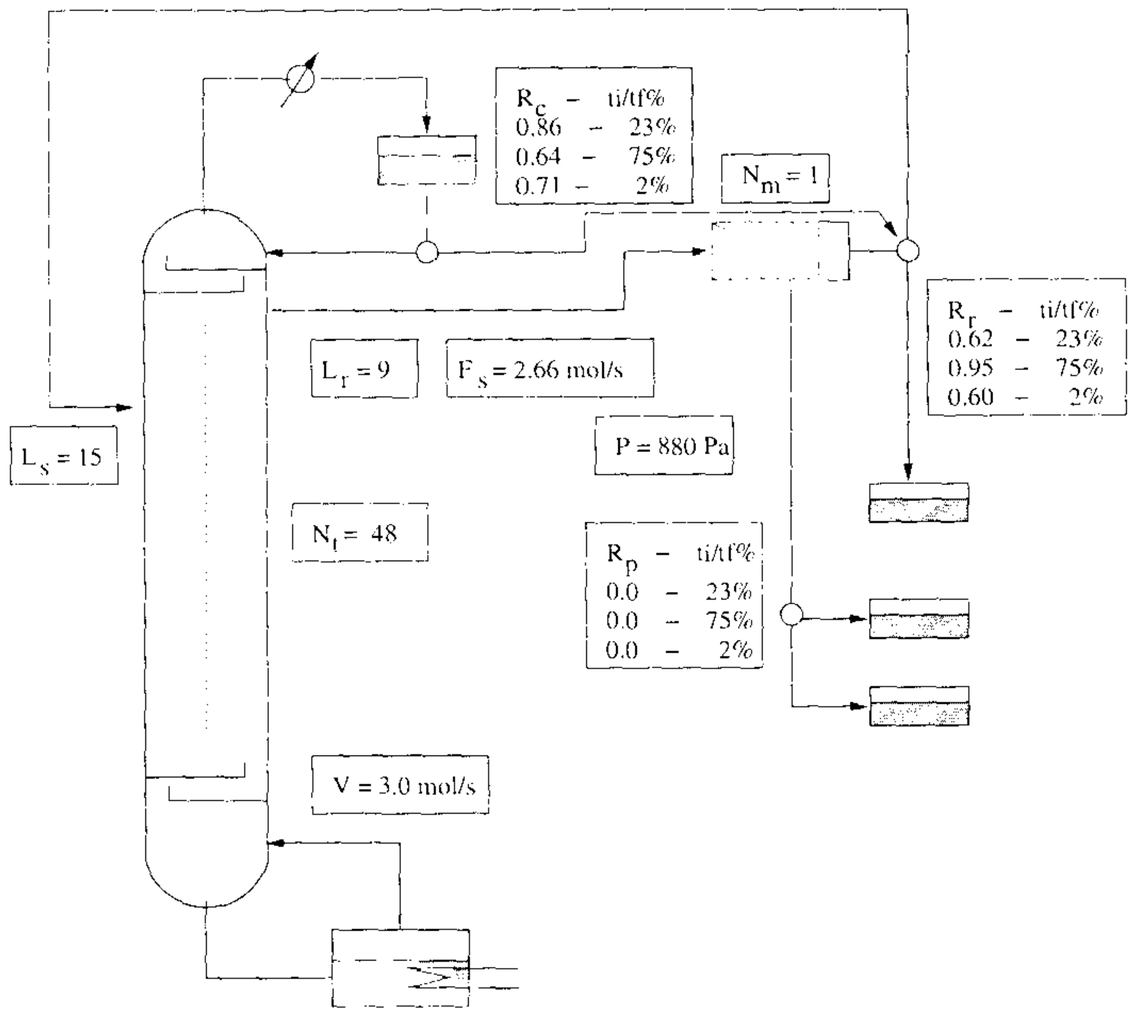

Figure 6.12: Flowsheet for hybrid process 1

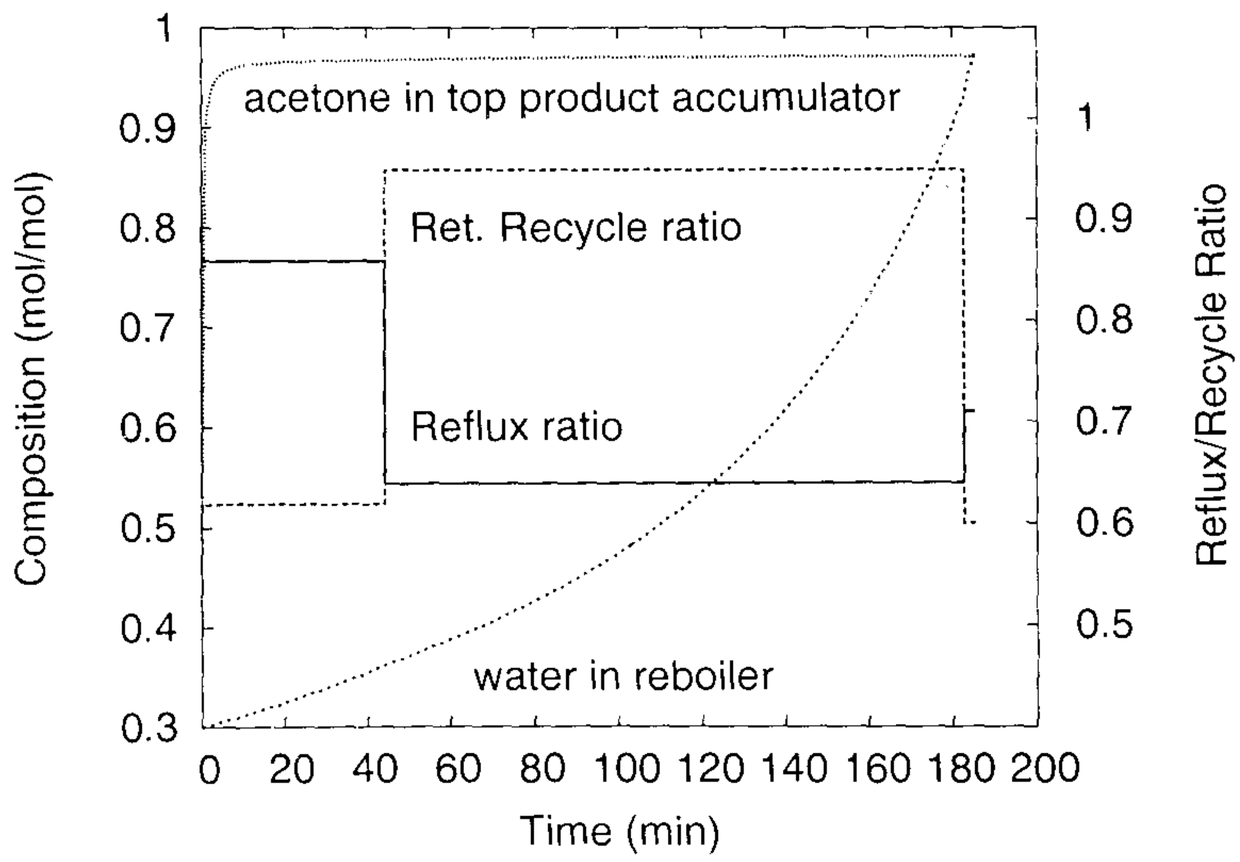

Figure 6.13: Product profile for hybrid process 1

6.8 Conclusions

This chapter focuses on the development of a multi-objective genetic algorithm for constrained multi-criteria engineering problems. The algorithm has been applied to the optimisation of batch distillation and batch hybrid distillation/pervaporation processes for a bi-criteria case. It has been demonstrated that the suggested algorithm can be applied successfully to generate the optimal Pareto set. It is also demonstrated that the elite distance based ranking results in the best optimal Pareto set compared to the other ranking procedures used. The convergence of such sets will, however, depend on the termination criterion chosen and whether sufficient penalty being applied to drive the solution towards feasibility and eventually Pareto non-dominance. The performance will also depend on the complexity of the engineering model implemented and whether an elitism operator is applied.

From the cases considered, it can be concluded that there are apparent trade-offs, as expected, between the process capital investment costs and energy consumption rates. Main factors affecting the investment costs were identified as the column number of trays in addition to the membrane number of modules for the hybrid column. The energy consumption rates of the distillation processes were found to be affected by the required batch time, reflux ratio and interval splits. The hybrid process energy consumption rates were mainly affected by the process permeate pressure and reflux and recycle ratios.

List of Publications

1. Barakat, T. and E. Sørensen, 2004, Optimal batch separation systems synthesis and design, *Proceedings of the AIChE Annual Meeting 2004*, Austin TX, USA, Paper 405d.

2. Barakat, T. and E. Sørensen, 2005, Optimal synthesis and design of hybrid batch separation processes, *Proceedings of the* 7^{th} *World Congress of Chemical Engineering*, Glasgow, Paper O87-002.

3. Barakat, T. and E. Sørensen, 2005, Optimal configuration, design and operation of hybrid batch distillation/pervaporation processes, *Proceedings of the AIChE Annual Meeting 2005*, Cincinnati OH, USA, Paper 445d.

4. Barakat, T., E. Fraga and E. Sørensen, 2006, Multi-objective optimisation of batch distillation processes, *Proceedings of the ESCAPE-16 and PSE'2006*, Garmisch-Partenkirc- hen, Germany, p955-960.

5. Barakat, T. and E. Sørensen, 2006, Optimal configuration, design and operation of hybrid batch distillation/pervaporation processes, *In Computer Aided Methods in Optimal Design and Operations*, World Scientific, p69-78.

6. Barakat, T. and E. Sørensen, 2006, Optimal configuration, design and operation of continuous hybrid distillation/pervaporation processes, *Proceedings of the International Conference on Distillation and Absorption 2006*, London, UK, p628-637.

7. Barakat, T., E. Fraga and E. Sørensen, 2006, Multi-objective optimisation of hybrid batch distillation/pervaporation processes, *Proceedings of the AIChE Annual Meeting 2006*, San Francisco CA, USA, Paper 409g, accepted.

Nomenclature

A	area	m^2
ACC_i	annualised equipment capital costs of i	$\$/yr$
AOC_i	annualised equipment operating costs of i	$\$/yr$
c_i	molar concentration of i	mol/m^3
c_i	problem constraint i value	-
CC_i	equipment capital costs of i	$
$C(s)$	transfer function of the controller	-
CRF_i	capital recovery factor of i	-
C_{ex}	installed heat exchanger cost	$
C_{feed}	cost price of feed	$\$/mol$
C_i	selling price of product i	$\$/mol$
C_{sh}	installed column shell cost	$
$C_{ut,i}$	utilities cost of equipment i	$\$/MJ$
d	process disturbances	-
d_i	distance i	-
D	column diameter	m
D	dispersion coefficient	m^2/s
e	error in control action	-
e_i	initial elitism size	-
e_s	elitism size	-
E_i	energy consumption rate of i	W
f	corrected objective function value	-

$f(g)$	objective value of solution g	-
f_i	function i	-
f_s	scaled genome fitness	
f_{sum}	sum of genome fitnesses	-
F_b	bottom flowrate	mol/s
F_f	feed flowrate	mol/s
F_m	membrane stage feed rate	mol/s
F_m	molar flux	mol/m^2s
F_r	retentate flowrate	mol/s
F_s	side-draw flowrate	mol/s
F_p	flowrate of permeate	mol/s
g	gravitational acceleration	m^2/s
g_i	solution set i	-
G	feasible solution space	-
$G(s)$	transfer function of the process	-
$G_d(s)$	transfer function of the process disturbances	-
h	enthalpy	J/mol
HP	hyperplane	-
H_i	segment i of hyperplane HP	-
J	molar flux through membrane	mol/m^2s
K_1	Guthrie's correlation coefficient for column shell cost	-
K_2	Guthrie's correlation coefficient for column exchangers cost	-
k_c	thermal conductivity	W/mK
l	level of liquid	m
L	liquid flowrate	mol/s
L_r	retentate recycle location	-
L_s	membrane feed location	-
m_f	feed amount	mol
m_i	product i recovery	mol

M	molar holdup	mol
M	large number	-
N_c	number of components	-
N_m	number of membrane modules	-
N_{front}	number of Pareto fronts	-
N_{obj}	number of objective functions	-
N_{pop}	number of genomes in genetic population	-
N_{sol}	number of solution sets	-
N_{seg}	number of hyberplane HP segments	-
N_t	number of column trays	-
P	pressure	Pa
P^{in}	pressure at unit inlet	Pa
P^{out}	pressure at unit outlet	Pa
P_A	annual profit	$\$/yr$
P_c	probability of crossover	-
P_m	probability of mutation	-
P_p	permeate pressure	Pa
P_s	probability of selection	-
P_{ss}	population overlap percentage	-
P^*	Pareto optimal set	-
PF^*	Pareto front	-
q	heat flux	W/m^2
Q	heat load	W
$Q_{m,h}$	pervaporation heat load	W
r	radial distance from centre (fibre)	m
r	controller setpoint	-
R	fibre inner radius	m
R	solution rank	-
$Rand$	random number	-

R_c	column internal reflux ratio	-
R_p	permeate offcut ratio	-
R_r	retentate recycle ratio	-
s	radial distance from centre (module)	m
S	fibre bundle radius	m
S_{front}	size of Pareto front (number of solutions)	-
t_f	total batch processing time	min
t_i	task i interval time	min
t_s	batch setup time	min
T	temperature	K
T_A	total production time available per annum	hr/yr
T_s	tournament pool size	-
U	internal energy	J/mol
UF	Update factor	\$
u	process input	-
u_d	vector of design variables	-
u_o	vector of operation variables	-
v	velocity	m/s
V	column vapour flowrate	mol/s
w_i	objective i weight	-
x	vector of state variables	-
x_i, X_i	molar fraction of component i in the vapour phase	-
x_i^{min}	minimum composition of component i in the mixture	-
y	process output	-
y_i	molar fraction of component i in the liquid phase	-
y_m	process output measurement	-
z	axial distance along fibre/module	m
z	mole fraction	-

Greek Letters

α	dry pressure drop coefficient	-
$\bar{\alpha}$	ratio of membrane surface area to volume	m^{-1}
β	aeration factor	-
η	efficiency	-
γ	condenser vapour flow coefficient	-
κ_i	penalty term i	-
λ_i	heat of vaporisation of component i	$Kcal/mol$
ν	volumetric flowrate	m^3/s
$\bar{\nu}$	molar volume	m^3/mol
Ω	objective function value	
ϕ	fugacity coefficient	-
ρ	molar density	mol/m^3
ρ^m	mass density	kg/m^3
σ	standard deviation	-
$\tilde{\rho}$	average mass density	kg/m^3
θ	angular direction	-
ϱ	sigma multiplier	-

Superscripts and Subscripts

anc	ancillary
ave	average
b	bottom product
c	column
cond	condenser
$f, feed$	feed stream
h	pervaporation membrane system feed heater
hyb	hybrid system
in	at the inlet
L	liquid phase
t	system turbine
p	system feed pump
m	membrane
out	at the outlet
s	column side-draw
r	radial direction
reb	reboiler
RC	reference case
tray	tray
V	vapour phase
vessel	vessel
z	axial direction

Bibliography

Aiouache, F., Goto, S., 2003. Reactive distillation-pervaporation hybrid column for tert-amyl alcohol etherification with ethanol. Chemical Engineering Science 58, 2465–2477.

Androulakis, I., Venkatasubramanian, V., 1991. A genetic algorithmic framework for process design and optimization. Computers & Chemical Engineering 15 (4), 217.

Avraam, M., Shah, N., Pantelides, C., 1999. A decomposition algorithm for the optimisation of hybrid dynamic processes. Computers & Chemical Engineering S23, S451.

Baker, R., 2000. Membrane Technology and Applications. McGraw-Hill.

Bansal, V., Sakizlis, V., Ross, R., Perkins, J., Pistikopoulos, E., 2003. New algorithm for mixed-integer dynamic optimisation. Comp. & Chem. Eng. 27, 647–668.

Bausa, J., Marquardt, W., 2000. Shortcut design methods for hybrid membrane/distillation processes for the separation of nonideal multicomponent mixtures. Ind. Eng. Chem. Res. 39, 1658–1672.

Bausa, J., Watzdorf, R., Marquardt, W., 1998. Shortcut methods for nonideal multicomponent distillation: 1. simple columns. AIChE Journal 44 (10), 2181–2198.

Benson, H., 1978. Existence of efficient solutions for vector maximization problems. Optimization Theory and Applications 26 (4), 469.

Binning, R., James, F., 1958. Now separate by membrane permeation. Pet. Refiner 37, 214–215.

Boston, J., Britt, H., Jirapongphan, S., Shah, V., 1980. An advanced system for the simulation of batch distillation operations. FOCAPD'80 (Mah and Seider, Eds.), New York II.

Chen, M., Eng, R., Glazer, J., Wensley, C., 1988. Pervaporation process for separating alcohols from ethers. US Patent 4 774 365.

Coley, D., 1999. An introduction to genetic algorithm for scientists and engineers, 1st Edition. World Scientific Publishing.

Daviou, M., Hoch, P., Eliceche, A., 2004. Design of membrane modules used in hybrid distillation/pervaporation systems. Industrial & Engineering Chemistry Research 43 (13), 3403–3412.

Deb, K., 2001. Multi-objective optimization using evolutionary algorithms. Wiley, Chichester, UK.

Deb, K., Pratap, A., Agarwal, S., Meyarivan, T., 2002. A fast and elitist multiobjective genetic algorithm: NSGA-II. IEEE Transactions on Evolutionary Computations 6 (2), 182–197.

Dedieu, S., Pibouleau, L., Azzaro-Pantel, C., Domenech, S., 2003. Design and retrofit of multiobjective batch plants via a multicriteria genetic algorithm. Computers & Chemical Engineering 27 (12), 1723–1740.

Douglas, J., 1988. Conceptual design of chemical processes. McGraw-Hill Book Company Inc., New York.

Duran, M., Grossmann, I., 1986. An outer-approximation algorithm for a class of mixed-integer nonlinear programs. Mathematical Programming 36, 307.

Eliceche, A., Daviou, M., Hoch, P., Uribe, I., 2002. Optimisation of azeotropic distillation columns combined with pervaporation membranes. Computers & Chemical Engineering 26, 563–573.

Fahmy, A., Mewes, D., Ohlrogge, K., 2002. On the integration of jet ejectors into hybrid dehydration processes. Journal of Membrane Science 196, 79–84.

Fontalvo, J., Cuellar, P., Timmer, J., Vorstman, M., Wijers, J., Keurentjes, J., 2005. Comparing pervaporation and vapor permeation hybrid distillation processes. Industrial & Engineering Chemistry Research 44 (14), 5259–5266.

Furlonge, H., Pantelides, C., Sørensen, E., 1999. Optimal operation of multivessel batch distillation columns. AIChE Journal 45 (781-801).

Garrard, A., Fraga, E., 1998. Mass exchange network synthesis using genetic algorithms. Computers & Chemical Engineering 22 (12), 1873.

Gear, C., 1971. Simultaneous numerical solution of differential and algebraic equations. IEEE Trans. Circuit Theory CT-18, 89–95.

Geoffrion, A., 1972. Generalized benders decomposition. Optimization Theory and Applications 10, 273.

Goldberg, D., 1989. Genetic algorithms in search, optimization and machine learning. Addison-Wesley.

Goldberg, D., Deb, K., 1991. Foundations of Genetic Algorithms. Morgan Kaufmann, Ch. A comparative analysis of selection schemes used in genetic algorithms.

González, B., Ortiz, I., 2001. Modelling and simulation of a hybrid process (pervaporation-distillation) for the separation of azeotropic mixtures of alcohol-ether. Chem. Technol. Biotechnol. 77, 29–42.

Guerreri, G., 1992. Membrane alcohol separation process-integrated pervaporation and fractional distillation. Trans. IChemE (Part A) 70, 501–508.

Haimes, Y., Lasdon, L., Wismer, D., 1971. On a bicriterion formulation of the problems of integrated system identification and system optimization. IEEE Transactions of Systems, Man and Cybernetics 1 (3), 296.

Hasebe, S., Kurooka, T., Hashimoto, I., 1995. Comparison of the separation performances of a multi-effect batch distillation system and a continuous distillation system. Proc. DYCORDq'95, Helsingor, Denmark, 249.

Hilmen, E., Skogestad, S., Doherty, M., Malone, M., 1997. Integrated design, operation and control of batch extractive distillation with a middle vessel. In: Proceedings of the AIChE Annual Meeting 1997. Los Angeles, USA.

Holland, J., 1962. Outline for a logical theory of adaptive systems. Journal of the ACM 4, 297.

Hömmerich, U., Rautenbach, R., 1998. Design and optimization of combined pervaporation/distillation processes for the production of mtbe. Journal of Membrane Science 146, 53–64.

IChemE, 1988. A guide to capital cost estimating, 3rd Edition. IChemE.

Ignizio, J., 1978. A review of goal programming: A tool for multiobjective analysis. Operations Research Society 29 (11), 1109.

Infochem, 2005. Infochem computer services ltd.

Kanji, N., Matsuo, M., 1994. Process for producing ether compound. US Patent 5 292 963.

Kita, H., Inoue, T., Asamura, H., Tanaka, K., Okamoto, K., 1997. Nay zeolite membrane for the pervaporation separation of methanol-methyl-tert-butyl-ether mixtures. Chem. Commun.

Klöker, M., Kenig, E., Hoffmann, A., Kreis, P., Górak, A., 2005. Rate-based modelling and simulation of reactive separations in gas/vapour-liquid systems. Chemical Engineering and Processing 44 (6), 617.

Kookos, I., 2003. Optimal design of membrane/distillation column hybrid processes. Ind. Eng. Chem. Res. 42, 1731–1738.

Kreis, P., Górak, A., 2006. Process analysis of hybrid separation processes combination of distillation and pervaporation. Chemical Engineering Research and Design 84 (A7), 595.

Kumar, R., Golden, T., White, T., Rokicki, A., 1992. Novel adsorption distillation hybrid scheme for propane/propylene separation. Sep. Sci. Technol. 27, 2157.

Lemanski, I., Lipscomb, G., 2000. Effect of fiber variation in the performance of counter-current hollow-fiber gas separation modules. Journal of Membrane Science 167, 241.

Levy, G., Dongen, D., Doherty, M., 1985. Design and synthesis of homogeneous azeotropic distillation. Ind. Eng. Chem. Fundam. 24 (4), 463–474.

Lewin, D., Wang, H., Shalev, O., 1998. A generalized method for HEN synthesis using stochastic optimization -i. general framework and MER optimal synthesis. Computers & Chemical Engineering 22 (10), 1503.

Lipnizki, F., Field, R., Ten, P., 1999. Pervaporation-based hybrid process: a review of process design, applications and economics. Journal of Membrane Science 153, 183–210.

Longsdon, J., Diwekar, U., Biegler, L., 1990. On the simultaneous optimal design and operation of batch distillation. Trans. Inst. Chem. Eng. 68 (A), 434.

Low, K., Sørensen, E., 2002. Optimal operation of extractive distillation in different batch configurations. AIChE Journal 48 (5), 1034–1050.

Low, K., Sørensen, E., 2003. Simultaneous optimal design and operation of multivessel batch distillation. AIChE Journal 49 (10), 2564–2576.

Low, K., Sørensen, E., 2004. Simultaneous optimal design and operation of mulipurpose batch distillation columns. Chem. Eng. & Prc. 43, 273–289.

Lu, Y., Zhang, L., Chen, H., Qian, Z., Gao, C., 2002. Hybrid process of distillation side-connected with pervaporation for separation of methanol/mtbe/c4 mixture. Desalination 149, 81–87.

Luo, G., Niang, M., Schaetzel, P., 1997. Separation of ethyl tert-butyl ether-ethanol by combined pervaporation and distillation. Chemical Engineering Journal 68, 139–143.

Marriott, J., 2001. Detailed modelling and optimal design of membrane separation systems. Ph.D. thesis, Department of Chemical Engineering, University College London.

Marriott, J., Sørensen, E., 2003a. A general approach to modelling membrane modules. Chem. Eng. Sci. 58 (22), 4975--4990.

Marriott, J., Sørensen, E., 2003b. The optimal design of membrane systems. Chem. Eng. Sci. 58 (22), 4991–5004.

Marriott, J., Sørensen, E., Bogle, D., 2001. Detailed mathematical modelling of membrane modules. Computers & Chemical Engineering 25 (4), 693.

Mitsui, 2005. Mitsui chemicals, inc., Japan.

Mohideen, M., Perkins, J., Pistikopoulos, E., 1996. Optimal design of dynamic systems under uncertainty. AIChE Journal 42, 2251.

Mujtaba, I. M., 1999. Optimization of batch extractive distillation processes for separating close boiling and azeotropic mixtures. Trans. Inst. Chem. Eng. 77, 588.

Nunes, S., Peinemann, K., 2001. Membrane Technology in the Chemical Industry. Wiley-VCH.

Obenaus, F., Droste, W., 1980. Hüels-process: Methyl tertiary butylether. Erdöl und Kohle-Erdgas-Petrochemie vereinigt mit Brennstoff-Chemie, Bd. 33, Heft 6.

Osyczka, A., Kundu, S., 1995. A new method to solve generalized multicriteria optimization problems using the simple genetic algorithm. Structural Optimization 10 (2), 94.

Pareto, V., 1896. Cours d'Economie Politique. Vol. I and II. F. Rouge, Lausanne.

Perry, R., Green, D., 1984. Perry's Chemical Engineers' Handbook. McGraw-Hill.

Pettersen, T., Argo, A., Noble, R., Koval, C., 1996. Design of combined membrane and distillation processes. separation Technology 6, 175–187.

Pettersen, T., Lien, K., 1995. Design of hybrid distillation and vapor permeation processes. Journal of Membrane Science, 21–30.

Pressly, T., Ng, K., 1998. A break even analysis of distillation-membrane hybrids. AIChE Journal 44 (1), 93–105.

PSE, 2005. gPROMS User Guide. Process Systems Enterprise Ltd.

Quesada, I., Grossmann, I., 1992. An LP/NLP based branch-and-bound algorithm for convex minlp optimization problems. Computers & Chemical Engineering 16, 937.

Rautenbach, R., Albrecht, R., 1989. Membrane Processes. Wiley, New York, pp. 363–422.

Sadomoto, H., Miyahara, K., 1983. Calculation procedure for multicomponent batch distillation. Int. Chem. Eng. 23, 56.

Sharif, M., Shah, N., Pantelides, C., 1998. On the design of multicomponent batch distillation columns. Computers & Chemical Engineering S22, S69.

Shindo, Y., Hakuta, T., Yoshitome, H., Inoue, H., 1985. Calculation methods for multicomponent gas separation by permeation. Sep. Sci. Technol. 20 (5,6), 445–459.

Sinnott, R. K., 1993. Coulson and Richardson's Chemical Engineering. Vol. 6. Pergamon Press, Oxford.

Smoker, E., 1938. Analytical determination of plates in fractionating columns. AIChE Journal 12, 165–172.

Srinivas, N., Deb, K., 1994. Multiobjective optimization using nondominated sorting in genetic algorithms. Evolutionary Computation 2 (3), 221–248.

Stephan, W., Noble, R., Koval, C., 1995. Design methodology for a membrane/distillation column hybrid process. Journal of Membrane Science 99, 259–272.

Streicher, A., Kremer, P., Tomas, V., Hubner, A., Ellinghorst, G., 1995. Development of new pervaporation membranes, systems and processes to separate alcohols/ethers/hydrocarbons mixture. Proceedings of the Seventh International Conference

on Pervaporation Processes in the Chemical Industry, bakish Material Corporation, NJ, USA.

Sulzer, 2005. Sulzer chemtech ltd, Switzerland.

Syswerda, G., 1989. Uniform crossover in genetic algorithms. In: Proceedings of the 3rd International Conference on Genetic Algorithms.

Szitkai, Z., Lelkes, Z., Rev, E., Fonyo, Z., 2002. Optimization of hybrid ethanol dehydration systems. Chemical Engineering and Processing 41, 613–646.

Tsuyumoto, M., Teramoto, A., Meares, P., 1997. Dehydration of ethanol on a pilot plant scale, using a new type of hollow-fibre membrane. Journal of Membrane Science 13 (1), 83–94.

Tusel, G., Ballweg, A., 1983. Method and apparatus for dehydrating mixtures of organic liquids and water. US Patent 4 405 409.

Van Hoof, V., Van den Abeele, L., Buekenhoudt, A., Dotremont, C., Leysen, R., 2004. Economic comparison between azeotropic distillation and different hybrid systems combining distillation with pervaporation for the dehydration of isopropanol. Separation and Purification Technology 37 (1), 33–49.

Viswanathan, J., Grossmann, I., 1990. A combined penalty-function and outer-approximation method for minlp optimization. Computers & Chemical Engineering 14, 769.

Viswanathan, J., Grossmann, I., 1993. An alternate minlp model for finding the number of trays required for a specified separation objective. Computers & Chemical Engineering 17 (9), 949–955.

Wall, M., 1999. Galib: C++ library of genetic algorithm components, version 2.4.5. http://lancet.mit.edu./ga.

Ward, W. I., 1970. Analytical and experimental studies of facilitated transport. AIChE Journal 16, 405–410.

Watzdorf, R., Bausa, J., Marquardt, W., 1999. Shortcut methods for nonideal multicomponent distillation: 2. complex columns. AIChE Journal 45 (8), 1615–1628.

Yang, B., Goto, S., 1997. Pervaporation with reactive distillation for the production of ethyl tert-butyl-ether. Sep. Sci. Technol. 32, 971–981.

Appendix A

Hybrid Distillation/Membrane Modelling

The mathematical models used in this thesis as discussed in Chapter 3 are outlined. The sub-models making up the hybrid column, i.e. the distillation and membrane models are presented. Section A.1 lists the distillation column sub-model equations followed by details of the membrane sub-model equations in Section A.2. Ancillary equipments models used within these units are outlined in Section A.4.

All connections between sub-models for the hybrid process as shown in Figure A.1 represent the flowrate, composition, pressure, temperature and enthalpy of that stream. Models to describe each sub-unit within the process superstructure are outlined next.

A.1 Distillation Model

The sub-models making up the distillation column include the reboiler, tray, condenser, pressure vessel, divider and, in case of a batch column, accumulators (Figure A.1). Equations describing these sub-models are now detailed.

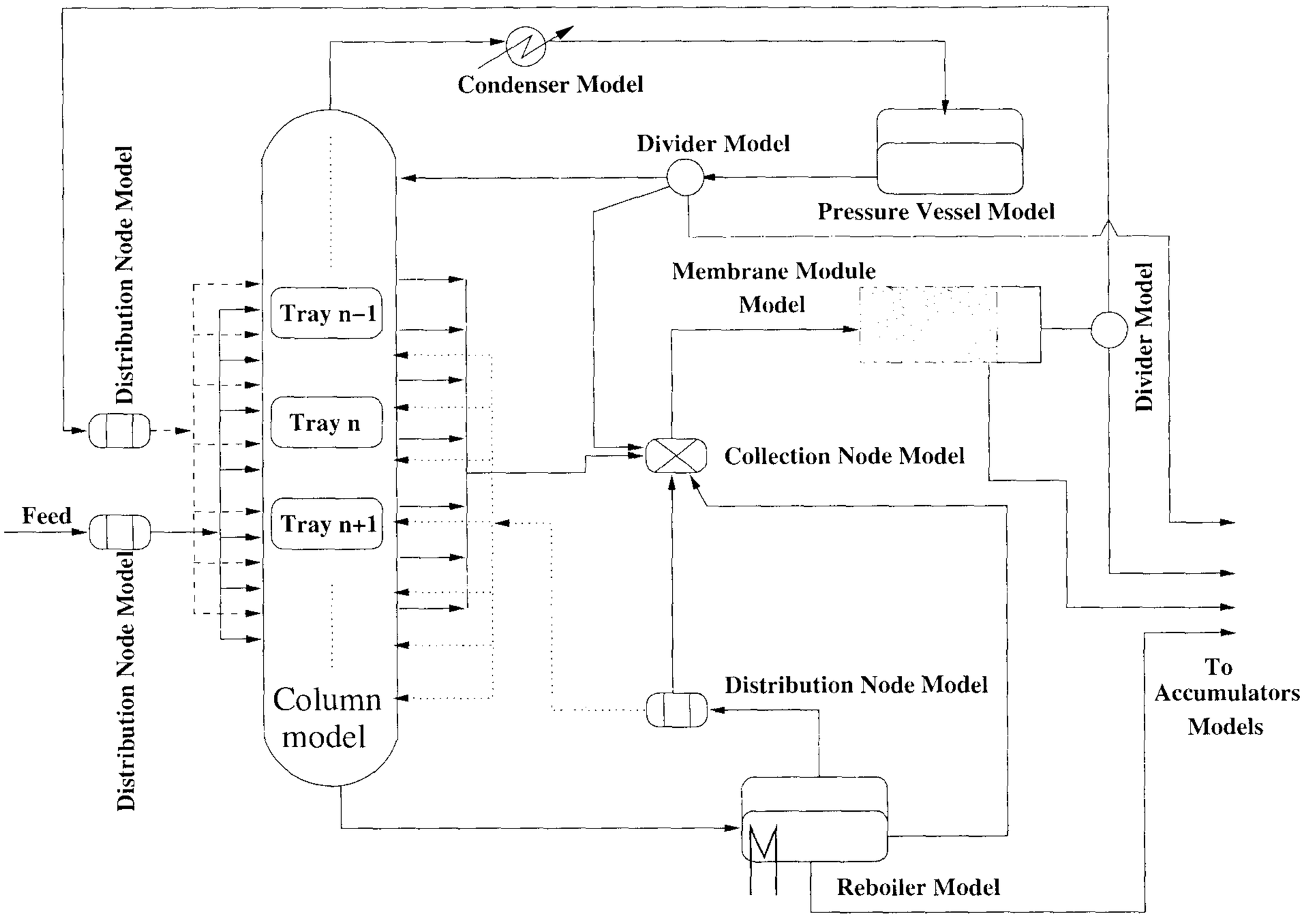

Figure A.1: Hybrid Process Model

A.1.1 Reboiler

Key Model Assumptions

- Perfect mixing of both liquid and vapour phases
- Thermodynamic phase equilibrium
- No liquid entrainment in the vapour stream
- Fast energy dynamics
- Negligible vapour holdup

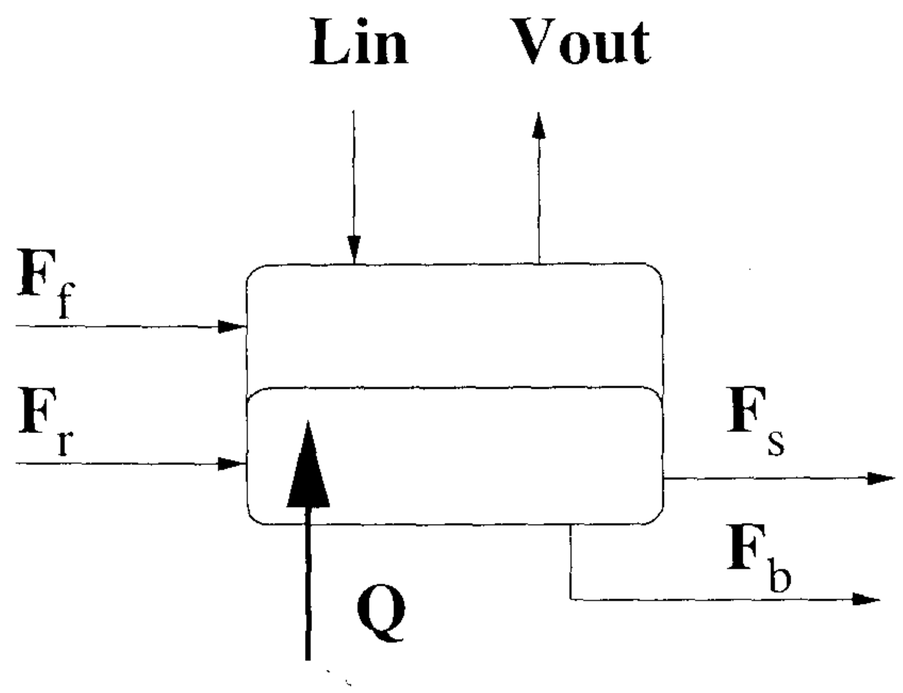

Figure A.2: Reboiler

Equations

Molar balance on component i:

$$\frac{dM_i}{dt} = F_f z_{i,f} + F_r z_{i,r} + L_{in} x_{in} - F_b x_i - F_s x_i - V_{out} y_i \qquad i = 1, .., N_C \qquad \text{(A.1)}$$

Energy balance:

$$Q_{reb} = F_f h_f + F_r h_r + L_{in} h_{in} - F_b h^L - F_s h^L - V_{out} h^V \qquad \text{(A.2)}$$

Component i molar holdup:

$$M_i = M^L x_i \qquad i = 1, .., N_C \qquad \text{(A.3)}$$

Normalisation equations:

$$\sum_{i=1}^{N_C} x_i = \sum_{i=1}^{N_C} y_i = 1 \qquad \text{(A.4)}$$

Phase equilibrium:

$$\phi_i^L x_i = \phi_i^V y_i \qquad i = 1, .., N_C \qquad \text{(A.5)}$$

When the reboiler model is used for a batch process, the feed F_f and bottom F_b stream flowrates are set to zero. The side stream F_s can still exit to provide a possible feed to the membrane unit in case of a hybrid distillation/membrane process.

A.1.2 Tray

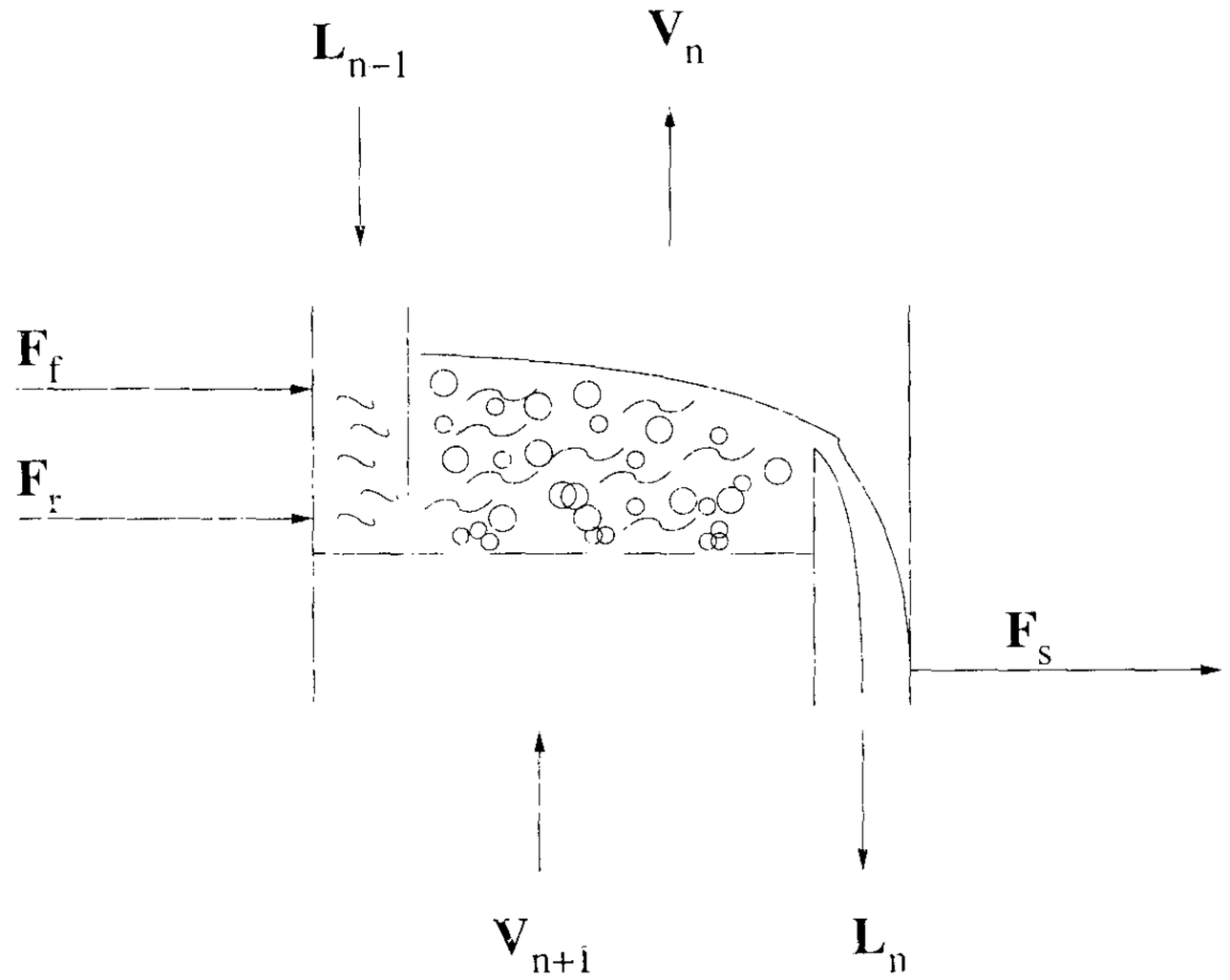

Figure A.3: Tray

Key Model Assumptions

- Liquid and vapour phases exist at all times
- Perfect mixing of liquid and vapour
- Thermodynamic phase equilibrium (Murphree plate efficiency = 1)
- No entrainment of liquid or vapour phase
- No weeping
- Neglected downcomer dynamics
- Fast energy dynamics
- Constant liquid holdup
- Negligible vapour holdup

Equations

Consider the nth tray.

Molar balance on component i:

$$\frac{dM_{i,n}}{dt} = F_f z_{i,f} + F_r z_{i,r} + L_{n-1} x_{i,n-1} + V_{n+1} y_{i,n+1} - L_n x_{i,n} - F_s x_{i,n} - V_n y_{i,n} \qquad (A.6)$$

$$i = 1, .., N_C$$

Flowrate balance:

$$F_f + F_r + L_{n-1} + V_{n+1} = F_s + L_n + V_n \qquad (A.7)$$

Energy balance:

$$F_f h_f + F_r h_r + L_{n-1} h^L_{n-1} + V_{n+1} h^V_{n+1} = L_n h^L_n + F_s h^L_n + + V_n h^V_n \qquad (A.8)$$

$$i = 1, .., N_C$$

Component i molar holdup:

$$M_i = M^L x_i \qquad i = 1, .., N_C \qquad (A.9)$$

Normalisation equations:

$$\sum_{i=1}^{N_C} x_i = \sum_{i=1}^{N_C} y_i = 1 \qquad (A.10)$$

Phase equilibrium:

$$\phi^L_i x_i = \phi^V_i y_i \qquad i = 1, .., N_C \qquad (A.11)$$

Pressure drop over plate:

$$\Delta P = P^V_{in} - P_{tray} \qquad (A.12)$$

when the tray model is used for a batch process, the feed F_f stream flowrate is set to zero.

A.1.3 Condenser Coil

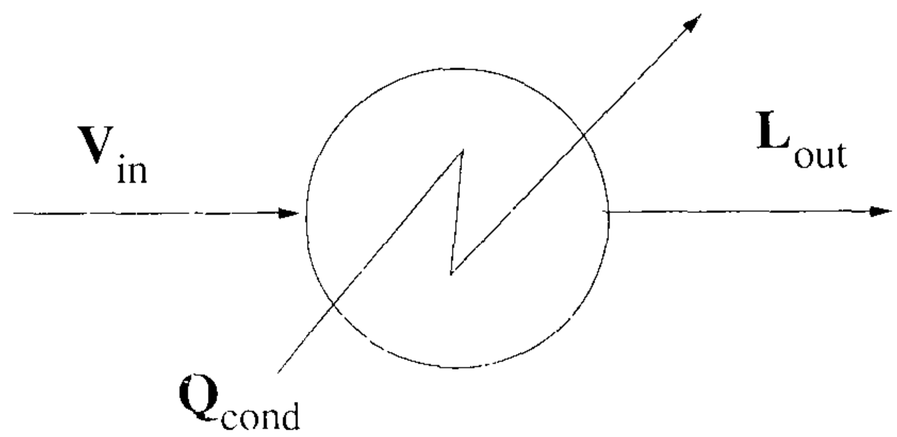

Figure A.4: Condenser coil

Key Model Assumptions

- Total condensation
- No subcooling

Equations

Molar balance:

$$V_{in} = L_{out} \tag{A.13}$$

$$x_i = y_i \qquad i = 1, .., N_C \tag{A.14}$$

Energy balance:

$$Q_{cond} = h_{in}^{V} V_{in} - h_{out}^{L} L_{out} \tag{A.15}$$

Normalisation equations:

$$\sum_{i=1}^{N_C} y_i = 1 \tag{A.16}$$

Phase equilibrium:

$$\phi_i^L x_i = \phi_i^V y_i \qquad i = 1, .., N_C \tag{A.17}$$

A.1.4 Reflux Drum

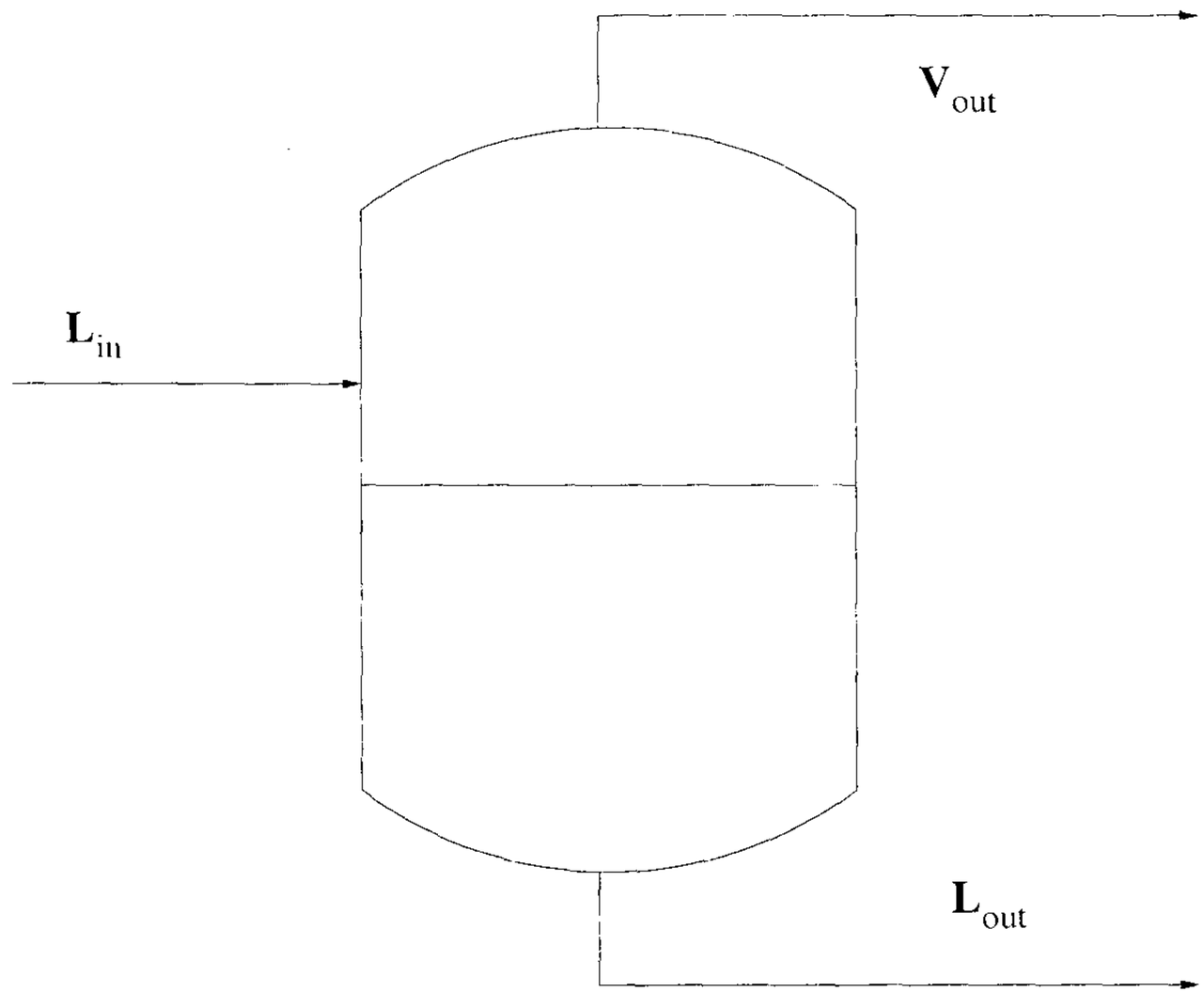

Figure A.5: Pressure vessel

Key Model Assumptions

- Perfect mixing in both phases
- Thermodynamic phase equilibrium
- Adiabatic
- Fast energy dynamics
- Negligible vapour holdup

Equations

Molar balance on component i:

$$\frac{dM_i}{dt} = L_{in}x_{i,in} - L_{out}x_i - V_{out}y_i \qquad i = 1,..,N_C \tag{A.18}$$

Energy balance:

$$L_{in}h_{in}^{L} = L_{out}h_{out}^{L} + V_{out}h_{out}^{V} \tag{A.19}$$

Component i molar holdup:

$$M_i = M^L x_i \qquad i = 1, .., N_C \tag{A.20}$$

Normalisation equations:

$$\sum_{i=1}^{N_C} x_i = \sum_{i=1}^{N_C} y_i = 1 \tag{A.21}$$

Phase equilibrium:

$$\phi_i^L x_i = \phi_i^V y_i \qquad i = 1, .., N_C \tag{A.22}$$

A.1.5 Accumulator Model

The model of the accumulators is identical to that of the reflux drum model with the exception that there are no flows leaving the unit, *i.e.* $L_{out} = V_{out} = 0$. No accumulators are used when the column is considered for steady-state operation.

A.1.6 Stream Divider

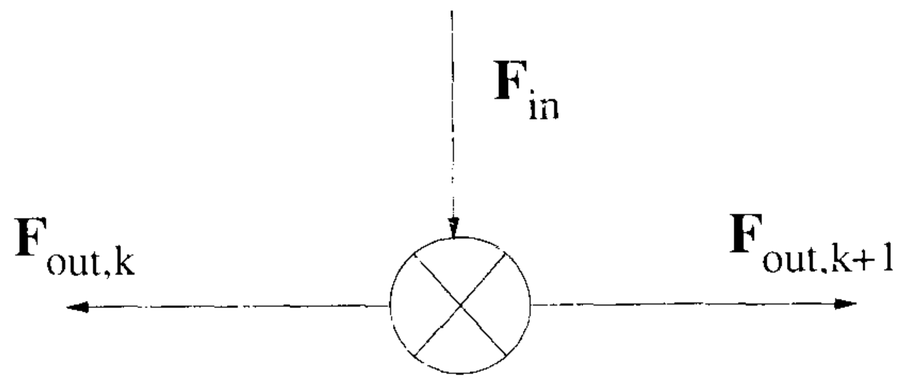

Figure A.6: Stream divider

Key Model Assumptions

- No pressure drop through the divider
- No change in composition and temperature

Equations

Molar balance:

$$F_{in} = \sum_{k=1}^{N_{out}} F_{out,k} \tag{A.23}$$

Inlet and outlet relationship:

$$x_{in} = x_{out,k} \qquad k = 1,..,N_{out} \tag{A.24}$$

$$P_{in} = P_{out,k} \qquad k = 1,..,N_{out} \tag{A.25}$$

$$T_{in} = T_{out,k} \qquad k = 1,..,N_{out} \tag{A.26}$$

$$h_{in} = h_{out,k} \qquad k = 1,..,N_{out} \tag{A.27}$$

A.2 Membrane Model

The derivations of the two membrane module models of different complexities described in Chapter 3 are outlined in the next sections. The sub-models making up the hollow-fibre membrane module include the fibre, shell and membrane characterisation sub-models. The sub-models are connected through a principal model representing the module as illustrated in Figure A.7.

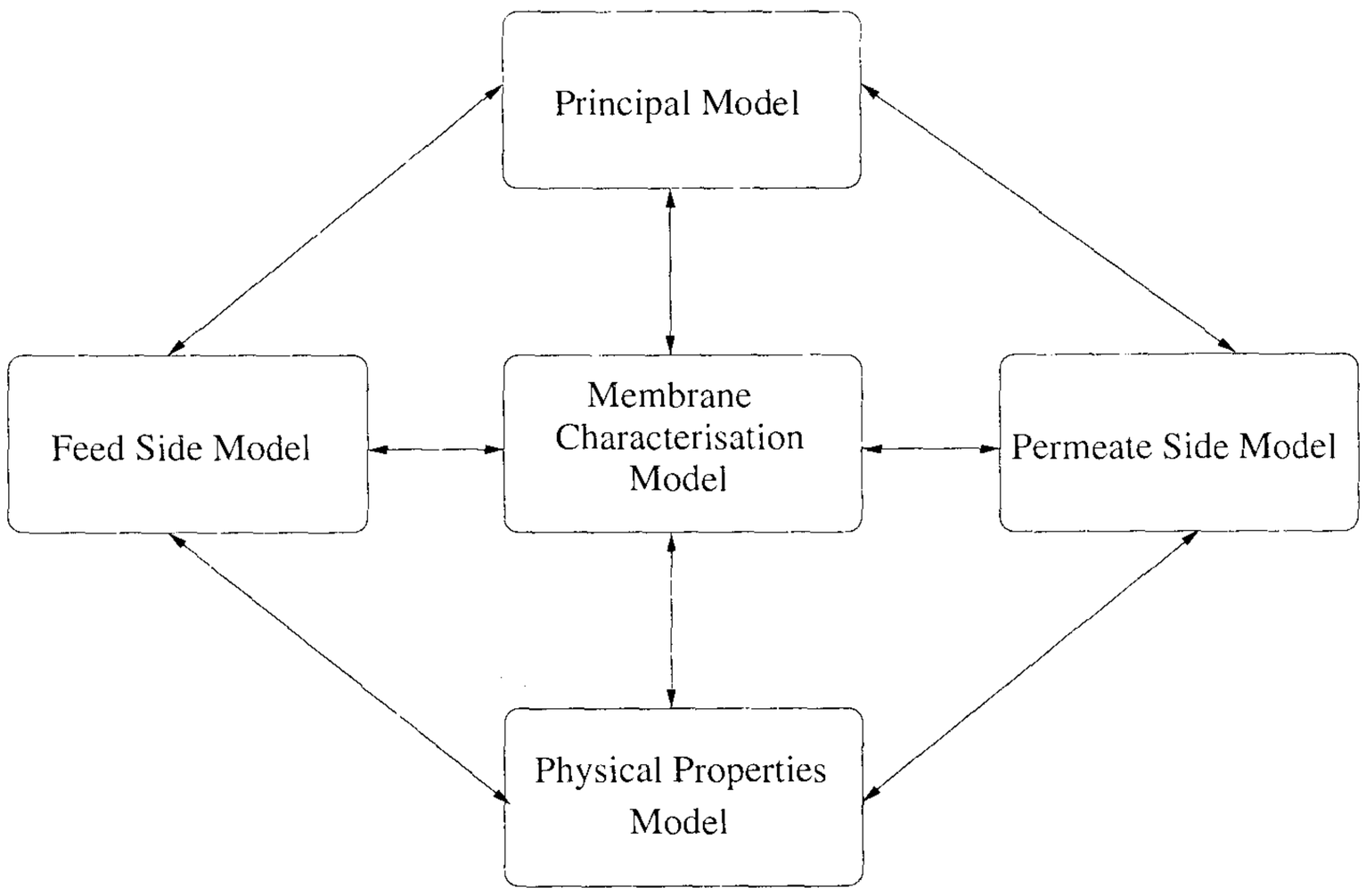

Figure A.7: Membrane model structure

A.2.1 Continuity Equations

The continuity equation in cylindrical coordinates is derived by considering the finite cylindrical element shown in Figure A.8 above with slides $dr, r.d\theta$ and dz. The velocity components normal to the r, θ and z faces of the finite element are v_r, v_θ and v_z, respectively.

Volume of element:

$$\Delta V = r\Delta\theta\Delta r\Delta z \tag{A.28}$$

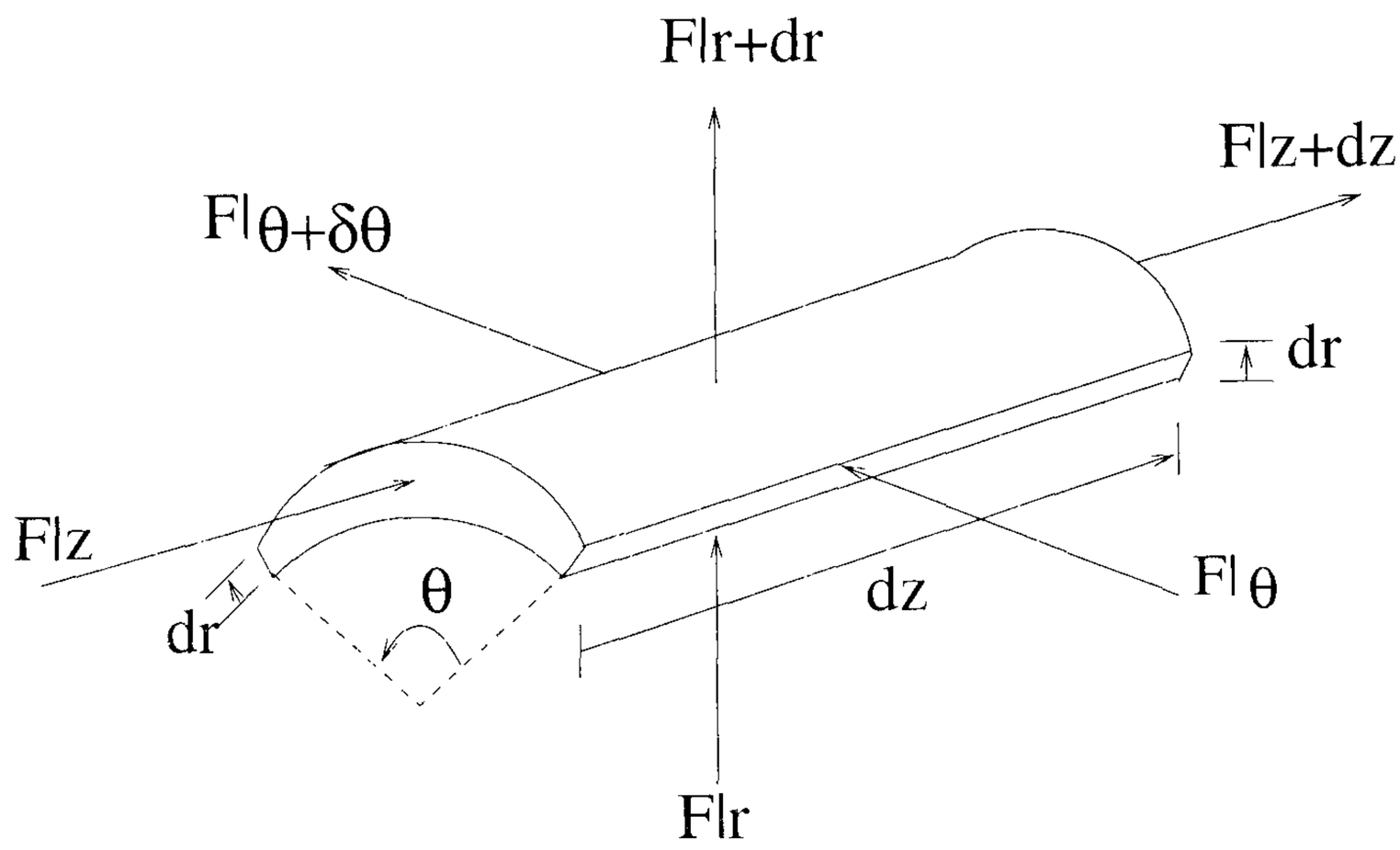

Figure A.8: Finite control volume

Conservation of mass in the volume element:

Mass accumulated in ΔV = Mass convected into ΔV - Mass convected out of ΔV (A.29)

Net convective flow on the θ-direction:

$$\Delta r \Delta z[\rho v_\theta|_\theta - \rho v_\theta|_{\theta+\Delta\theta}] \tag{A.30}$$

Net convective flow on the r-direction:

$$\Delta\theta \Delta z[\rho v_r|_r.(r - \Delta r) - \rho v_r|_{r+\Delta r}.(r)] \tag{A.31}$$

Net convective flow on the z-direction:

$$r\Delta\theta \Delta r[\rho v_z|_z - \rho v_z|_{z+\Delta z}] \tag{A.32}$$

Combining equations A.30 to A.32 then dividing by ΔV, also assuming for a small Δr that $(r - \Delta r) = r$, taking $lim_{\Delta V \to 0}$, and invoking the definition of the partial derivative leads to:

$$\frac{\partial \rho}{\partial t} = -\frac{1}{r}\frac{\partial}{\partial r}(\rho r v_r) - \frac{1}{r}\frac{\partial}{\partial \theta}(\rho v_\theta) - \frac{\partial}{\partial z}(\rho v_z) \tag{A.33}$$

Similarly, the energy continuity equation can be obtained as follow:

$$\frac{\partial \rho \hat{U}}{\partial t} = -\frac{1}{r}\frac{\partial}{\partial r}(\rho r q_r) - \frac{1}{r}\frac{\partial}{\partial \theta}(\rho q_\theta) - \frac{\partial}{\partial z}(\rho q_z) \tag{A.34}$$

A.2.2 Two-Dimensional Model

Hollow-Fibre Module, Fibre Side Sub-Model

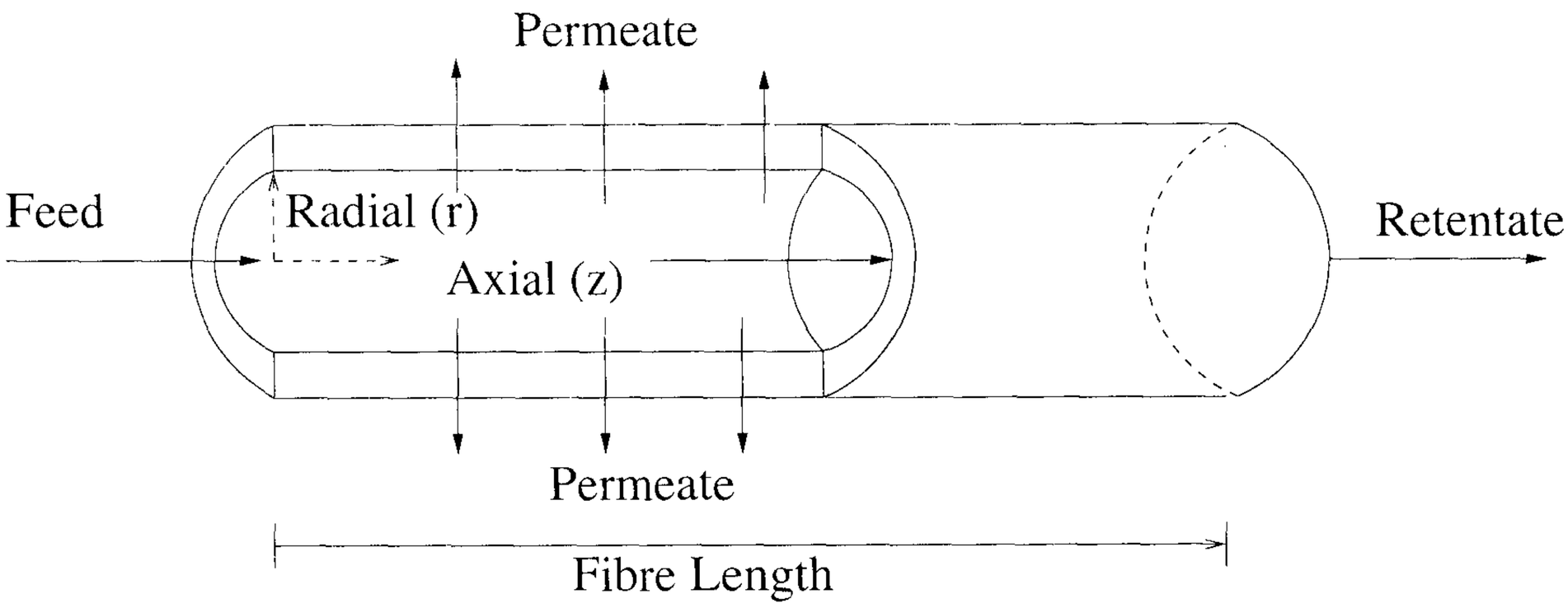

Figure A.9: Single hollow-fibre with fibre feed

Key Model Assumptions

- Non-ideal plug flow model
- Radial symmetry at the centre of the fibre
- No slip conditions at the fibre wall

Molar balance on component i:

$$\frac{\partial c_i}{\partial t} = -\frac{1}{r}\frac{\partial}{\partial r}(r F^r_{m,i}) - \frac{\partial}{\partial z}(F^z_{m,i}) \tag{A.35}$$

Energy balance on molar basis:

$$\frac{\partial \rho^m \hat{U}}{\partial t} = -\frac{1}{r}\frac{\partial}{\partial r}(\rho r q_r) - \frac{\partial}{\partial z}(\rho q_z) \tag{A.36}$$

Radial and axial molar fluxes:

$$F^r_{m,i} = c_i v_r - D_i \frac{\partial c_i}{\partial r} \tag{A.37}$$

$$F^z_{m,i} = c_i v_z - D_i \frac{\partial c_i}{\partial z} \tag{A.38}$$

Molar density:

$$\rho^m = \sum_{i=1}^{N_C} c_i \tag{A.39}$$

Radial and axial energy fluxes:

$$q_r = \rho \bar{v}_r h - k_c \frac{\partial T}{\partial r} \tag{A.40}$$

$$q_z = \rho \bar{v}_z h - k_c \frac{\partial T}{\partial z} \tag{A.41}$$

Radial boundary conditions:

$$v_r|_{r=0} = 0 \qquad \forall z \tag{A.42}$$

$$v_z|_{r=R} = 0 \qquad \forall z \tag{A.43}$$

$$F^r_{m,i}|_{r=R} = J_i \qquad \forall z \tag{A.44}$$

Axial boundary conditions:

$$\frac{\partial c_i v_z}{\partial z}|_{z=L} = 0 \qquad \forall r \tag{A.45}$$

$$\frac{\partial T}{\partial z}|_{z=L} = 0 \qquad \forall r \tag{A.46}$$

$$v_r|_{z=[0,L]} = 0 \qquad \forall r \tag{A.47}$$

Hollow-Fibre Module, Shell Side Sub-Model

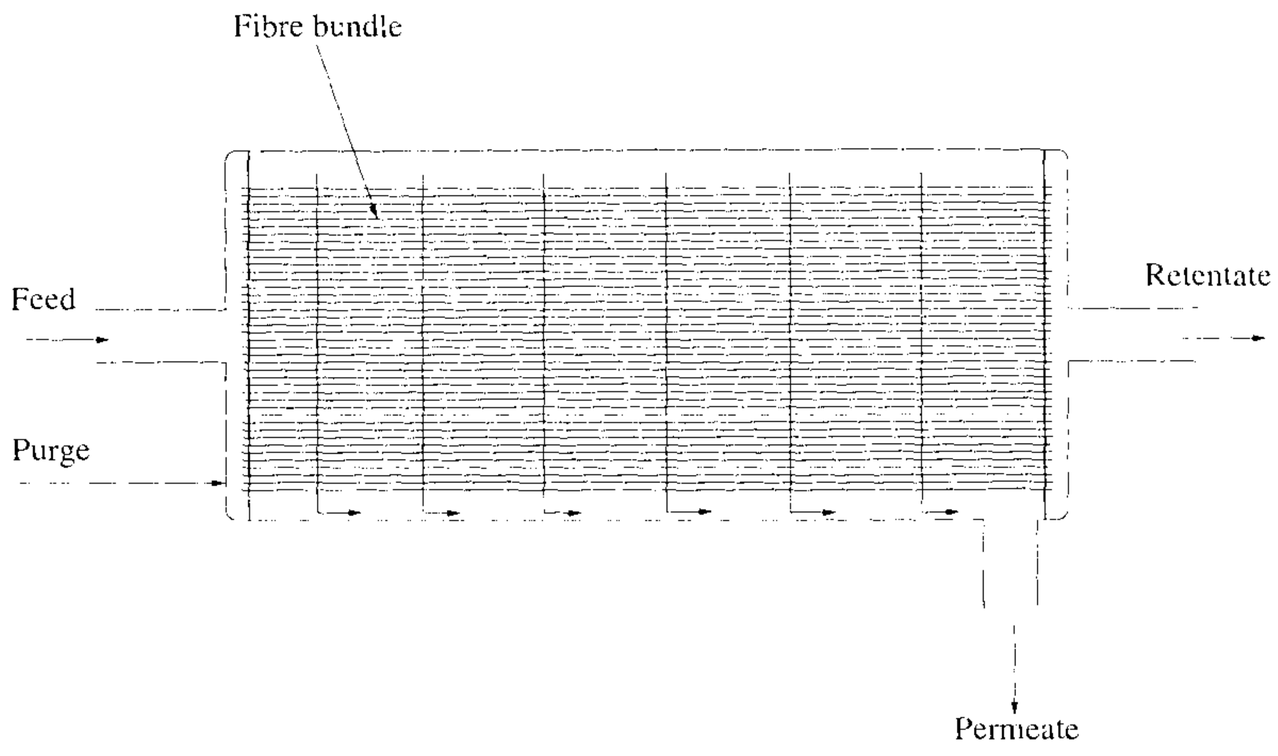

Figure A.10: Hollow-fibre module with fibre feed

Key Model Assumptions

- The fibre bundle is treated as a continuous radially symmetric porous medium
- Non-ideal plug flow
- Radial symmetry at the centre of the fibre bundle
- No slip conditions at the fibre bundle wall

Molar balance on component i:

$$\frac{\partial c_i}{\partial t} = -\frac{1}{s}\frac{\partial}{\partial s}(sF^s_{m,i}) - \frac{\partial}{\partial z}(F^z_{m,i}) - \bar{\alpha}J_i \tag{A.48}$$

Energy balance on molar basis:

$$\frac{\partial \rho^m \hat{U}}{\partial t} = -\frac{1}{s}\frac{\partial}{\partial s}(\rho s q_s) - \frac{\partial}{\partial z}(\rho q_z) \tag{A.49}$$

Radial and axial molar fluxes:

$$F^s_{m,i} = c_i v_s - D_i \frac{\partial c_i}{\partial s} \tag{A.50}$$

$$F^z_{m,i} = c_i v_z - D_i \frac{\partial c_i}{\partial z} \tag{A.51}$$

Molar density:

$$\rho^m = \sum_{i=1}^{N_C} c_i \tag{A.52}$$

Radial and axial energy fluxes:

$$q_s = \rho \bar{v}_s h - k_c \frac{\partial T}{\partial s} \tag{A.53}$$

$$q_z = \rho \bar{v}_z h - k_c \frac{\partial T}{\partial z} \tag{A.54}$$

Radial boundary conditions:

$$v_z|_{s=S} = 0 \qquad \forall z \tag{A.55}$$

$$\frac{\partial c_i v_s}{\partial s}|_{s=S} = 0 \qquad \forall z \tag{A.56}$$

$$\frac{\partial T}{\partial s}|_{s=S} = 0 \qquad \forall z \tag{A.57}$$

Axial boundary conditions:

$$v_z|_{z=[0,L]} = 0 \qquad \forall s \tag{A.58}$$

A.2.3 One-Dimensional Model

Fibre Sub-Model

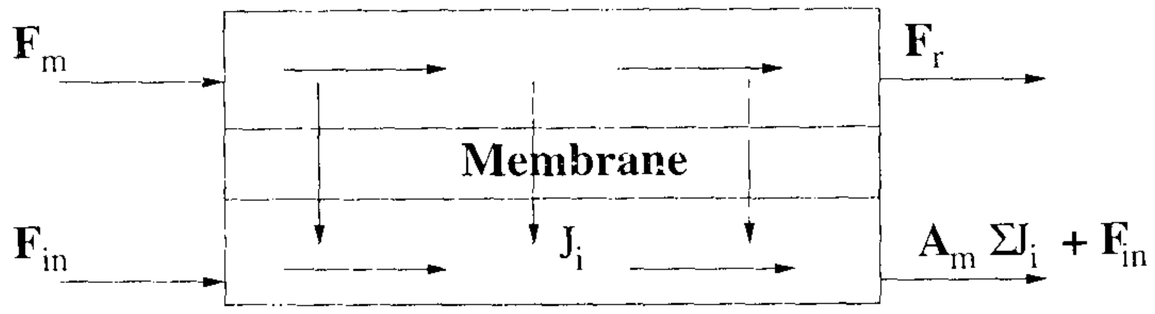

Figure A.11: General membrane module

Key Model Assumptions

- Ideal plug flow
- Perfect mixing inside fibres

Mass balance:

$$\frac{dM_i}{dt} = F_m z_m - F_r x_r - A_{mem} J_i \qquad i = 1, .., N_C \tag{A.59}$$

Energy balance:

$$\frac{dU}{dt} = F_m h_m - F_r h_r - A_{mem} Q_{mem} \tag{A.60}$$

Component i molar holdup:

$$M_i = M^L x_i \qquad i = 1, .., N_C \tag{A.61}$$

Total energy

$$U = M^L h^L \tag{A.62}$$

Normalisation equations:

$$\sum_{i=1}^{N_C} x_i = 1 \tag{A.63}$$

Shell Sub-Model

Key Model Assumptions

- Ideal plug flow
- Perfect mixing inside shell
- Purge gas inlet

Mass balance:

$$\frac{dM_i}{dt} = F_{in} z_{in} - F_{out} x_i + A_{mem} J_i \qquad i = 1, .., N_C \tag{A.64}$$

Energy balance:

$$\frac{dU}{dt} = F_{in} h_{in} - F_{out} h + A_{mem} Q_{mem} \tag{A.65}$$

Component i molar holdup:

$$M_i = M^V y_i \qquad i = 1, .., N_C \tag{A.66}$$

Total energy

$$U = M^V h^V \tag{A.67}$$

Normalisation equations:

$$\sum_{i=1}^{N_C} y_i = 1 \tag{A.68}$$

Membrane Characterisation Sub-Model

Tsuyumoto et al. (1997) described the fluxes of both water and ethanol through a polyin complex membrane that preferentially permeates water to dehydrate ethanol-water mixtures. They also showed experimental studies to validate this model. The water flux through the membrane is described by a solution-diffusion model where:

$$J_W = \frac{D_{W0}K_{cw}}{\delta^m}\left(\gamma_{1W}x_{1W} - \frac{P_2}{P_W^{sat}}x_{2W}\right) + \frac{D_{W0}K_{cw}^2 k_{dw}}{2\delta^m}\left((\gamma_{1W}x_{1W})^2 - \left(\frac{P_2}{P_W^{sat}}x_{2W}\right)^2\right) \quad \text{(A.69)}$$

The ethanol flux is described by:

$$J_E = Q_E w_E (P_1 - P_2) \quad \text{(A.70)}$$

The model parameters are given by Tsuyumoto et al. (1997) as

$$D_{W0}K_{cw} = 8.086 \times 10^6 \exp^{\frac{-11500}{T}} \quad mol/ms \quad \text{(A.71)}$$

$$\frac{D_{W0}K_{cw}^2 k_{dw}}{2} = 3.441 \times 10^{-3} \exp^{\frac{-3390}{T}} \quad mol/ms \quad \text{(A.72)}$$

$$Q_E = 1.72 \times 10^{-10} \quad mol/m^2 sPa \quad \text{(A.73)}$$

Models that chracterise other membrane similar to the one described above, can easily be implemented as illustrated in Figure A.7.

A.3 Membrane Models Simulation Studies

While distillation process modelling is well established, membrane process modelling is relatively newer and highly dependent on the type of membrane characterisation equations used. The accuracy of membrane models coupled with real membrane characterisation equations will need to be compaced to real experimental values to determine its validity for describing the process. In this section, the accuracy of the two hollow-fibre membrane

models as presented earlier is assessed against experimental data (Tsuyumoto et al., 1997) and similar, but more detailed models in terms of the momentum balances, developed by Marriott et al. (2001). An ethanol dehydration system is considered as the bases for the comparison with the process specifications showed in Table A.1.

Results

The hollow-fibre membrane module was simulated for a continuous fibre feed flow mode with a co-current shell flow arrangements. The permeate is collected in the shell and then removed with a purge gas. As shown in Table A.2, the 2-D model and to a lesser extent the 1-D model, show a good agreement with experimental results (Tsuyumoto et al., 1997) and similar simulations (Marriott et al., 2001). It is also noted that for optimisation purposes, the 2-D model developed will result in a significant increase in solution time compared to the 1-D model developed. The use of the 1-D model for these purpose is therefore justified, especially as there is minimal loss in accuracy.

Property	Value	Units
Module		
Operation	Continuous	-
Flow arrangements	Co-current	-
Feed mode	Fibre feed	-
Shell		
Purge gas flowrate outlet	1×10^{-12}	mol/s
Purge gas temperature	333	K
Permeate pressure	400	Pa
Fibres		
Feed pressure	1.01×10^{5}	Pa
Feed temperature	353	K
Feed eth. wt%	94.0-96.8	-
Feed mass flowrate	44.8-248.5	kg/hr

Table A.1: Module properties for the ethanol dehydration system

Feed rate (kg/hr)	44.8	248.5
Feed wt% ethanol	94.0	96.8
Product wt% ethanol		
Experimental (Tsuyumoto et al., 1997)	97.2	97.4
Marriott et al. (2001), 1-D	97.5	97.4
Marriott et al. (2001), 2-D	97.3	97.4
This work, 1-D	97.0	97.8
This work, 2-D	97.3	97.4

Table A.2: Comparison of model results

A.4 Ancillary Equipment Models

A number of information streams has been used in conjunction with the membrane and distillation models. These correspond to actual stream flows on the real plant. The additional models required to describe the ancillary equipment operation are detailed in this section.

Distribution Node Model

The distribution node determines the destination of an inlet stream. It has single input but multiple outputs. The node uses a binary variable α_i to select the properties for stream i to be used as the outlet stream. In case no real inlet stream is needed, *e.g.* where no feed flowrate is present for a batch process (Figure A.1), a dummy stream of zero flowrate is selected. The equations representing this unit can be written as:

$$F = \sum_{k=1}^{N_{out}} \alpha_i F_{out,k} \qquad \sum \alpha_i = 1 \quad \alpha_i \in \{0,1\} \tag{A.74}$$

$$x = \sum_{k=1}^{N_{out}} \alpha_i x_{out,k} \qquad \sum \alpha_i = 1 \quad \alpha_i \in \{0,1\} \tag{A.75}$$

$$P = \sum_{k=1}^{N_{out}} \alpha_i P_{out,k} \qquad \sum \alpha_i = 1 \quad \alpha_i \in \{0,1\} \tag{A.76}$$

$$T = \sum_{k=1}^{N_{out}} \alpha_i T_{out,k} \qquad \sum \alpha_i = 1 \quad \alpha_i \in \{0,1\} \tag{A.77}$$

$$h = \sum_{k=1}^{N_{out}} \alpha_i h_{out,k} \qquad \sum \alpha_i = 1 \quad \alpha_i \in \{0,1\} \tag{A.78}$$

(A.79)

Collection Node Model

The Collection node determines the origin of an outlet stream. It has multiple inputs but single output. The node uses a binary variable β_i to select the properties for stream i to

be used as the inlet stream. A dummy stream is introduced where all inputs are required to be zero, *e.g.* where the structure is considered for pure distillation process there is no feed to the membrane unit. The equations representing this unit can be written as:

$$F = \sum_{k=1}^{N_{in}} \beta_i F_{in,k} \qquad \sum \beta_i = 1 \quad \beta_i \in \{0,1\} \tag{A.80}$$

$$x = \sum_{k=1}^{N_{in}} \beta_i x_{in,k} \qquad \sum \beta_i = 1 \quad \beta_i \in \{0,1\} \tag{A.81}$$

$$P = \sum_{k=1}^{N_{in}} \beta_i P_{in,k} \qquad \sum \beta_i = 1 \quad \beta_i \in \{0,1\} \tag{A.82}$$

$$T = \sum_{k=1}^{N_{in}} \beta_i T_{in,k} \qquad \sum \beta_i = 1 \quad \beta_i \in \{0,1\} \tag{A.83}$$

$$h = \sum_{k=1}^{N_{in}} \beta_i h_{in,k} \qquad \sum \beta_i = 1 \quad \beta_i \in \{0,1\} \tag{A.84}$$

(A.85)

Heater Exchanger

The heat exchanger model is used to calculate the energy load of the membrane feed heater as well as permeate condenser as follow:

$$Q_h = F_{in}|(h_{in} - h_{out})| \tag{A.86}$$

Liquid Pump

The energy load on the pump is calculated as:

$$Q_p = \frac{\nu_p}{\eta_p}\left(P_p^{out} - P_p^{in}\right) \tag{A.87}$$

Vacuum Turbine

The energy load on the turbine is calculated as:

$$Q_t = \frac{\nu_t}{\eta_t} \times P_t^{in} \ln\left(\frac{P_t^{out}}{P_t^{in}}\right) \tag{A.88}$$

Appendix B

General Dynamic Optimisation Problem Statement

The general form of the dynamic optimisation problem for hybrid batch distillation/pervaporation processes as used in this thesis is outlined.

B.1 Model

The mathematical model describing the hybrid batch distillation/pervaporation process operations (Appendix A) used for the optimisation of these processes, has the general form:

$$f(x(t), \dot{x}(t), y(t), u(t), v, t) = 0 \quad \forall\, t \in [0, t_f] \tag{B.1}$$

where

- $x(t)$: differential variables (*e.g.* component molar holdups and internal energy)
- $y(t)$: algebraic variables (*e.g.* compositions, flowrate, temperature and pressure)
- $u(t)$: time-dependent decision variables (*e.g.* reflux ratio)

- v : time-invariant parameters (*e.g.* reboiler heat duty and membrane feed flowrate if kept constant throughout the operation)

B.2 Initial conditions

The *initial conditions* required for initialisation of the DAE system have the general form:

$$I(x(0), \dot{x}(0), y(0), u(0), v) = 0 \tag{B.2}$$

The values of the initial holdups, temperatures and compositions throughout the column may represent suitable initial conditions. All of these are algebraic variables in our case. Therefore, the initial conditions used are of the simpler form:

$$\hat{y}(0) - \hat{y}_0 = 0 \tag{B.3}$$

where $\hat{y}$ represents a subset of the algebraic variables y, and $\hat{y}_0$ are *given* initial values.

B.3 Constraints

There are usually different types of constraints which need to be satisfied. *Path constraints*, which hold at all times, may generally be represented as:

$$h(x(t), \dot{x}(t), y(t), u(t), v, t) \leq 0 \qquad \forall\, t \in [0, t_f] \tag{B.4}$$

The liquid holdup in the reboiler drum, for instance, can have a Path constraint in the liquid level if this must not exceed the maximum level (to avoid over-filling), nor fall below a minimum level (to prevent damage to a heating coil) at *any* time throughout the operation of the column.

Constraints which hold at a particular instant in time, t_λ, are known as *point constraints*, and these have the following general form:

$$g(x(t_\lambda), \dot{x}(t_\lambda), y(t_\lambda), u(t_\lambda), v, t_\lambda) \leq 0 \qquad \lambda = 1, 2, .. \tag{B.5}$$

End point constraints are of particular interest (that hold at the final time), as they normally represent specifications imposed on the purities and quantities of the final products (Chapters 4-6):

$$k(x(t_f), \dot{x}(t_f), y(t_f), u(t_f), v, t_f) \leq 0 \tag{B.6}$$

B.4 Bounds

There are also bounds on the control variables and on the time-invariant parameters, which define the optimisation search space:

$$u^{\min} \leq u(t) \leq u^{\max} \qquad \forall\, t \in [0, t_f] \tag{B.7}$$

$$v^{\min} \leq v \leq v^{\max} \tag{B.8}$$

For instance, the internal reflux ratio must lie between 0 and 1 ($0 \leq R(t) \leq 1$).

There may also be limitations on the batch processing time:

$$t_f^{\min} \leq t_f \leq t_f^{\max} \tag{B.9}$$

B.5 Objective Function

The *objective function* is generally of the form:

$$\min \Phi\,(x(t_f), \dot{x}(t_f), y(t_f), u(t_f), v, t_f) \tag{B.10}$$

B.6 General Optimisation Problem Statement

The general dynamic optimisation problem formulation for hybrid batch distillation/ pervaporation may therefore be summarised as follows:

$$\min \Phi\left(x(t_f), \dot{x}(t_f), y(t_f), u(t_f), v, t_f\right) \tag{B.11}$$

subject to

$$f(x(t), \dot{x}(t), y(t), u(t), v, t) = 0 \qquad \forall\, t \in [0, t_f] \tag{B.12}$$

$$I(x(0), \dot{x}(0), y(0), u(0), v) = 0 \tag{B.13}$$

$$h(x(t), \dot{x}(t), y(t), u(t), v, t) \leq 0 \qquad \forall\, t \in [0, t_f] \tag{B.14}$$

$$g(x(t_\lambda), \dot{x}(t_\lambda), y(t_\lambda), u(t_\lambda), v, t_\lambda) \leq 0 \qquad \lambda = 1, 2, .. \tag{B.15}$$

$$k(x(t_f), \dot{x}(t_f), y(t_f), u(t_f), v, t_f) \leq 0 \tag{B.16}$$

$$u^{\min} \leq u(t) \leq u^{\max} \qquad \forall\, t \in [0, t_f] \tag{B.17}$$

$$v^{\min} \leq v \leq v^{\max} \tag{B.18}$$

$$t_f^{\min} \leq t_f \leq t_f^{\max} \tag{B.19}$$

Appendix C

Genetic Algorithm Parameters Tuning

The sensitivity of the GA parameters discussed in Chapter 3 is analysed in this appendix. The base case process for the separation of acetone-water mixture described in Chapter 4 is used to conduct the analysis.

The main parameters within the GA framework are: 1) the population size N_{pop}, 2) the crossover rate P_c, 3) the mutation rate P_m, in addition to 4) the population overlap percentage P_{ss} (steady state GA only). The choice of the values of these parameters influences the outcomes of the optimisation. Another important determining factor in obtaining a good final solution is the termination criterion employed and, for constrained optimisation problems, the penalty method used. These parameters are often tuned manually depending on the problem at hand. This appendix outlines the effects of the GA population size N_{pop}, mutation percentage P_m, penalty function and termination criteria employed on the algorithm's performance as employed in this work.

Considerable theoretical studies have been carried out in order to link the population size, N_{pop}, with the number of variables of the optimisation problem and to better tune mutation and crossover rates. The tuning operation, because of the stochastic nature

Parameter	**Value**
Population size N_{pop}	100*, (50, 100, 120)†
Crossover rate P_c	75%*
Mutation rate P_m	10%*, (0%, 5%, 10%, 15%, 20%)†
Population overlap percentage P_{ss}	25%*
Penalty equation (Eq. C.1-C.2)	C.1* (C.1,C.2)†
Termination criteria	Population best* , $\geq$ 95%
	(Population best $\geq$ 95%, No. of Generations$\geq$ 200)†

Table C.1: GA parameters, * base case, † sensitivity

of the algorithm, nevertheless should be performed for each specific problem at hand, *especially* where the genetic algorithm approach has not been applied before (*e.g.* GA optimisation of hybrid separation processes as considered in this thesis).

The general procedure to tune the GA parameters is first to obtain good initial guesses for their values based on general heuristics and rules of thumb (Goldberg, 1989) or from past experience of similar chemical engineering optimisation problems where GA has been applied (*e.g.* Marriott (2001) and Garrard and Fraga (1998)). For instance, most of the applications in various fields, including outside chemical engineering, points to high crossover rates and low mutation rates, *e.g.* above 70% and below 20%, respectively. This is then followed by an appropriate tuning of the parameters achieved conventionally through either a sensitivity analysis, as presented in this study, or parametric optimisation which presents further complexity to the problem. Analysis conducted in this appendix use the base case parameters as outlined in Table C.1.

C.1 Population Size and Overlap Percentage

The size of the population should be sufficiently large to provide a diversity within the GA populations. Lewin et al. (1998) report that genetic algorithm are generally insensitive

Population size	**50**	**100**	**120**
Final best solution $\$/yr$	0.92*	11.8×10^6	$150.\times10^6$
Final average solution $\$/yr$	0.85*	2.77×10^6	12.1×10^6
Constraint violation in final best%	8.5*	0	0
Generations to convergence	48*	59	68

Table C.2: Effects of population size on GA performance, * infeasible solution

to the population size provided that this is not very small. Garrard and Fraga (1998) studied the effect of population size and percentage overlap for a range $N_{pop} \in [10, 100]$ and $P_{ss} \in [25\%, 75\%]$, respectively. They concluded that higher population size and percentage overlap result in a better standard deviation of the population from the optimum solution value, but with higher computational costs. The value of P_{ss} is thus a trade-off between reliability of the final solution and computational costs as long as the critical population size is established.

Figures C.1a and C.1b show the effect of varying the population size on the average and best solutions with all the other parameters at the base case (see Table C.1). It can be seen that a population size of 120 yields the best average and best solutions compared to the other sizes (Table C.2). With a small population size (50) for the optimisation of hybrid separation processes, the final solution is infeasible as there is no enough diversity in the genetic population to evolve effectively. If a population size of 100 is considered, a 27% decrease (Table C.2) on the best solution value is observed compared to 120. The improvement of using the extra 20 genomes in the population, however, increases the computational time, as the population size of 120 converged in 68 generations compared to 59 generations with $N_{pop} = 100$. The decision of which size to use will depend on the required accuracy and the available computational time which is essentially decided by the purpose of the optimisation procedure (*e.g.* rigorous, initial screening).

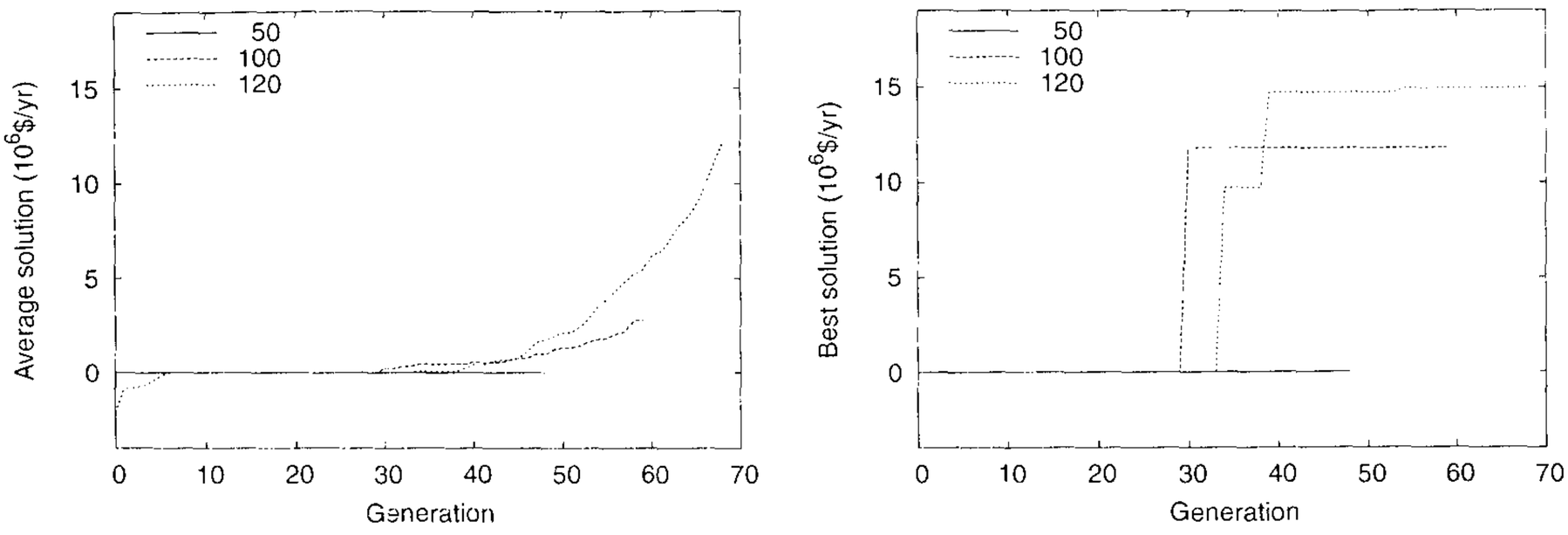

(a) (b)

Figure C.1: Effects of population size on solutions, a, population average solution, b, population best solution

C.2 Mutation Rate

The mutation rate is the likelihood that a gene in an offspring genome will change. It is used to control the rate of introducing new genetic material into the population. A high mutation rate will override the effect of genome crossover, but a value set too low will cause the algorithm to converge prematurely. It is therefore important that an appropriate value for the mutation rate be chosen.

The mutation rate, as all genetic operators, is dependent on the type of the problem being solved. Garrard and Fraga (1998) and Low and Sørensen (2003) found that a mutation rate of 10% resulted in better solutions than other values for mass exchanger network synthesis and optimisation of batch distillation processes, respectively. A mutation rate of 20%, however, has been found to be better for the optimisation of pervaporation membrane systems (Marriott, 2001). It is therefore expected that a value between these two will be appropriate for hybrid processes.

The effects of mutation rate is investigated with all other parameters fixed as in the base case (Table C.1). Figures C.2a and C.2b show the effect of different mutation rates on

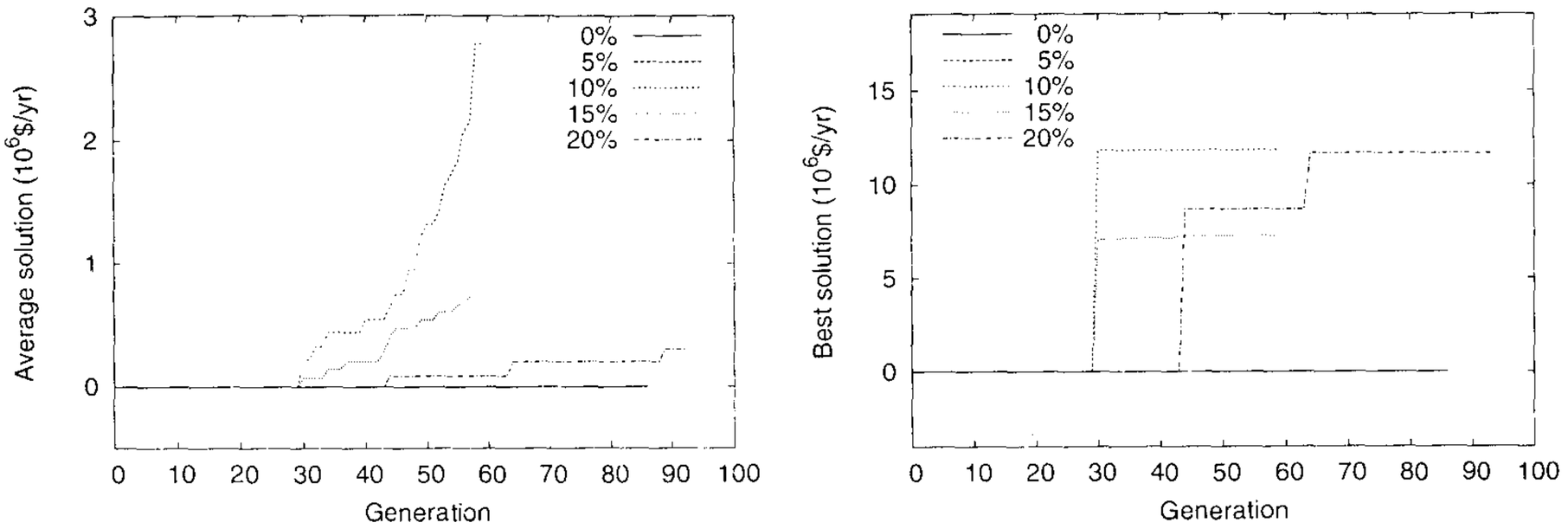

(a) (b)

Figure C.2: Effects of the mutation rate on solutions, a, population average solution, b, population best solution

Mutation rate	**0%**	**5%**	**10%**	**15%**	**20%**
Final best solution $\$/yr$	0.98*	0.99*	11.8×10^6	7.25×10^6	11.7×10^6
Final average solution $\$/yr$	0.98*	0.98*	2.77×10^6	0.73×10^6	0.30×10^6
Constraint violation in final best %	2.3*	0.36*	0	0	0
Generations to convergence	86*	45*	59	59	93

Table C.3: Effects of mutation rate on GA performance, * infeasible solution

the average and best solutions, respectively. It is observed that with low mutation rates (0% and 5%) the final population converged to infeasible solutions using a convergence setting of $\geq 95\%$ of the best solution compared to the best solution within the previous 30 generations. The largest constraints violation was found to be 2.3% (see Table C.3) for the case with a 0% mutation. Lower violations (0.36%) and hence solution closer to feasibility, resulted for the case of 5% mutation rate. Mutation rate of 10% was found to yield the best solution in terms of the final solution's best and average values. A mutation rate of 15% was found to result in a lower average and best solution compared to a 10% mutation rate but with convergence at the same population (after 59 generations). A similar final solution was found although slightly less (see Table C.3) using a 20% mutation rate but at a significant increase in the required population for convergence compared to 10% mutation rate (93 generations).

C.3 Penalty Function

A penalty function is applied to infeasible solutions to drive the algorithm to feasibility and subsequently to optimality. A method of hard (absolute) constraints' satisfaction (Eq. C.1) is proposed in this work. This method is a variant of the soft constraints handling equation (Eq. C.2) presented by Low and Sørensen (2003).

Absolute Constraints Handling

$$\kappa_i = \begin{cases} \left[1 - \frac{c_i^{\min} - c_i(t_f)}{c_i^{\min}}\right] & \text{if} \quad c_i(t_f) < c_i^{\min} \qquad \forall\, i = 1, .., n_c \\ 1 & \text{otherwise} \end{cases}$$

$$f = \begin{cases} \Omega & \text{when} \quad \text{feasible} \\ \prod_{i=1}^{n_c} \kappa_i & \text{when} \quad \Omega \geq 0 \quad \text{(profit and infeasible)} \\ \Omega\,(2 - \prod_{i=1}^{n_c} \kappa_i) & \text{when} \quad \Omega < 0 \quad \text{(loss and infeasible)} \end{cases} \tag{C.1}$$

Soft Constraints Handling

$$\kappa_i = \begin{cases} \left[1 - \frac{c_i^{\min} - c_i(t_f)}{c_i^{\min}}\right]^{p_i} & \text{if} \quad c_i(t_f) < c_i^{\min} \qquad \forall\, i = 1, .., n_c \\ 1 & \text{otherwise} \end{cases}$$

$$f = \begin{cases} \Omega \prod_{i=1}^{n_c} \kappa_i & \text{when} \quad \Omega \geq 0 \quad \text{(profit)} \\ \Omega \left(2 - \prod_{i=1}^{n_c} \kappa_i\right) & \text{when} \quad \Omega < 0 \quad \text{(loss)} \end{cases} \tag{C.2}$$

The difference between the two methods is that the hard constraints handling method assigns low fitness values to infeasible solutions (a value between 0 and 1) relative to the constraint violations whereas the soft method multiplies the objective value (*i.e.* profit) by the constraint violations (a value between 0 and 1) and thus reduces the objective value proportional to the violation. The problem with the method is that if a feasible solution can achieve, for instance, $\$1 \times 10^6$ profit, an infeasible solution with a 9% violation but an uncorrected profit figure of $\$10 \times 10^6$ will be preferred by the optimisation procedure as the corrected profit will then be $10 \times 10^6 \times (100\% - 9\%) = \$9.1 \times 10^6$. It should be noted that the objective value is proportional to the amount of product collected and capital and operating costs incurred, regardless of the final product purities and recoveries as these two are usually formulated as constraints to the optimisation problem (*e.g.* Eq. 4.2 in Chapter 4). The effects of using either function is considered next.

As shown in Table C.4, the method proposed in Eq. C.1 results in better constraint satisfaction and convergence time (*i.e.* populations required). The soft constraints handling method resulted in a final solution which failed to tackle the separation of the difficult region (*e.g.* acetone-water tangent-pinch) and hence a small violation was acceptable for lower operating costs and thus higher profit value (without feasibility). The method proposed here (Eq. C.1) will also eliminate the need to specify the value of the parameter p_i in Eq. C.2. Note that the comparison reported in Table C.4 is based on a parameter value $p_i = 8$ as used by Low and Sørensen (2003) for the optimisation of batch distillation processes.

Penalty function	**Eq. C.1**	**Eq. C.2**
Final best solution $/yr	11.8×10^6	$19.4\times10^{6*}$
Final average solution $/yr	2.77×10^6	$17.1\times10^{6*}$
Constraint violation in final best %	0	5.2*
Generations to convergence	59	101*

Table C.4: Effects of penalty function used on GA performance, * infeasible solution

C.4 Termination Criteria

The accuracy of the final solution of the GA procedure depends on the termination criteria employed. Common convergence criteria used are genome, population or generation based. Genome and population based criteria have similar characteristics, with the former depending on the similarity of the best solution from generation to another and the latter depending on the similarity of the genomes inside the population. The population convergence typically takes longer to converge than does the genome convergence. Another common technique is to terminate the GA when a particular number of generations or/and objective function evaluations has been exceeded. The effects of these termination criteria is investigated with all other parameters as in the base case (Table C.1).

Table C.5 shows the results for the genome based and maximum number of generation methods applied to the optimisation of hybrid processes. It is noted that both methods result in solutions that satisfy all the constraints. The maximum number of generation convergence is based on a maximum of 200 generations. The genome convergence criteria is based on that the best solutions should have $\geq 95\%$ resemblance compared to the best solution during the previous 30 generations. The maximum number of generation method resulted in a better solution (61% higher) than the genome convergence criteria. Which method to use will depend on the required accuracy and the available computational resources.

Termination criteria	Population best	Maximum generations
Final best solution $/yr	11.8×10^7	19.02×10^6
Final average solution $/yr	2.77×10^6	15.2×10^6
Constraint violation in final best %	0	0
Generations to convergence	59	200 *

Table C.5: Effects of termination criteria used on GA performance, * fixed

C.5 Conclusions

Based on the sensitivity studies presented here, *general* guidelines are now available for appropriate algorithm parameter values in hybrid separation system optimisation. Note that the sensitivity trials presented were based on a single hybrid distillation/pervaporation problem (base case in Chapter 4), hence further parameter values adjustment may be needed when the size or complexity of the optimisation problem varies widely from case to case. The values of the GA parameters used in conducting the optimisation work in this thesis are given in the relevant chapters. These values are within a typical range that have been used and shown to be effective in most genetic algorithm applications on a wide range of problems including those outside of the chemical engineering field. This has also been confirmed by the sensitivity analysis of the hybrid distillation/pervaporation problem as presented in this appendix.

Appendix D

Derivation of Cost Correlations

This section details the costing data for the distillation, pervaporation and the hybrid as used in Chapters 4, 5 and 6 of this thesis.

D.1 Distillation Column

D.1.1 Capital Costs

The annualised capital costs associated with the installed equipment costs for the column shell can be described using Guthrie's correlations (Douglas, 1988) as follow:

$$C_{sh} = C_{sh,RC}\left(\frac{N}{N_{RC}}\right)^{0.862}\left(\frac{D}{D_{RC}}\right)^{1.066} \tag{D.1}$$

where N is the number of trays, D is the diameter of the column and RC represents the reference case column on which the Guthrie's correlation is based. Assuming the column diameter varies as the square root of the column vapour loading, $D \propto \sqrt{V}$ (Douglas, 1988), Equation D.1 can be written as:

$$C_{sh} = C_{sh,RC}\left(\frac{N}{N_{RC}}\right)^{0.802}\left(\frac{V}{V_{RC}}\right)^{0.533} \tag{D.2}$$

Another contribution to the column cost are the reboiler and condenser installation costs. Guthrie (Douglas. 1988) proposed that the annual installed cost of heat exchangers can be describe by:

$$C_{ex} = C_{ex,RC}\left(\frac{A}{A_{RC}}\right)^{0.65} \tag{D.3}$$

where the heat exchanger area, A, is calculated:

$$Q = VC_p\Delta t = UA\Delta T_m \tag{D.4}$$

where Δt is the temperature difference of the exchanger fluid (reboiler or condenser) and ΔT_m is the mean temperature difference across the heat exchanger. Assuming constant values of heat capacities, C_p, and the overall heat transfer coefficient, U, and substituting for A in Equation D.3 with D.4 gives:

$$C_{ex} = C_{ex,RC}\left(\frac{V}{V_{RC}} \times \frac{\Delta t}{\Delta t_{RC}} \times \frac{\Delta T_{m,RC}}{\Delta T_m}\right)^{0.65} \tag{D.5}$$

If the stream temperatures are fixed, a simple model for the heat exchangers costs in terms of flows can be obtained from Eq. D.5:

$$C_{ex} = C_{ex.RC}\left(\frac{V}{V_{RC}}\right)^{0.65} \tag{D.6}$$

Equations D.2 and D.6 can be written respectively as:

$$C_{sh} = K_1 N^{0.802} V^{0.533} \tag{D.7}$$

$$C_{ex} = K_2 V^{0.65} \tag{D.8}$$

The values of the correlation coefficients K_1 and K_2 can be calculated from the reference case column:

$$K_1 = \frac{C_{sh,RC}}{N_{RC}^{0.802} V_{RC}^{0.533}} \tag{D.9}$$

$$K_2 = \frac{C_{ex,RC}}{V_{RC}^{0.65}} \tag{D.10}$$

D.1.2 Operating Costs

The main contribution to operating costs in a distillation column are the reboiler heating and condenser cooling duties. The annual operating costs, AOC_c, for the distillation column is therefore given by:

$$AOC_c = C_{ut,reb}Q_{reb} + C_{ut,cond}Q_{c,cond} \tag{D.11}$$

where $C_{ut,reb}$ and $C_{ut,cond}$ represent the unit cost of utility in the reboiler and condenser, respectively. Q_{reb} and $Q_{c,cond}$ represent the reboiler heating and condenser cooling duties, respectively.

D.2 Pervaporation Unit

D.2.1 Capital Costs

The annualised capital cost for the pervaporation membrane process can also be correlated using Guthrie's correlation from values of a reference case including pumps and heaters (Sulzer, 2005) such that:

$$ACC_m = ACC_{m,RC} \times \left(\frac{A_m}{A_{m,RC}} \times \frac{F_m}{F_{m,RC}} \times \frac{F_p}{F_{p,RC}} \right)^{0.3} \tag{D.12}$$

The membrane stage flowrate, F_m, membrane area, A_m, and permeate flowrate, F_p, are the main parameters affecting membrane system performance and are hence included in the cost equation for comparison with the reference case. The scale exponent is estimated to be 0.3 (Eq. D.12), the lowest recommended value (IChemE, 1988) in order to accurately predict the pervaporation capital costs.

Based on the reference case specifications given in Table D.1, the annualised capital cost of the base case can be calculated as:

$$ACC_{m,RC} \approx \$350,000 \times \frac{1}{3} + \$20,000 \approx \$136,000 \tag{D.13}$$

Property	**Value**	**Units**
Membrane Area, $A_{m,RC}$	6	m^2
Feed flowrate, $F_{m,RC}$	0.73	mol/s
Permeate flowrate, $F_{p,RC}$	0.0365	mol/s
Purchase cost of module	$\approx 350,000$	\$
Equipment service cost	$\approx 20,000$	\$/yr
Capital recovery factor, CRF_m	$\approx \frac{1}{3}$	-

Table D.1: Membrane reference case estimates (Sulzer, 2005)

D.2.2 Operating Costs

The feed stream heater and the permeate side cooler, in addition to the membrane feed pump and the permeate vacuum turbine, are considered to be the main contributions to the operating cost of the membrane unit. The operating costs for the membrane process are therefore given by:

$$\begin{aligned} AOC_m &= (C_{ut,m,h} \times Q_{m,h} + C_{ut,m,cond} \times Q_{m,cond} \\ &\quad + C_{ut,p} \times Q_{m,p} + C_{ut,t} \times Q_{m,t}) \times \left(\frac{T_A}{t_s + t_f}\right) \end{aligned} \tag{D.14}$$

$$Q_{m,p} = \frac{\nu_p}{\eta_p}\left(P_p^{out} - P_p^{in}\right) \tag{D.15}$$

$$Q_{m,t} = \frac{\nu_t}{\eta_t} \times P_t^{in} \ln\left(\frac{P_t^{out}}{P_t^{in}}\right) \tag{D.16}$$

where $C_{ut,i}$ represent cost of utilities of equipment i, $Q_{m,h}$ and $Q_{m,cond}$ represent the pervaporation unit total feed tank heat duty and permeate condenser cooling duty. $Q_{m,p}$ and $Q_{m,t}$ are the total energy load of the membrane unit feed pump and permeate vacuum turbine, respectively. T_A represents the total available time for operation per annum and t_s and t_f represent the process startup and operating time respectively. ν_i is the flowrate entering the ancillary equipment, i and η_i is the efficiency of the equipment i. P_i^{in} and P_i^{out} represent the pressure at the inlet and outlet of the relevant equipment, i, respectively.

D.3 Hybrid Process Costs

The annualised capital costs, ACC_{hyb}, and the operating costs, AOC_{hyb}, for the hybrid distillation column are the summation of the cost contributions of the constituent processes and are therefore given by:

$$ACC_{hyb} = ACC_c + ACC_m \tag{D.17}$$

$$AOC_{hyb} = AOC_c + AOC_m \tag{D.18}$$